FACULTY OF ECONOMICS AND BUSINESS

DEPARTMENT OF ECONOMICS AND ECONOMICS HISTORY

VNiVERSiDAD
Đ SALAMANCA

MACRO-FINANCIAL STABILITY UNDER A SEMI-NONPARAMETRIC APPROACH

DOCTORAL THESIS

JUAN FERNANDO RENDÓN GARCÍA

Thesis directors:

JAVIER PEROTE PEÑA

LINA MARCELA CORTÉS DURÁN

June 2023, Salamanca

Esta tesis está dedicada:

A mis sobrinos Matías y David, para quienes quiero ser ejemplo de transformación a través del conocimiento. A mi amada Diana que me ha brindado su amor, apoyo moral, psicológico y logístico para que yo pudiera sacar adelante este proyecto. A mi mamá y a mis hermanas que siempre me han apoyado de manera incondicional y que han sido fundaméntales no solo en este proceso, sino en todos los procesos de mi vida. Por último, a mis perros Nietzsche, Lou, Quevedo y Copito y a mis gatos, Pulga, Chuchu y la negrita, que han sido tan importantes en mi bienestar.

AGRADECIMIENTOS

Afortunadamente existe esta sección en donde puedo hacer explícito mi profundo agradecimiento a mis directores de tesis, la Doctora Lina Marcela Cortés y el Doctor Javier Perote Peña por haber hecho posible este proceso. Específicamente quiero agradecerles haber posibilitado el cambio personal que ha implicado para mí este proyecto; su calidez humana, su experiencia como investigadores, su producción científica que es una guía, que facilita los avances en cada capítulo, y su experiencia en la redacción científica de la cual saco uno de los mayores aprendizajes obtenidos. Destaco la disposición de la Doctora Lina para atender con paciencia y dedicación las tareas que le implicaron su labor como directora, y a el Doctor Javier por su hospitalidad, su disposición para atender rápidamente las solicitudes y su eficiencia comunicativa.

Agradezco al Instituto Tecnológico Metropolitano (ITM) de Medellín que es la institución que ha patrocinado este proceso otorgándome una comisión de estudios y brindándome apoyo para asistir a eventos científicos en donde he presentado avances de la tesis doctoral. Agradezco al ITM su compromiso con la formación integral de los docentes y la confianza que depositaron en mí al apoyarme.

También quiero aprovechar esta ocasión a la Doctora Inés Jiménez y al doctor Andrés Mora Valencia por facilitarme su desarrollo computacional del modelo DCC-SNP y al Doctor Alfredo Trespalacios quien me introdujo en el proceso de estimación de los modelos SNP.

ABSTRACT

This thesis proposes a set of tools for measuring and managing financial risks related to the stability of banking systems and for establishing macroprudential policies aimed at preventing the materialization of systemic risks. It is based on accurately modeling probability density functions associated with banking stability indicators. The methodologies used respond to the second pillar of the Basel Committee on Banking Supervision agreement, which states the need to determine and monitor the Economic Capital banks' need to cover losses caused by the materialization of financial risks with a certain level of confidence and for a given time horizon. Semi-nonparametric statistics were used to parameterize stylized facts such as asymmetries and heavy and wavy tails observed in the empirical probability distributions of financial stability indicators. Analytical and simulated solutions for probability measures and economic capital settings are proposed. Applications are made on aggregate solvency indicators and their components, the bank leverage indicator for developed and emerging economies, and interactions between these indicators and monetary policy were analyzed. The results point to the need to model the skewness and kurtosis of the probability distributions of the financial stability indicators for not to underestimate risk and the level of economic capital. The hypothesis of an interaction between prudential and monetary policy and the need to jointly consider the decision-making of both policies is confirmed.

RESUMEN

Esta tesis propone un conjunto de herramientas para la medición y administración de riesgos financieros relacionados con la estabilidad de los sistemas bancarios, y para el establecimiento de políticas macroprudenciales destinadas a prevenir la materialización de riesgos sistémicos. Se parte de la modelación precisa de las funciones de densidad de probabilidad asociadas a indicadores de estabilidad bancaria. Las metodologías utilizadas responden al segundo pilar del acuerdo del Comité de Supervisión Bancaria de Basilea, el cual plantea la necesidad de determinar y monitorear el Capital Económico que necesitan los bancos para cubrir las pérdidas ocasionadas por la materialización de riesgos financieros, con un determinado nivel de confianza y para un horizonte temporal dado. Se utiliza estadística semi-noparamétrica que permite la parametrización de hechos estilizados como asimetría, y colas pesadas y ondeadas observadas en las distribuciones de probabilidad empíricas de los indicadores de estabilidad financiera. Se proponen soluciones analíticas y simuladas para las mediciones de probabilidad y el establecimiento del capital económico. También, se realizan aplicaciones sobre los indicadores agregados de solvencia y sus componentes, y el indicador de apalancamiento bancario para economías desarrolladas y emergentes. Además, se analizan interacciones entre estos indicadores y la política monetaria. Los resultados señalan la necesidad de modelar el sesgo y la curtosis de las distribuciones de probabilidad de los indicadores de estabilidad financiera, para no subestimar el riesgo y el nivel de capital económico. Se confirma la hipótesis de interacción entre la política prudencial y la política monetaria y la necesidad de considerar la toma de decisiones de ambas políticas de manera conjunta.

CONTENT

LIST OF TABLES

LIST OF FIGURES

CHAPTER I. Introduction to the study

I.1. Introduction

The limitation of human beings as finite individuals attempting to understand an infinite world has led to the construction of the cultural idea of uncertainty, which in general is related to the ignorance of the occurrence of future unknown events (Martínez, 2006).

The concept of uncertainty has been developed in different fields of knowledge, such as philosophy, where authors such as Plato in the myth of the Cave pose how human beings are denied absolute knowledge of the world and only manage to see shadows and reflections of this (La República, 2009); Kant states the impossibility of knowing " Thing-in-itself" and that it is only possible to construct an idea of things for ourselves (Kant, 1967, p. 48); Albert Camus in his book the myth of Sisyphus (Camus, 2021) assumes existential uncertainty as a human condition and renounces the support offered by the gods, to adhere to the metaphysics of the absurd, of what is hidden from human lucidity and becomes gods.

The concept of uncertainty in physics has been developed within the framework of measurement and probability theory (Alemán Berenguer, 2010). From the perspective of physics, uncertainty refers to imprecision or inaccuracy in measurements and predictions of physical phenomena caused by sources such as imprecision in measurement instruments, limitations of theory, the impossibility of simultaneously measuring certain variables, and the presence of random and systematic errors in the data, among others (Smith & Vul, 2013; Taylor, 1997). Although Einstein asserted that "God does not play dice," quantum theory and chaos theory have had to introduce uncertainty in the face of the impossibility of knowing the physical laws that govern the universe with sufficient precision.

In economics and finance, uncertainty about the future of the different financial and macroeconomic variables plays a fundamental role in decision-making (Martínez, 2006). The complexity of the interactions between the agents and economic factors and the incomplete

information has led to the development of decision-making models where the uncertainty about the expected results is considered.

Probability is a field of mathematics concerned with quantifying and modeling uncertainty or randomness in events (Evans & Rosenthal, 2004). In particular, the probability is used to address the problem of forecasting uncertain or random future events, i.e., to determine the probability that a given event will occur. Probability theory provides a formal framework for dealing with uncertainty. It is applied in different fields such as economics, physics, medicine, engineering, and biology, among others., where future outcomes are uncertain, and decision-making depends on the probability of occurrence of certain events.

The normal distribution is one of the most important and widely used distributions in probability theory and statistics since the central limit theorem states that the sum of a large number of independent random variables approximates a normal distribution regardless of their distribution (Durrett, 2019). This theorem is fundamental to inferential statistics, as it allows us to use normal distribution to make inferences about population means from samples.

Within the economic and financial theory, the normal distribution has played a fundamental role in developing probabilistic models since the behavior of many economic and financial phenomena approximates the behavior of Gaussian random variables. The normal distribution has been widely used in the analysis of risk and uncertainty in investments, the valuation of financial assets, the analysis of income and wealth distribution, the modeling of macroeconomic phenomena, and the analysis of economic and financial data. Some financial models widely used by academics and practitioners assume the normality assumption. Markowitz's portfolio optimization model assumes that financial asset returns follow a normal distribution (Markowitz, 1959), the option pricing model proposed by Black-Scholes assumes that stock prices follow Gaussian stochastic processes (Merton, 1973), the CAPM model (Sharpe, 1964) which is widely used for estimating the cost of capital allocated to project finance. In the context of credit risk, Vasicek (2002) proposes a model that starts from a Gaussian stochastic process to determine the probability distribution of the value of a credit portfolio. Chava et al. (2011). Belkin et al. (1998) and Schönbucher (2002), among others, have also modeled the distribution of credit risk materialization losses from the normality

assumption. Frachot et al. (2001) approximated the loss distribution for operational risk VaR estimation to a Gaussian distribution in the context of operational risk.

In financial risk measurement, it is common for empirical probability distributions to have certain distortions concerning the normal distribution, such as skewness and heavy tails. Authors such as Rosenberg & Schuermann (2006), Daníelsson et al. (2013), Sandström (2007), Bølviken & Guillen (2017), Brio et al. (2009), Le Maistre & Planchet (2013), Dutta & Perry (2006), De Fontnouvelle et al. (2003), Feria-Domínguez et al. (2015), Kretzschmar et al. (2010); Bateni et al. (2014); Madan (2009); and Lynn Wirch & Hardy (1999) Jiménez et al. (202020), Brio et al. (2009), Del Brio et al. (2011), have addressed the problem of bias and heavy tails in the measurement of market, credit, operational, liquidity and solvency risks, both univariate and multivariate.

The problem addressed in this research project is the study of the probability distributions involved in the integral management of financial risks to which banking institutions are exposed. The objective is to propose models that adjust more precisely to the empirical characteristics of the risk distributions generated by the financial intermediation activity.

For fitting more accurate pdfs, this paper uses models that generalize the normal pdf from the Taylor series expansion of its characteristic function (which is the Fourier transform of the pdf) and recovering the pdf from the inverse of the Fourier transform. (Cohen, 1998; Dharmani, 2018; Kolassa, 2006).

These procedures make explicit the parameters for modeling high-order moments, such as skewness and kurtosis, and allow relaxing the assumption that these high-order moments are equal to zero, as in the normal distribution. This natural extension of the normal distribution is obtained from Taylor series expansions truncated at a finite order, so that parameters modeling the higher order moments can be estimated from data. This procedure is known as Gram-Charlier and Edgeworth expansions and is framed in Semi-Non-Parametric statistics (SNP) fields, since although the asymptotic expansions capture the true data generating process, the truncated expansions result in parametric pdfs. SNP distributions have some critical advantages over parametric and nonparametric distributions. The SNP approach is more flexible than the parametric distributions from which they start since they can be

adapted to different shapes of the empirical distributions. Concerning nonparametric distributions, SNP pdfs have properties of parametric pdfs that allow unique identification of the pdf, facilitate comparison between measurements, and can be more efficient in parameter estimation.

Gram-Charlier expansions have been applied in various fields where the accuracy in tail fitting of pdfs is essential for the correct measurement of the occurrence of outliers. In finance, Mauleon & Perote (2000), Mora-Valencia et al. (2017), Ñíguez & Perote (2012), and Perote (2012) have developed and made use of these methodologies for modeling univariate and multivariate financial phenomena.

I.2. Objectives of the study

I.2.1 General Objective

This thesis proposes methodologies for financial risk management within the prudential policy based on the adjustment of SNP probability distributions. As an application case, this manuscript measures macrofinancial risks required in the macroprudential decision-making process.

The economic costs caused by the financial crisis of 2007-08, unleashed by the materialization of systemic risks in the banking system in the United States and some countries globally, have led macroprudential policy to establish itself as an area of financial policy to prevent excessive risk-taking in the financial sector and mitigate its effects on the real economy (Bengtsson, 2020). The relationship between the stability of the financial system as a whole and the economy's performance has become a priority for policymakers and academics as the conception of financial stability policy has changed (Ebrahimi Kahou & Lehar, 2017).

I.2.2 Specific objectives

In this framework, the study accomplishes several targets:

- Determine the empirical characteristics of probability distributions of macrofinancial stability indicators.

- Introduce SNP models based on the Gram-Charlier series to quantify macro-financial risks and contrast their accuracy of fit with the results obtained under parametric distributions.
- Apply the proposed models for risk measurement in international banking systems to monitor macro-financial stability indicators and thus infer the best macro-prudential policies.

The results show that the empirical pdfs associated with bank solvency and leverage present significant skewness and kurtosis distortions concerning the normal distribution. These distortions could be modeled from SNP econometric models that allowed the estimation of higher-order moments. These models serve as an early warning tool for systemic risks and for formulating macroprudential policies such as creating countercyclical capital buffers. In addition, the multivariate approach allows the formulation of macroprudential stress test models used in decision-making under uncertainty.

The main contributions of this research are a set of tools for the measurement and management of financial risks in the banking system and for the establishment of prudential policies, which respond to the principles established in the Second Pillar of the Basel Committee on Banking Supervision agreements. It proposes univariate and multivariate models better adapted than the normal distribution to the particular conditions of the observed risk distributions of the financial stability indicators. It incorporates parameters that model the general cyclical behavior of credit portfolios and businesses.

These models are applied to measure the probability that bank capital will absorb losses due to the materialization of financial risks breaching regulatory limits and generating imbalances in banking systems. They are also used to establish prudential policies in terms of the amount of capital that banks must hold in order not to cross regulatory limits, for a given time horizon, with a certain level of confidence that depends on risk appetite. Models are included to estimate countercyclical capital buffers to absorb systematic risks in their time dimension.

The analytical solution for estimating countercyclical capital buffers to absorb systematic risks in their time dimension is highlighted. This solution is similar to the model proposed by Black-Scholes for estimating the financial option premium, where the regulatory thresholds are analogous to the exercise price of the options.

Another methodological contribution is the proposal of models that combine harmonic analysis with SNP probability distributions in the context of financial risk modeling. At this point, contributions are made to estimate the harmonic components.

The notation used to describe semi-nonparametric statistical models is based on literature from the fields of physics. It is more compact than the notation typically used in finance.

I.3. Structure of the document

This thesis is written as independent and self-contained chapters that are divided as follows: Chapter II proposes risk measures based on SNP distributions on the changes of the bank solvency indicator and its components, which allows the measurement of the probability of regulatory intervention and the establishment of prudential policies related to the capital destined to absorb losses generated by the materialization of financial risks. A case analysis is made of the effect of the monetary policy measures used to respond to the COVID-19 pandemic in Colombia on the aggregate solvency indicator in Colombia.

Chapter III presents a long-run model that assumes that the Capital Adequacy Ratio (CAR) follows a generalized Ornstein Uhlenbeck stochastic process under SNP expansions. Harmonic analysis is used to model the financial cycles to incorporate periodic functions in the mean CAR. This model estimates the probability of breaching the minimum capital threshold and the countercyclical bank capital buffer established as a macroprudential measure in the Basel III agreement. As a case of analysis, the model was adjusted to the observed time series of the CAR for the United States, Germany, the Netherlands, and Colombia.

Chapter IV presents a model for macroprudential stress testing based on the joint modeling of the probability distributions of a leverage indicator and the monetary policy interest rate. For the modeling of the marginal probability distributions, the DCC-SNP model is used, which allows the modeling of the dynamic conditional correlation and the skewness and kurtosis of the marginal pdfs. In addition, bivariate harmonic analysis is applied to analyze the dynamics between the cycles of the analysis variables. This chapter also includes

applying the proposed stress test model to analyze the impact of different regimes of monetary policy interest rate scenarios on a bank leverage indicator.

References

Alemán Berenguer, R. A. (2010). Incertidumbre, predictibilidad e indeterminación en la ciencia física. *Thémata (2010, Vol. 43, p. 27-40)*.

Bateni, L., Vakilifard, H., & Asghari, F. (2014). The influential factors on capital adequacy ratio in iranian banks. *International Journal of Economics and Finance*, *6*(11), 108–116. https://doi.org/10.5539/ijef.v6n11p108

BCBS, B. I. (2011). Basel III: A global regulatory framework for more resilient banks and banking systems. *Bank for International Settlements, Basel, Switzerland*. https://www.bis.org/publ/bcbs189.htm

Belkin, B., Suchower, S., & Forest, L. R. (1998). The effect of systematic credit risk on loan portfolio value-at-risk and loan pricing. *CreditMetrics Monitor*, 17–28. https://www.z-riskengine.com/media/1037/the-effect-of-systematic-credit-risk-on-loan-portfolios-and-loan-pricing.pdf

Bengtsson, E. (2020). Macroprudential policy in the EU: A political economy perspective. *Global Finance Journal*, *46*, 100490. https://doi.org/https://doi.org/10.1016/j.gfj.2019.100490

Bølviken, E., & Guillen, M. (2017). Risk aggregation in solvency II through recursive log-normals. *Insurance: Mathematics and Economics*, *73*, 20–26. https://doi.org/https://doi.org/10.1016/j.insmatheco.2016.12.006

Brio, E. B. D., Ñíguez, T.-M., & Perote, J. (2009). Gram–charlier densities: A multivariate approach. *Quantitative Finance*, *9*(7), 855–868. https://doi.org/10.1080/14697680902773611

Camus, A. (2021). *El mito de sísifo*. RANDOM HOUSE.

Chava, S., Stefanescu, C., & Turnbull, S. (2011). Modeling the loss distribution. *Management Science*, *57*(7), 1267–1287. https://doi.org/https://doi.org/10.1287/mnsc.1110.1345

Cohen, L. (1998). Generalization of the gram-charlier/edgeworth series and application to time-frequency analysis. *Multidimensional Systems and Signal Processing*, *9*(4), 363–372. https://doi.org/https://doi.org/10.1023/A:1008454223082

Daníelsson, J., Jorgensen, B. N., Samorodnitsky, G., Sarma, M., & de Vries, C. G. (2013). Fat tails, VaR and subadditivity. *Journal of Econometrics*, *172*(2), 283–291. https://doi.org/https://doi.org/10.1016/j.jeconom.2012.08.011

De Fontnouvelle, P., Jesus-Rueff, D., Jordan, J. S., Rosengren, E. S., et al. (2003). Using loss data to quantify operational risk. *Available at SSRN 395083*. https://doi.org/http://dx.doi.org/10.2139/ssrn.395083

Del Brio, E. B., Ñíguez, T.-M., & Perote, J. (2011). Multivariate semi-nonparametric distributions with dynamic conditional correlations. *International Journal of Forecasting*, *27*(2), 347–364. https://doi.org/https://doi.org/10.1016/j.ijforecast.2010.02.005

Dharmani, B. C. (2018). Multivariate generalized gram–charlier series in vector notations. *Journal of Mathematical Chemistry*, *56*, 1631–1655.

Durrett, R. (2019). *Probability: Theory and examples* (Vol. 49). Cambridge university press.

Dutta, K., & Perry, J. (2006). *A tale of tails: An empirical analysis of loss distribution models for estimating operational risk capital*. https://www.bostonfed.org/publications/research-department-working-paper/2006/a-tale-of-tails-an-empirical-analysis-of-loss-distribution-models-for-estimating-operational-risk-capital.aspx

Ebrahimi Kahou, M., & Lehar, A. (2017). Macroprudential policy: A review. *Journal of Financial Stability*, *29*, 92–105. https://doi.org/https://doi.org/10.1016/j.jfs.2016.12.005

Evans, M. J., & Rosenthal, J. S. (2004). *Probability and statistics: The science of uncertainty*. Macmillan.

Feria-Domínguez, J. M., Jimenez-Rodriguez, E., & Sholarin, O. (2015). Tackling the over-dispersion of operational risk: Implications on capital adequacy requirements. *The North American Journal of Economics and Finance*, *31*, 206–221. https://doi.org/https://doi.org/10.1016/j.najef.2014.11.004

Frachot, A., Georges, P., & Roncalli, T. (2001). Loss distribution approach for operational risk. *Available at SSRN 1032523*. https://papers.ssrn.com/sol3/papers.cfm?abstract_id=1032523

Javier Perote, E. B. D. B. &. (2012). Gram–charlier densities: Maximum likelihood versus the method of moments. *Insurance: Mathematics and Economics*, *51*(3), 531–537. https://doi.org/https://doi.org/10.1016/j.insmatheco.2012.07.005

Jiménez, I., Mora-Valencia, A., Ñíguez, T.-M., & Perote, J. (2020). Portfolio risk assessment under dynamic (equi)correlation and semi-nonparametric estimation: An application to cryptocurrencies. *Mathematics*, *8*(12). https://doi.org/10.3390/math8122110

Kant, I. (1967). *Crítica de la razón pura: Estética trascendental y analítica trascendental. Vol. 1* (Vol. 1). Losada.

Kolassa, J. E. (2006). *Series approximation methods in statistics* (Vol. 88). Springer Science & Business Media. https://link.springer.com/book/10.1007/0-387-32227-2

Kretzschmar, G., McNeil, A. J., & Kirchner, A. (2010). Integrated models of capital adequacy–why banks are undercapitalised. *Journal of Banking & Finance*, *34*(12), 2838–2850. https://doi.org/https://doi.org/10.1016/j.jbankfin.2010.02.028

La república. (2009). Ediciones Akal. https://books.google.com.co/books?id=aAk3O462g1QC

Le Maistre, A., & Planchet, F. (2013). A proposal of interest rate dampener for solvency II framework introducing a three factors mean reversion model. *ISFA-Laboratory SAF*. https://www.semanticscholar.org/paper/A-proposal-of-interest-rate-dampener-for-Solvency-a-Maistre/00bc83d8d5ebc17e062d86456a67a5ae44d46cfe

Lynn Wirch, J., & Hardy, M. R. (1999). A synthesis of risk measures for capital adequacy. *Insurance: Mathematics and Economics*, *25*(3), 337–347. https://doi.org/https://doi.org/10.1016/S0167-6687(99)00036-0

Madan, D. B. (2009). Capital requirements, acceptable risks and profits. *Quantitative Finance*, *9*(7), 767–773. https://doi.org/10.1080/14697680903314456

Markowitz, H. (1959). Portfolio selection. *Investment Under Uncertainty*.

Martínez, F. V. (2006). *Riesgos financieros y económicos : Productos derivados y decisiones económicas bajo incertidumbre*. THOMSON. https://books.google.com.co/books?id=AZzaPBYFIuAC

Mauleon, I., & Perote, J. (2000). Testing densities with financial data: An empirical comparison of the EdgeworthSargan density to the students t. *The European Journal of Finance*, *6*(2), 225–239. https://doi.org/10.1080/13518470050020851

Merton, R. (1973). Theory of rational option pricing. *The Bell Journal of Economics and Management Science*, 229–288. https://doi.org/10.1142/9789812701022_0008

Mora-Valencia, A., Ñíguez, T.-M., & Perote, J. (2017). Multivariate approximations to portfolio return distribution. *Computational and Mathematical Organization Theory*, *23*, 347–361.

Ñíguez, T.-M., & Perote, J. (2012). Forecasting heavy-tailed densities with positive edgeworth and gram-charlier expansions*. *Oxford Bulletin of Economics and Statistics*, *74*(4), 600–627. https://doi.org/https://doi.org/10.1111/j.1468-0084.2011.00663.x

Rosenberg, J. V., & Schuermann, T. (2006). A general approach to integrated risk management with skewed, fat-tailed risks. *Journal of Financial Economics*, *79*(3), 569–614. https://doi.org/https://doi.org/10.1016/j.jfineco.2005.03.001

Sandström, A. (2007). Solvency II: Calibration for skewness. *Scandinavian Actuarial Journal*, *2007*(2), 126–134. https://doi.org/10.1080/03461230701250481

Schönbucher, P. (2002). Taken to the limit: Simple and not-so-simple loan loss distributions. *The Best of Wilmott*, *1*, 143–160.

Sharpe, W. F. (1964). Capital asset prices: A theory of market equilibrium under conditions of risk. *The Journal of Finance*, *19*(3), 425–442.

Smith, K. A., & Vul, E. (2013). Sources of uncertainty in intuitive physics. *Topics in Cognitive Science, 5*(1), 185–199.

Taylor, J. (1997). *Introduction to error analysis, the study of uncertainties in physical measurements*.

Vasicek, O. (2002). The distribution of loan portfolio value. *Risk, 15*(12), 160–162

CHAPTER II. Prudential regulation and Bank Solvency Based on Flexible Distributions: An Example for Evaluating the Impact of Monetary policy[1]

II.1. Introduction

Prudential regulation has become more relevant in recent years for preserving investors' protection and the financial system's stability. Prudential regulation seeks to promote the solvency and liquidity of financial institutions and ensure their ability to meet their obligations and manage risks. At the International level, Basel Committee on Banking Supervision (BCBS) defines capital adequacy as the main way to cover losses that can destabilize a bank and the financial system (BCBS, 1988). The indicator used in BCBS for measuring capital adequacy is the solvency ratio (*SR)*, calculated by dividing regulatory capital *(RC)* by risk-weighted assets *(RWAs)* whose value should not fall below a certain value set by regulators. However, the Basel accord was insufficient for protecting the banking system in the 2008 financial crisis, which revealed the need to reevaluate policies, business models, and financial risk management systems (Borio, 2008). A significant concern in measuring, monitoring, and controlling solvency risk is the provision of accurate and flexible methodologies. In this framework, we focus on modeling probability density functions (*pdfs*) that can be applied in the context of the Basel Accords to measure and limit solvency risk.

We measure the probability that a bank may fall below the minimum solvency required as a prudential policy and for controlling risk by setting regulatory constraints based on defining minimum solvency levels from quantile risk measures. These pdfs reflect banks' risk profile and can be used in the context of prudential regulation to dampen banks' appetite for risk. Also, stylized facts of the pdfs, including skewness and excess kurtosis observed in the sample data, should be considered because these parameters contain more precise information about the bank risk profile. Therefore, to estimate the pdf of the variations in the *SR*, the risk portfolio, and the capital supporting this portfolio, we propose seminonparametric (SNP) techniques based on Gram–Charlier (GC) expansions.

[1] A version of this Chapter has been accepted for publication in The World Economy.

The SNP distribution enables us to capture the stylized facts in the tails of the probability distribution, such as skewness, leptokurtosis, and other aspects, such as multimodality in the extreme values of the distribution, which would not be possible under the assumption of normality and other typical parametric specifications. This approach is consistent with autoregressive moving average (ARMA) and generalized autoregressive conditional heteroscedasticity (GARCH) models for capturing the mean-variance time-varying patterns in the solvency risk measures.

As a case study, we apply the proposed methodology using Colombian data from the following variables: (i) the solvency decline rate (SDR), which is calculated as the negative first logarithmic difference of the *SR*; (ii) the portfolio growth rate (PGR), which is calculated as the first logarithmic difference of the value of the risk portfolio; (iii) the tier decline rate (TDR), which is calculated as the negative first logarithmic difference of the value of tier capital that supports the risk portfolio of the banks. These risk measures can be used to estimate the risk of regulatory intervention and define policies that establish the minimum *SR*s required by bank regulators based on an estimation of Quantile Risk Metrics (*QRMs*). For this purpose, we collected data on the solvency indicators of the banking system in Colombia (a country that has followed the standards set by the Basel Committee) and data on the monetary measures implemented by its central bank to deal with the effects of COVID-19 on economic performance. The rationale behind this case study is that banks regulated through prudential policy are used as a transmission channel for monetary policy. Emphasis is placed on the period corresponding to the COVID-19 pandemic, given that during this period, an extraordinary monetary policy regime was applied to mitigate the effects of the lockdown.

According to our findings, implementing COVID-19 monetary policy measures in Colombia increased banks' regulatory intervention risk by acting as a transmission channel. Also, we find that the frequency distributions of *SDR* and its components (*TDR* and *PGR*) have time-varying patterns in the mean and variance, which can be captured using ARMA-GARCH models. The modeling of excess kurtosis at higher moments of the probability distributions is significant for all the variables, and the same is true of skewness for *PGR*. Overall, the performance tests indicate that *GC* densities fit the observed frequency histograms of solvency risk better than normal densities; thus, they are an adequate tool for ensuring the implementation of prudential policy.

Since 2008, most central banks have adopted unprecedented expansionary monetary policy measures to inject liquidity into their economies in an attempt to restore economic stability. This response, however, posed higher financial and reputational risks for banks involved in the transmission mechanism of monetary policy, as it increased (or reduced) their level of leverage (solvency) and led to unsustainable debt levels (International Monetary Fund, 2020). This scenario created several uncertainties in the banking industry, as stated by KPMG (2020): Will some companies' *SR* plunge to the point that they require regulatory actions? What is the impact of these decreases on solvency? How does the decline in equity ratios affect rating agencies' opinions at the corporate and industry level?

The answers depend on the "risk-taking channel," which links monetary policy and the perception and valuation of risk by financial institutions used as a transmission mechanism (Borio and Zhu, 2012). One of the main drawbacks is that the current macroeconomic models are not flexible enough to incorporate such a channel, reducing their effectiveness in designing monetary policy. Many studies provide empirical evidence of monetary policy's impact on transmission channel risk. However, these studies are focused mainly on the effects of risk in banks' loan portfolios, which affect bank solvency, as suggested by de Moraes et al. (2016), who stated that banks react to monetary policy by changing the amount of loan-loss provisions and the capital adequacy ratio (CAR).

The rest of this paper is structured as follows. Section 2 provides the theoretical framework, which decomposes the solvency risk into different risk sources and accurately estimates regulatory capital. Section 3 proposes solvency risk measures and models to estimate them. Section 4 describes the dataset used in this study and the monetary policy measures adopted by the central bank of Colombia during the COVID-19 period. In addition, it presents the results of the detection and adjustment of the PGR, TDR, and SDR time series by Additive Outliers, the results of the unit root tests, and the results of the tests for detecting structural changes. Section 5 presents the empirical results. Finally, Section 6 draws our conclusions and offers some practical recommendations.

II. 2 Theoretical Framework

The Basel Accords are founded on three pillars. The first pillar requires *SR* to be measured in a standard manner so that different agents' aspects can be compared and aggregated. The second pillar calls for banks to develop more precise risk management techniques that consider the relationship between these risks and banks' risk profile and environment. This pillar, in turn, requires banks to measure their capital requirements using regulatory and rigorous models to calculate economic capital *(EC)*, defined by Elizalde and Repullo (2007) and Tiesset and Troussard (2005) as the level of capital required to cover banks' losses at a given confidence level for a given time horizon. Balthazar (2006) stressed the importance of pillar 2 in the regulatory framework's evolution. This pillar promotes *EC*, instead of *RC*, as the capital necessary to cover the losses of a risk portfolio. The reason for this is that *EC* is calculated using internal models, adapts to the risk profile of each bank, and considers their risk appetite, as it is based on *QRMs*, which generalize the concept of value at risk *(VaR)*. In calculating *QRMs* (see Section 3), excess kurtosis and skewness must be considered characteristics of banks' risk portfolio components (commonly described in the financial literature) so that risks are not underestimated. The third pillar is associated with market discipline and complements the other two pillars by allowing market players to assess banks' capital adequacy.

Capital adequacy requirements (*CARs*) encompass both regulatory and economic capital. Basel II aims to establish more risk-sensitive minimum capital requirements so that regulatory capital is closer to a bank's economic capital (Caruana, 2005). According to the BCBS (1998), tier regulatory capital is divided into two components: (1) Tier 1 capital, or core capital, which includes equity capital and disclosed reserves, and (2) Tier 2 capital, or supplementary capital, which includes revaluation reserves, general provisions, hybrid capital instruments, and subordinated debt. *RC* and *EC* requirements are determined as a function of the risk portfolio. From a modeling and computational perspective, accurately calculating risk portfolios takes work (Wason et al., 2004). The risk of each module that makes up the risk portfolio can be measured, and these modules can be aggregated at different levels.

Greater disaggregation implies a more accurate, but also more complex measurement (Sandström, 2007). Assuming a multivariate normal distribution and a linear correlation between the risk modules to be aggregated, the solvency capital required to cover the

portfolio can be estimated as the α percentile. As described by Wason et al. (2004), this method coincides with the one used under the Solvency II guidelines in European Union law, which states that the solvency capital requirement must be sufficient for surviving extreme losses over a one-year horizon (with a minimum confidence level of 99.5%). The solvency capital requirement incorporates insurance, market, credit, operational, and counterparty risks and must be recalculated at least once a year.

From the regulatory perspective of the BCBS framework, the *CAR* establishes the proportion of *RC* required to support a certain amount of *RWA*s, which determines the value of the risk portfolio (consisting of credit, market, and operational risks), as expressed in Equation 1.

$$RWA = \sum_{i=1}^{n} w_i * asset_{i.} \quad (1)$$

Under the standard method, each source of risk (i) is multiplied by a standardized factor (w_i), which is expected to be conservatively set in each jurisdiction. In this weighted aggregation of the risk portfolio, correlations between assets are not considered, and relative weights (w_i) are assigned as arbitrary constants. Under Basel's internal models' approach, banks, subject to certain minimum conditions and disclosure obligations, can develop their internal estimates of risk components to determine the capital requirement for that position. Banks sometimes have to use a supervisory value instead of an internal estimate for one or more risk components (BCBS, 2004). The internal models approach assumes that the loss distributions are close to the normal distribution and consider correlations between assets. These correlations are defined in a regulatory manner for certain groups of assets. However, the assumption of a normal distribution of the risk portfolio components in finance and insurance is implausible because of the high occurrence of outliers and a high level of skewness (Wason et al., 2004).

For instance, Balthazar (2006) highlights the presence of heavy tails to the right of the loss distribution. Measuring the solvency risk of a bank's portfolio depends on measuring each portfolio component's risk, and the loss probability distribution estimation is fundamental. In the literature, it is common to find models that assume Gaussian distributions, such as those proposed by Merton (1973), Merton (1974), Vasicek (2002), Jiménez and Mencía (2009), Chava et al. (2011), Belkin et al. (1998), Frachot et al. (2001), and Shevchenko (2010), which, in most cases, underestimate risk by overlooking

the frequency of extreme events that cause distortions in the tails of the probability distributions.

Several studies have demonstrated that the normal distribution differs significantly from the distributions observed in the variables related to banks' financial risks. Regarding deviations from normality, Sandström (2007) analyzes the skewness of the probability distributions of the different components of a bank's risk portfolio and the effect of not parameterizing it using some underlying distribution. This author proposes using a Cornish–Fisher expansion to parameterize it and finds that if a normal multivariate risk distribution is assumed (without considering module skewness), the capital requirement can be well below the risk threshold when skewness is omitted. According to Bølviken and Guillen (2017), the accuracy of risk aggregation in solvency can be improved by recursively updating skewness when the risk of specific instruments is measured. For their part, Del Brio et al. (2009) demonstrate that Pearson's correlation coefficients differ depending on whether they are estimated under the assumption of normality or using SNP approaches. Le Maistre and Planchet (2013) show that the standard approach used in the Basel Framework to assess interest rate risk leads to biased risk measurement.

In the context of operational risk measurement, Dutta and Perry (2006), De Fontnouvelle et al. (2003), and Feria-Domínguez et al. (2015) reveal that the distributions of losses due to the materialization of operational risks exhibit skewness and have fat tails. Kretzschmar et al. (2010), Bateni et al. (2014), Madan (2009), and Wirch and Hardy (1999) study probability distributions in the estimation of both aggregated and disaggregated solvency risks and reported that skewness and kurtosis do not correspond to the parameters of a normal distribution.

To correct the distortions between the loss frequency distributions of the components of a bank's risk portfolio and the normal distribution, recent studies propose using *GC* expansions. These expansions were introduced by Edgeworth (1896) and have been widely studied and employed to approximate the probability curves of random variables in various scientific fields. Sargan (1975) introduced this methodology in SNP econometrics to approximate the confidence intervals of *t* ratios and concluded that these intervals are more accurate than the usual asymptotic confidence intervals for large samples. Since then, the use of *GC* expansions in econometrics has been expanded to model random variables that show significant deviations from the normal distribution. Jarrow and Rudd (1982), Lee (1984), Corrado and Su (1996), Mauleón and Perote (2000),

Jondeau and Rockinger (2001), Ñíguez and Perote (2012), and Brio and Perote (2012) are among those who use *GC* expansions in financial econometrics. In addition to the problems of skewness and excess kurtosis that arise in measuring financial portfolio risks, banking regulations can also negatively affect solvency risk.

II.3. Description of the Proposed Solvency Risk Measures and Estimation Methodology

The proposed methodology provides accurate probability measures to estimate the loss distribution and thus measure solvency risk. This measurement can be performed at different levels of aggregation of the solvency risk components. The *SDR* variable has the highest level of aggregation, which groups all the components of the risk portfolio and capital supporting it. The *TDR* and *PGR* variables have the first level of disaggregation.

II.3.1. Probability of Regulatory Intervention

Let η be the minimum *SR* at time *t*, defined by a banking regulator to cover unexpected losses in the risk portfolio. Thus, a bank must maintain a SR_t equal to or greater than η in order to avoid regulatory intervention $(SR_t \geq \eta)$.

SR_t is calculated by dividing $Tier_t$ by RWA_t; hence, at $t+1$, it can be expressed as in Equation 2.

$$SR_{t+1} = \frac{Tier_t * exp(-TDR_{t+1})}{RWA_t * exp(PGR_{t+1})} = \frac{Tier_t}{RWA_t * exp(PGR_{t+1} + TDR_{t+1})} \quad (2)$$

Because $SDR_{t+1} = PGR_{t+1} + TDR_{t+1}$, then $SR_t * e^{-SDR_{t+1}} \geq \eta$ must be satisfied to avoid regulatory intervention. Therefore, given a regulatory *SR*, (η), the maximum value that SDR_{t+1} can take is given by Equation 3.

$$RID_t = \ln(SR_t) - \ln(\eta). \quad (3)$$

where RID is the logarithmic regulatory intervention distance. Thus, the probability of regulatory intervention can be expressed as in Equation 4.

$$p(SDR_{t+1} > RID_t) = 1 - F_{SDR}(RID_t). \quad (4)$$

where F_{SDR} is the cumulative density function (*CDF*) of *SDR*. Therefore, if a decline in the *SR* is only due to an increase in the risk portfolio or tier capital, the probability of regulatory intervention is $1 - F_{PGR}(RID)$ for the risk portfolio component and $1 - F_{TDR}(RID)$ for the capital component. In this case, F_{PGR} and F_{TDR} are the *CDFs* of *PGR* and *TDR*, respectively.

The need for regulatory action against a bank with a *SR* below the regulatory minimum is justified by its solvency and the reputational risks involved.

II.3.2. Policies Based on Quantile Risk Metrics (QRMs)

The second pillar established by the Basel Committee requires the development of risk management policies based on measures that reflect banks' risk profile and appetite. Under this framework, *EC* should be estimated as a quantile of the *pdf* of losses in a bank's risk portfolio (*RWA*). The estimation of this quantile considers the bank's risk profile, which is reflected in the different parameters of the *pdf* (e.g., those that capture variance, skewness, and kurtosis), as well as its risk appetite associated with the loss probability (α) assumed in the decision-making process. Alexander (2009) defines quantile risk metrics (*QRMs*), for any α between 0 and 1, as the x_α quantile of the distribution of a continuous random variable (X) such that $P(X < x_\alpha) = \alpha$. $QRMs$ can be calculated using the quantile function (F_X^{-1}) of a given CDF F_x, as defined in Equation 5.

$$QRMs_\alpha = F_X^{-1}(\alpha) = \ inf\{x \in R: \alpha \leq F_X(x)\}. \quad (5)$$

Policies based on *QRMs* make it possible to set the minimum *SR* in which a bank can withstand the maximum expected shock, $F_X^{-1}(\alpha)$, which would reduce solvency if it falls below the minimum regulatory ratio (η). In general, random variable X is any source of risk on which banks' solvency depends, such as the *PGR*, the *TDR*, or the *SDR*. Let $SR_t^{\eta,\alpha}$ (*SR* based on QRMs) be the *SR* required to withstand the maximum expected shock, $F_X^{-1}(\alpha)$. Then, given a confidence level of $1 - \alpha$, it can be expressed as in Equation 6.

$$SR_t^{\eta,\alpha} = \eta * e^{F_X^{-1}(\alpha)}. \quad (6)$$

If the risk portfolio cannot be rebalanced, then *SR* will depend on an *EC* readjustment. Therefore, the *EC* that must be held at the beginning of period $t + 1$ to support $F_X^{-1}(\alpha)$

meets the following condition: $Tier_t \geq \eta * RWA_t * e^{F_X^{-1}(\alpha)}$. Thus, *EC* depends not only on the value of the risk portfolio and the minimum regulatory ratio (η) but also on the risk appetite (α) and the risk profile, which are reflected in F_X^{-1}.

II.3.3. Determination of the Probability Density Functions of PGR, TDR, and SDR

To measure the probability of regulatory intervention and establish policies based on $QRMs_\alpha$, the conditional *pdf* of the sources of solvency risk must be determined. For this purpose, we assume that ARMA and GARCH models, respectively, can determine the dynamics of the mean and variance. The estimation of the higher-order moments, however, requires specification of the full *pdf*, which we model with the *SNP* approach based on the *GC* expansion. For notational convenience, the *pdf* of a random variable *X* (representing any source of solvency risk) is defined in its standardized form (i.e., with location and scale parameters of 0 and 1, respectively).

Mean-variance model

We propose using ARMA models to calculate the mean of random variable ω because they are sensitive to short-term variations and capture the time-varying dependence patterns observed in the series under analysis. Let ω represent a random variable that captures any source of solvency risks, such as *PGR*, *TDR*, or *SDR*. The dynamics of these variables are characterized by the *ARMA(p,q)* model in Equation 7:

$$\omega_t = \phi_0 + \sum_{i=1}^{p} \phi_i \, \omega_{t-i} + \sum_{j=1}^{q} \theta_j \, a_{t-q} + a_t. \tag{7}$$

where ϕ is the autoregressive (AR) parameters; θ is the moving average (MA) parameters; and a is model errors. The conditional variance (σ_t) of errors is assumed to follow a GARCH(i,j) model, i.e.,

$$a_t = \sigma_t X_t. \tag{8}$$

where

$$\sigma_t = \sqrt{\alpha_0 + \sum_{i=1}^{m} \alpha_i a_{t-i}^2 + \sum_{j=1}^{s} \beta_i \sigma_{t-j}^2}. \tag{9}$$

and X_t is randomly distributed as a standard *GC pdf* as described below.

Gram–Charlier expansion

To introduce the *GC pdf*, we follow the methodology Davis (1976) and Kolassa (2006) used. They propose a model that considers high-order approximations of a density f_X of random variable X from a reference density f_Y of a random variable Y. We define $X = Z + Y$, where Z is a pseudovariate with a zero mean and variance (because the mean and variance of X and Y are assumed to be equal) with the same higher-order cumulants ($k_3, k4, \ldots$) as X, which contain the corresponding information about the distortions of f_X with respect to the normal distribution. Z and Y are orthogonal, which implies that they are linearly independent.

Let $Z = \frac{\sum_{j=1}^{n} Y_j}{\sqrt{n}}$ be the standardized sum of independent and identically distributed (i.i.d.) n variables ($Y_1, Y_2, Y_3, \ldots, Y_n$). Then, its characteristic function, $\zeta(u)$, defined as the Fourier inverse transform of a μ probability measure into R^n, can be written as in Equation 10.

$$\zeta(u) = \int e^{i(u,\vartheta)} \mu(d\vartheta). \tag{10}$$

where i is the imaginary unit. Hence, the characteristic function of Z is $\varphi_Z(u) = E[e^{i(u,Z)}] = \int e^{i(u,z)} f_Z(dz)$, where f_Z is the *pdf* of Z and always exists because they are just Fourier transforms of the probability measures (Jacod & Protter, 2012). By conditioning $Z = z$, X has a *pdf*, and by expanding f_Y as a Taylor series, we have $f_Y(x - z) = \sum_{j=0}^{\infty} f_Y^{(j)}(x)(-z)^j/j!$. Thus, according to Kolassa (2006), the unconditional density of X is given by Equation 11.

$$f_X(x) = \sum_{j=0}^{\infty} f_Y^{(j)}(x) \frac{(-1)^j \mu_j^*}{j!}. \tag{11}$$

where μ_j^* denotes the moments of Z that need to be added to Y to obtain X. Furthermore, the jth-order cumulant (k_j^*) associated with Z is the cumulant j of X minus the corresponding cumulant of Y. Multiplying $f(x)$ by $f_Y(x)$ in the numerator and the denominator, we obtain the following equation:

$$f_X(x) = \frac{f_Y(x) \sum_{j=0}^{\infty} f_Y^{(j)}(x)(-1)^j \mu_j^*}{j! f_Y(x)}, \text{ and}$$

by defining $h_j = \frac{(-1)^j f_Y^{(j)}(x)}{f_Y}$, it can be expressed as

$$f_X(x) = \frac{f_Y(x)\sum_{j=0}^{\infty} h_j(x)\mu_j^*}{j!}. \quad (12)$$

h_j is the ratio between $f_Y^{(j)}$, which is the jth-order derivative of the weight function f_Y, and f_Y. If f_Y is the normal density *pdf*, $\phi(x)$, then h_j corresponds to the polynomial functions known as Hermite polynomials (HPs), which are orthogonal to $\phi(x)$. The infinite series in terms of HPs express a function $\theta(x)$ such that $\theta(x) = \sum_{j=1}^{\infty} \delta_j h_j$, where δ_j is given by Equation 13.

$$\delta_j = \frac{1}{j!}\int_{-\infty}^{\infty} h_j(x)\phi(x)dx. \quad (13)$$

In addition, f_X and $\phi(x)$ have the same mean and variance.

h_j is given by:

$$h_j = \frac{(-1)^j\left[\frac{d^j}{dx^j}e^{\frac{-x^2}{2}}\right]}{e^{\frac{-x^2}{2}}}. \quad (14)$$

The orthogonality condition is satisfied such that:

$$\int_{-\infty}^{\infty} h_j(z)h_i(z)\phi(x) = 0, \quad \forall j \neq i. \quad (15)$$

According to Equation 15, *HPs* represent an orthogonal basis for weight function $\phi(x)$. In the empirical application of the model, this property of orthogonality with respect to the weight function makes it possible to truncate the *HP* series to an order n, thus defining a family of functions as in Equation 16. Because of this orthogonality property, this family defines the *GC pdf*s in regions that were recently described by Wu et al. (2020).

$$f_{X,n}(x) = \frac{\phi(x)\sum_{j=0}^{n} h_j(x)\mu_{j,n}^*}{j!}. \quad (16)$$

This expansion density may also be characterized in terms of *CDFs*. In particular, F_Y and F_X are the *CDFs* of f_Y and f_X, respectively. Then, F_X can be approximated as follows:

$$F_X = F_Y(x) - f_Y(x)\sum_{j=1}^{\infty} h_{j-1}(x)\mu_j^*/j!. \quad (17)$$

If the weight function is the normal density $\phi(x)$, with *CDF* denoted by $\Phi(x)$, the *CDF* is given by Equation 18.

$$F_{X,n} = \Phi(x) - \phi(x)\sum_{j=1}^{n} h_{j-1}(x)\mu_{j,n}^*/j!. \quad (18)$$

For convenience, moments μ_j^* are replaced with cumulants k_j^*, and it is usually assumed that $\mu_{0,n}^* = 1$, $\mu_{1,n}^* = \mu_{2,n}^* = 0$. Thus, $f_{X,n}(x) = g(x;d)$ is expressed as in Equation 19, as stated by Cortés et al. (2016) and other authors.

$$g(x;\boldsymbol{d}) = \left[1 + \sum_{j=3}^{n} d_j\, h_j(x)\right]\phi(x). \quad (19)$$

In Equation 19, the vector of parameters $\boldsymbol{d} = (d_1, d_2, , \ldots, d_n,)$ contains the corresponding information about the distortions of f_X with respect to the normal distribution $\phi(x)$ and guarantees that $g(x;d) \geq 0\ , \forall x \in \mathbb{R}$. The *GC* series can accurately approximate the sample distribution as f_X because $\lim_n g(x;d) = f_X$. In practice, most applications of this distribution include only third- and fourth-order *HPs*, which are related to skewness and excess kurtosis (Del Brio and Perote, 2012), i.e.,

$$g(x;d_3,d_4) = [1 + d_3(x^3 - 3x) + d_4(x^4 - 6x^2 + 3)]\phi(x). \quad (20)$$

Estimation of Gram–Charlier Parameters

In most applications of *GC* expansions, parameters are estimated with the maximum likelihood (ML) method. Assuming that the first two moments of the distribution are well specified, the global optima guarantees that $g(x;\boldsymbol{d})$ is positive. Del Brio and Perote (2012) compare parameter estimation via the *ML* method using the method of moments *(MM)* and conclude that both methods provide similar results. However, the *MM* can only guarantee positive values for $g(x;\boldsymbol{d})$ in the asymptotic expansion and does not ensure positivity when the series is truncated with few terms. In our applications, we use the *ML* method and expand the series until the fourth moment to capture skewness and kurtosis. Thus, for a sample size *T*, the log-likelihood function, $log(L)$, is given by Equation 21:

$$log(L) = -\frac{T}{2}log(2\pi) - \frac{1}{2}\sum_{t=1}^{T} l\,og(x_t^2) + \sum_{t=1}^{T} l\,og\left(\left[1 + \sum_{j=3}^{n} d_j\, h_j(x_t)\right]\right). \quad (21)$$

II.4. Case study

This section applies the methodology proposed in this study to measure the solvency risk of the Colombian banking system, emphasizing the period at the beginning of the COVID-19 pandemic, in which an extraordinary monetary policy regime was applied to mitigate the impact of the lockdown on the local economy. This case study allows us to analyze the impact of the application of this extraordinary monetary policy regime on the risk of regulatory intervention due to the solvency deficit of the banks used as a transmission channel.

We collected monthly data on the solvency of fifteen banks in Colombia from January 2002 to November 2021.[2] In the sample under analysis, 60% of the banks are international banks that hold more than 80% of total domestic banking assets. Colombian banking regulations are currently transitioning from Basel II to Basel III. Hernández et al. (2018) provide a general overview of the implementation of Basel III standards in Colombia and highlight the need to add a capital conservation buffer of 2.5%, a countercyclical buffer between 0% and 2.5%, and a systemic buffer between 1% and 3.5% for minimum solvency of 9%, as established by Basel III. With this adjustment, the minimum *SR* of some financial institutions could reach 16.5%. To analyze solvency in Colombia, we calculated *Tier* capital by adding up the capital of all the banks in the sample, and *RWA* was calculated by adding up the portfolio, i.e., $Tier = \sum_{j=1}^{K} Tier_j$ and $RWA = \sum_{j=1}^{K} RWA_j$, where $Tier_j$ and RWA_j are the capital and portfolio of bank j, respectively, and K is the aggregate number of banks.

COVID-19 Monetary Policy Measures

Cantú et al. (2021) present a global database of central banks' monetary responses to COVID-19 and divide them into five types of tools: interest rate measures, reserve policies, lending operations, asset purchase programs, and foreign exchange operations. Table II.1 reports the number of monetary policy announcements by the central bank of Colombia at the beginning of the COVID-19 pandemic (March, April, May, and June 2020). It announced four asset purchases, eleven foreign exchange operations, twelve lending operations, and one reserve policy. These measures adopted by the central bank

[2] The database is available on the website of the Superintendencia Financiera de Colombia (Financial Superintendence of Colombia, https://www.superfinanciera.gov.co/jsp/index.jsf/), which is responsible for regulating the Colombian banking system.

to inject liquidity into the economy sought to protect the payment system, maintain the credit supply, stabilize key markets under pressure, and stimulate economic activity. Asset purchase operations comprised public and private debt securities and swaps of public debt securities with the Colombian government, delivering short-term debt securities and receiving long-term debt securities. A new exchange rate hedging mechanism was adopted through non-deliverable forwards. US dollars were auctioned in swaps (FX Swaps), in which the Central Bank sells dollars in cash and will buy them in futures contracts (at 60 days), and IMF approved a successor two-year arrangement for Colombia under the flexible credit line (FCL), designed for crisis prevention.

Table II.1 Monetary responses by the central bank of Colombia to COVID-19

Row labels	Asset purchases	Foreign exchange operations	Lending operations	Reserve policies
Mar	2	4	5	0
Apr	1	2	3	1
May	1	3	2	0
Jun	0	2	2	0
Total	4	11	12	1

Notes: This table reports the number of monetary policy announcements by the central bank of Colombia at the beginning of the COVID-19 pandemic (March, April, May, and June 2020).
Source: Cantú et al. (2021).

In lending operations, private debt was allowed, new access to the central bank's transitory repurchase agreements was expanded, and definitive expansion auctions were conducted using public and private debt instruments, among other measures. Among the reserve policies, reserve requirements for liabilities were reduced.

Table II.2 lists the changes and targets of the interest rate measures adopted in Colombia from March 2020 to December 2021. In March 2020, the annual interest rate was 4.25%, and in September 2020, it fell to a historic low of 1.75%.

Table II.2 Interest rates in Colombia during the COVID-19 period

Date	Variation	Target
03/29/20		4.25%
03/30/20	-0.50%	3.75%
05/04/20	-0.50%	3.25%
06/01/20	-0.50%	2.75%
07/01/20	-0.25%	2.50%
08/03/20	-0.25%	2.25%
09/01/20	-0.25%	2.00%
09/28/20	-0.25%	1.75%
10/01/21	0.25%	2.00%
11/02/21	0.50%	2.50%
12/20/21	0.50%	3.00%

Notes: This table presents the variations and targets of the interest rate measures adopted in Colombia from March 2020 to December 2021.
Source: Authors' calculations based on data from the central bank of Colombia (https://www.banrep.gov.co/es/estadisticas/tasas-interes-politica-monetaria/).

Figure II.1 Monthly time series of the aggregate solvency ratio (SR) (a), tier capital (b), and risk-weighted assets (RWAs) (c) in the Colombian banking system

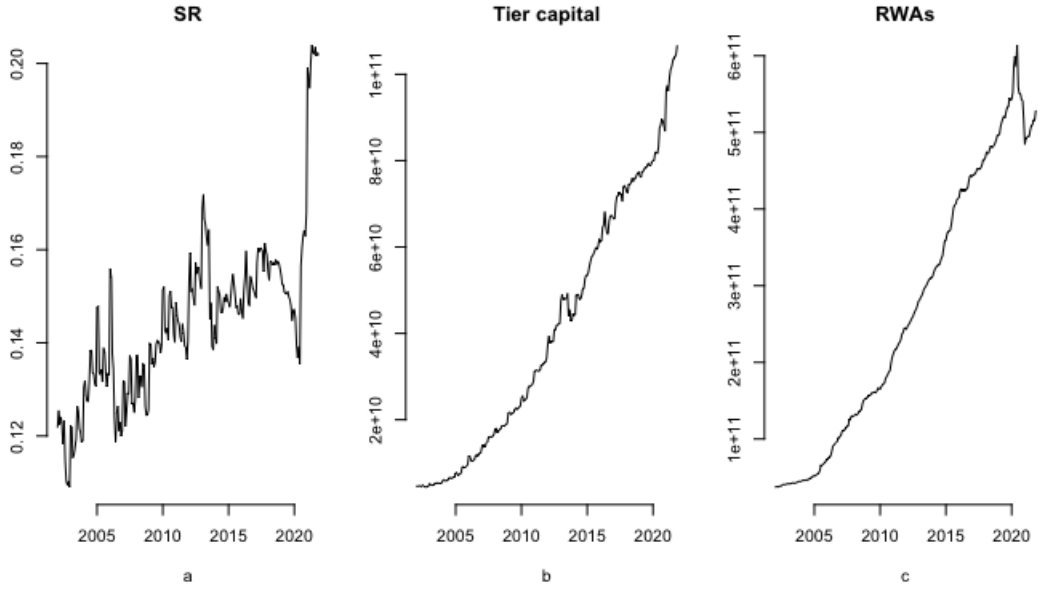

Figure II.1 illustrates the evolution of the *SR*, tier capital, and *RWA* in Colombia from 2005-2020. In Figure II.1a, *SR* trended upward and reached a peak (17%) in February 2013. In 2017, it reached a value close to 16% and then decreased to 14.5% in February 2020. In March 2020, the central bank of Colombia began to implement monetary policy measures to mitigate the effects of COVID-19 on its economy, which caused the banking system's solvency to fall to 13.6%. These trends have yet to be observed since the end of 2013. From February to June 2020, *SR* decreased by more than 7%, whereas *RWAs* increased by almost 10% (Figure II.1c). Tier capital (Figure II.1b) showed no significant changes at the beginning of the COVID-19 pandemic. An increase in *RWAs* without an increase in tier capital led to a marked decline in solvency.

Table II.3 shows the correlations between *PGR*, *TDR*, and *SDR*, in which the correlation is much greater between *SDR* and *TDR* than between *SDR* and *PGR*, which implies that solvency is more sensitive to variations in tier capital than to variations in the risk portfolio. The low correlation (negative sign) between *PGR* and *TDR* suggests that tier

capital does not increase as the value of the risk portfolio increases. It also indicates that the conversion of tier capital to *RWAs* does not always occur in the same period.[3]

Table II.3 Correlation matrix of the variations in the components of SR

	PGR	TDR	SDR
PGR	1.000	-0.065	0.402
TDR	-0.065	1.000	0.888
SDR	0.402	0.888	1.000

Note: This table presents the correlations between *PGR*, *TDR*, and *SDR*.
Source: Authors' calculations based on data from the Financial Superintendence of Colombia.

Table II.4 presents the basic descriptive statistics on *PGR*, *TDR*, and *SDR*, in which the average monthly growth rate of *RWAs* was 1.1% and that of tier capital was 1.3%, indicating that tier capital grew in proportion to risk. However, the standard deviation of *TDR* was higher than that of *PGR*, and the mean of *SDR* was close to zero. The positive excess kurtosis in all the time series suggests the presence of fat tails. *PGR* skewed to the right, whereas *TDR* and *SDR* skewed to the left

Table II.4 Descriptive statistics

	Min	Max	Mean	Std. deviation	Skewness	Excess kurtosis	q5	q10	q90	q95
PGR	-0.093	0.112	0.011	0.018	0.192	11.179	-0.006	-0.003	0.026	0.037
TDR	-0.180	0.113	-0.013	0.035	-1.054	4.942	-0.081	-0.050	0.015	0.031
SDR	-0.170	0.124	-0.002	0.038	-1.006	4.216	-0.069	-0.040	0.030	0.054

Note: This table presents the descriptive statistics of *PGR*, *TDR*, and *SDR*.
Source: Authors' calculations based on data from the Financial Superintendence of Colombia.

Figure II.2 shows both time-varying patterns in the mean (given the frequency of the reported financial statements) and volatility clusters in the time series. In March, April, and June 2020, *RWAs* had positive shocks, which represented an increase of more than 12% over the January levels, followed by a fall of 9.25% in July 2020 (which was the maximum historical negative variation) and a cumulative drop of almost 24% by January 2021. According to the Q-Q plots of *PGR*, *TDR*, and *SDR* (Figures II.2b, 2e, and 2h), the quantile of the normal distribution was close to that of the frequency distribution, whereas the right and left tails of the frequency distribution were fatter than those of the normal distribution. Regarding dispersion in the time series, the *SDR* time series (Fig. 2d) had

[3] The cross-correlation diagram in Appendix Figure II.1 shows that the highest correlation between PGR and capital CDR occurs at lags 5 and 10, which means that tier capital adjustments are five months ahead of the variations in this component. However, a high correlation is also observed in period -2, which means that some increases in the risk portfolio are compensated by capital increases two months later.

volatility clusters. The autocorrelation function (ACF) correlograms (Figs. 3c, 3f, and 3i) show that the most significant autocorrelations are those of orders 6, 12, and 18.

Figure II.2 Monthly time series, Q-Q plot, and correlogram of portfolio growth rate (PGR) (a, b, c), tier decline rate (TDR) (d, e, f), and solvency decline rate (SDR) (g, h, i)

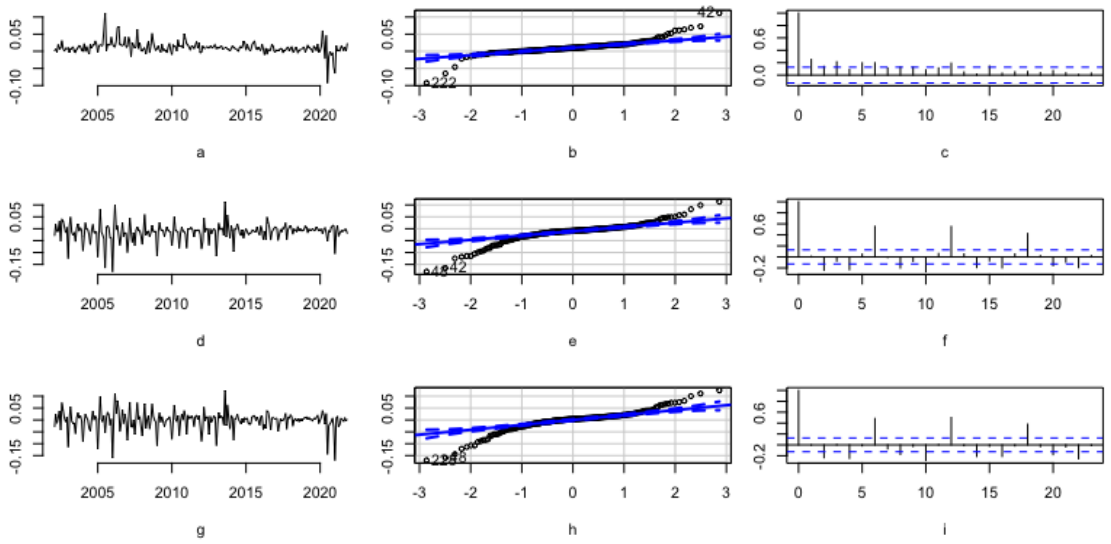

Figures II.2a, 2d, and 2g show potential Additive Outliers that, according to Franses & Haldrup (1994), can produce spurious stationarity, thus rejecting the null hypothesis of the presence of unit roots. Haldrup et al. (2005) point out that outliers can severely affect the inference of seasonal unit roots depending on their frequency, magnitude, and persistence. To control the effect of Additive Outliers on unit root tests, we apply the approach described by Chen & Liu (1993) and computationally implemented in Lopez-de-Lacalle (2019). Under this approach, outliers are detected in the series in levels through the t-statistics associated with the parameters that measure the effect of the outliers modeled from the incorporation of dummy variables in the estimation of the ARMA model used in the unit root tests. Perron & Rodriguez (2003) demonstrate, through simulations, that the test on the variable in levels is appropriate for detecting a single outlier under the null hypothesis of no outliers. Still, it can yield excessive outliers when applied iteratively to select multiple outliers. The outliers must have enormous values for the power of the test to be acceptable. As an alternative, they offer a methodology based on the first difference in the data. This alternative presents a better test power, but compared to the procedure based on the data series in levels, it has the

disadvantage that the limiting distribution depends on the specific distribution of the model errors.

Figure II.3 Monthly time series adjusted for additive outliers and outliers' effects of portfolio growth rate (PGR) (a), tier decline rate (TDR) (b), and solvency decline rate (SDR) (c)

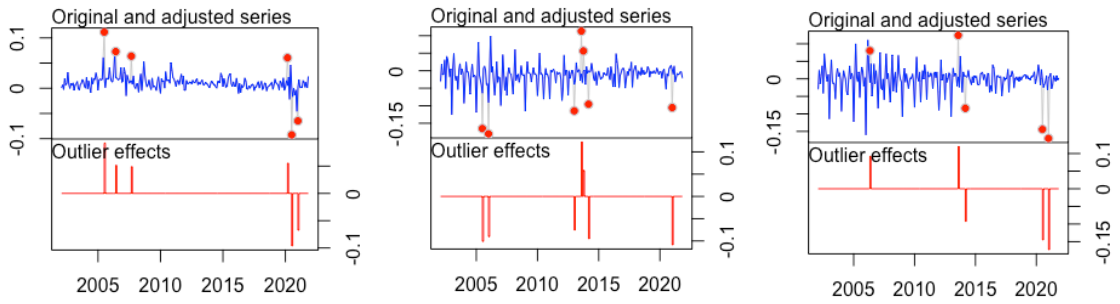

(a) (b) (c)

Figure II.3 presents the time series adjusted by Additive Outliers and the effects of the PGR, TDR, and SDR outliers. The PGR time series presents four positive outliers in July 2005, June 2006, September 2007, and March 2020 and two negative outliers in July 2020 and January 2021. The TDR time series presents five negative outliers in July 2005, January 2006, January 2013, March 2014, and January 2021, and two positive outliers in August and October 2013. The SDR time series presents four negative outliers in January 2013, March 2014, July 2020, and January 2021, and one positive outlier in August 2013. The outliers in 2020 and 2021 are related to the implementation of monetary policy during COVID-19 and to prudential policy adjustments aligned with the regulatory framework established in Basel III.

Table II.5 presents the results of the unit root tests for the PGR, TDR, and SDR time series adjusted for Additive Outliers. The classical Augmented Dickey-Fuller test was performed, with one lag selected by the BIC criterion. However, the hypothesis of the existence of unit roots is rejected, given the seasonal behavior of the analyzed series. The DF-GLS test, proposed by Elliott et al. (1996), improves the power of the test by taking into account the serial correlation of the error term, and the HEGY test proposed by Hylleberg et al. (1990), which tests for the presence of seasonal unit roots, are also displayed. Drift was included in both tests. The DF-GLS test's lag selection was performed using the BIC criterion. Elliott et al. (1996) indicate that this criterion

represents a reasonable trade-off between size and power. The selection of the number of lags for the HEGY test is based on the AIC criterion since, according to Barrio Castro et al. (2016), this criterion provides a more reliable size than lag selection methods based on hypothesis testing or the BIC criterion. At the 1% significance level, all hypotheses stating the presence of unit roots are rejected, except for the Hd hypothesis of the HEGY test stating the existence of unit roots of the quarterly seasonal component, where the rejection of the hypothesis is done at a 10% significance level. The Ljung-Box serial autocorrelation test reveals autocorrelation in all three series.

Table II.5 Unit Root tests

	p-value (PGR)	p-value (TDR)	p-value (SDR)
Augmented Dickey-Fuller			
y_{t-1}	0.000	0.000	0.000
ADF-GLS			
y_{t-1}	0.001	0.000	0.000
HEGY			
Ha	0.053	0.059	0.003
Hb	0.000	0.000	0.000
Hc	0.000	0.000	0.000
Hd	0.000	0.095	0.064
He	0.000	0.001	0.001
Hf	0.000	0.019	0.034
Hg	0.000	0.000	0.000
Ljung-Box			
X-squared	0.000	0.000	0.000

Note: This table presents the p-values of the Augmented Dickey-Fuller, DF-GLS, and HEGY unit root tests and the Ljung-Box autocorrelation test of PGR, TDR, and SDR. The Augmented Dickey-Fuller test and ADF-GLS test include drift, and the number of lags is selected using the BIC criterion (1 lag for three variables in the Augmented Dickey-Fuller test and four lags for the three variables in the ADF-GLS test). The HEGY test includes drift, and the number of lags is selected using the AIC criterion. The presence of unit roots is tested with the corresponding null hypotheses: Ha: non-seasonal unit root, Hb: bi-monthly unit root, Hc: unit root for four-month periods, Hd: quarterly unit root, He: semi-annual unit root, Hf: root a the frequency $5\pi/6$, Hg: annual unit root. The Ljung-Box test was performed on 20 lags.
Source: Authors' calculations based on data from the Financial Superintendence of Colombia.

To analyze potential structural changes in the mean and variance of the models, we used the methodology proposed by Bai & Perron (1998) on the Additive Outliers adjusted time series of PGR, TDR, and SDR. Table II.6 presents the values obtained from the BIC criterion to detect between 0 and 5 break points in the mean and variance of the analyzed series. Since the data-generating process is assumed to be an ARMA process, lags up to order 12 were used as regression variables for the mean. The variance was estimated as the square of the errors of the mean model, and only structural level changes from a constant were considered. The BIC criterion states that the models should include no structural changes for both mean and variance.

Table II.6 Structural Changes detection

Breakpoints		0	1	2	3	4	5
	mean	-1.29E+03	-1.25E+03	-1.20E+03	-1.14E+03	-1.08E+03	-1.01E+03
BIC (PGR)	variance	-2.96E+03	-2.96E+03	-2.95E+03	-2.94E+03	-2.93E+03	-2.92E+03
	mean	-1.08E+03	-1.04E+03	-9.91E+02	-9.40E+02	-8.86E+02	-8.24E+02
BIC (TDR)	variance	-2.65E+03	-2.65E+03	-2.64E+03	-2.63E+03	-2.62E+03	-2.61E+03
	mean	-1.01E+03	-9.65E+02	-9.13E+02	-8.51E+02	-7.89E+02	-7.26E+02
BIC (SDR)	variance	-2.50E+03	-2.49E+03	-2.49E+03	-2.48E+03	-2.47E+03	-2.46E+03

Note: This table presents the value of the BIC criterion for the Bai and Perron test to detect between 0 and 5 breakpoints in the mean and variance parameters of PGR, TDR, and SDR. For the mean, lagged regressors up to order 12 were used as regression variables. The variance is estimated from the square of the errors obtained from the mean model with regressors lagged up to order 12, and level changes are analyzed from a constant.

II.5. Results

II. 5.1 Fitted distribution

Table II.7 lists the estimated parameters of the conditional moments of the probability distributions of *PGR*, *TDR*, and *SDR*. In the three-time series, the mean had significant time-varying patterns in quarterly multiples (3, 6, and 12 months). Additionally, *PGR* had an autoregressive effect on order 1. The estimated variances correspond to the ARCH(2) process for *TDR* and *SDR* (parameters a0, a1, and a2) and the ARCH (1) process for *PGR* (parameters a0 and a1). The kurtosis parameters for *GC* were significant for the three series, whereas skewness was significant only for *PGR*.

Table II.7 Fitted conditional densities of the ARMA-GARCH model under a GC probability distribution

PGR parameters					*TDR parameters*					*SDR parameters*				
	Estimate	Std. error	t-value	p-value		Estimate	Std. error	t-value	p-value		Estimate	Std. error	t-value	p-value
ar1	0.225	0.062	3.610	<.0001***	ar6	0.203	0.056	3.629	<.0001***	ar6	0.284	0.059	4.856	<.0001***
ar3	0.183	0.062	2.936	0.003***	ar12	0.692	0.067	10.314	<.0001***	ar12	0.400	0.061	6.555	<.0001***
intercept	0.007	0.001	4.743	<.0001***	ma12	-0.418	0.089	-4.686	<.0001***	a0	0.001	0.000	11.696	<.0001***
a0	0.000	0.000	16.470	<.0001***	a0	0.000	0.000	8.477	<.0001***	a1	0.000	0.058	0.000	1.000
a1	0.508	0.066	7.649	<.0001***	a1	0.517	0.089	5.814	<.0001***	a2	0.113	0.062	1.840	0.066*
d3	0.091	0.034	2.645	0.008***	a2	0.149	0.056	2.673	0.008***	d4	0.129	0.015	8.560	<.0001***
d4	0.119	0.014	8.400	<.0001***	d4	0.094	0.015	6.388	<.0001***					

Notes: This table presents the estimated parameters of the portfolio growth rate (*PGR*), tier decline rate (*TDR*), and solvency decline rate (*SDR*) under an ARMA-GARCH with Gram–Charlier distributed errors. *, **, and *** significant at the 10%, 5%, and 1% levels, respectively. The ARMA-GARCH models were selected based on AIC.

Figures II.4a, 4c, and 4e compare the fit of the *GC pdf* to the *PGR*, *TDR*, and *SDR* series, respectively, to the normal fit. The *GC pdfs* captured the fat tails of the frequency histograms and the right-tail skewness of *PGR*. Figures II.4b, 4d, and 4f compare the *GC CDF*s of *PGR*, *TDR*, and *SDR* to their normal counterparts. For *PGR*, the differences between the *CDF* of the *GC* and the normal in the left tail were less pronounced than in the right tail. This difference between the right and left tails was not marked for TDR and the SDR.

Figure II.4 Comparison between the frequency histograms of the standardized residuals of the mean model, the normal (solid line), and GC (dotted line) probability density functions of portfolio growth rate (PGR), tier decline rate (TDR), and solvency decline rate

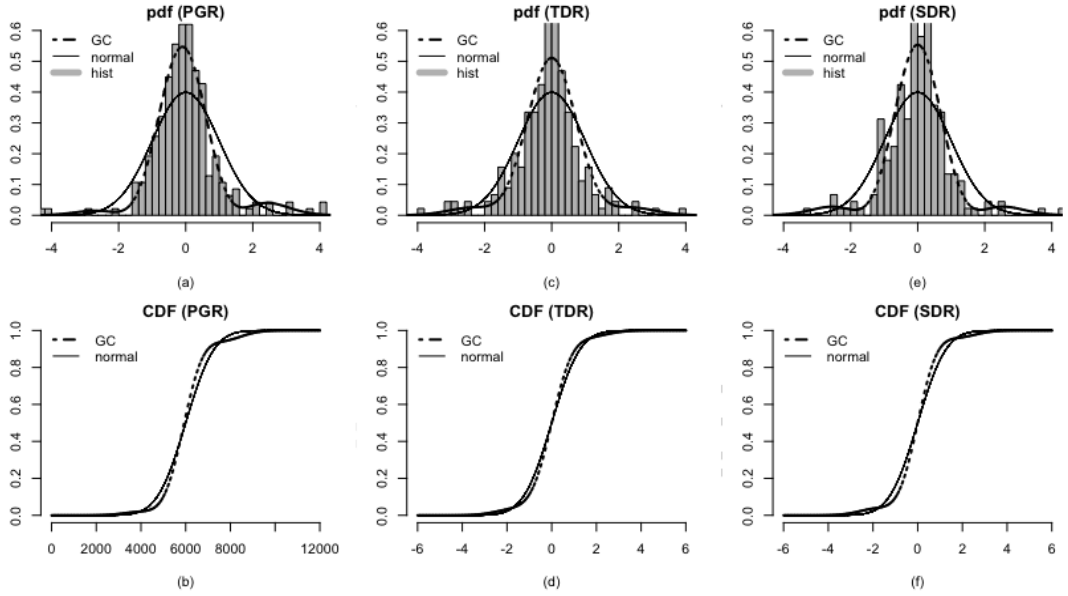

II. 5.2 Performance Testing

We used Kupiec's and Lopez's tests to measure and compare the performance of the QRMs estimated using a *GC pdf* and a normal *pdf* for PGR, TDR, and SDR. Table II.8 presents the results of both tests. According to the results, Kupiec's test only rejected the normal model for TDR, which compares the theoretical and empirical quantiles through a ratio comparison hypothesis test. Meanwhile, the results of Lopez's test, which considers the distance between the estimated *QRMs* and the exceptions observed, revealed that the score obtained was lower when using a *GC* distribution than when using a normal distribution in all the series: the scores obtained were 50% lower using *GC pdf*s than with normal *pdf*s for *TDR* and *SDR* and 40% lower for *PGR*.

Table II.8 Forecasting performance tests under Gram–Charlier and normal distributions

Component	p-value Kupiec's test Gram–Charlier	p-value Kupiec's test Normal	Score Lopez' test Gram–Charlier	Score Lopez' test Normal	p-value log-likelihood ratio test
PGR	0.865	0.376	4	7.002	<.0001
TDR	0.403	0.075	2.001	4.003	<.0001
SDR	0.303	0.321	1.002	4.004	<.0001

Note: This table reports the log-likelihood ratio (LR) between the normal and Gram–Charlier *pdfs*, and the results of Kupiec's and Lopez's tests, which were used in this study to measure the performance of the *QRMs* estimated using *GC* and normal distributions.

Table II.8 also reports the log-likelihood ratio *p*-value between the normal and *GC pdfs* for *PDR, TDR,* and SDR. In both cases, the results show strong evidence favoring the *GC* model. This log-likelihood ratio test confirmed that incorporating the d_s parameters is critical and enables the *GC* model to outperform the normal model. This evidence reinforces the flexibility of the model to dynamically adapt skewness and kurtosis (and higher-order parameters, if necessary) to the new scenarios (structural breaks) triggered by extreme events, such as those produced by the COVID-19 crisis and the monetary policy unconventional measures in response to them.

II. 5.3 Measuring the Impact of COVID-19 Monetary Policy Measures on Solvency Risk

Table II.9 reports the estimated *GC* quantiles associated with *SDR, PGR,* and *TDR* during the implementation of COVID-19 monetary policy measures in Colombia. The measures adopted in March 2020 increased the risk portfolio by 6.04% (exceeding the 99th percentile of the F_{PGR} and a decline in the solvency of 3.9% (exceeding the 94th percentile of the F_{SDR}. This increase is associated with the twelve monetary policy measures that were implemented. For instance, the repo operations quota was increased by 38 percent. Also, the term for repo operations was extended from 30 to 90 days. Moreover, the purchase operations for the permanent injection of liquidity totals COP 2 trillion in private securities and COP 2 trillion in public securities, and the intervention rate was cut by half a percentage point.

Table II.9 Quantiles associated with SDR, PGR, and TDR

Date	Quantile_SDR	Quantile_PGR	Quantile_TDR
01/01/20	42.11%	40.87%	26.10%
02/01/20	61.84%	71.47%	47.78%
03/01/20	94.32%	99.92%	27.86%
04/01/20	74.53%	55.17%	54.00%
05/01/20	15.12%	0.80%	73.13%
06/01/20	91.61%	91.60%	19.47%
07/01/20	0.00%	0.02%	1.84%
08/01/20	8.97%	54.52%	44.63%
09/01/20	24.03%	12.08%	38.47%
10/01/20	22.36%	43.30%	70.26%
11/01/20	59.02%	34.57%	80.24%
12/01/20	7.51%	0.05%	89.78%
01/01/21	0.02%	3.39%	0.12%

Note: This table reports the estimated *GC* quantiles associated with *SDR*, *PGR*, and *TDR* during the implementation of COVID-19 monetary policy measures in Colombia.

Solvency fell to its lowest value during the pandemic in June 2020, when all the other COVID-19 monetary policies had been implemented. From May to June 2020, it declined by 2.7% (which corresponds to the 92nd percentile of CDF_{SDR} because of an increase in $RWAs$ of 4.6% (which corresponds to the 92nd percentile of CDF_{PGR}. In July 2020, the risk portfolio decreased by 9%, which was below the first percentile of CDF_{PGR}, and coincided with the extension of the maturity period of the March repos to 90 days. Tier capital increased by more than 5% (which corresponds to the second percentile of CDF_{TDR}. A decrease in the risk portfolio and an increase in tier capital led to an increase in the solvency of more than 14%, from 13.5 to 15.7 percentage points (this variation was below the first percentile of CDF_{SDR}. The value of the risk portfolio continued to fall through January 2021. *PGR* values were below the first percentile of CDF_{PGR} by December 2020 and below the fourth percentile by January 2021. Tier capital increased by more than 10% in January 2021, which was below the first percentile of CDF_{TDR}. These risk portfolio and tier capital variations resulted in a 17% increase in solvency, bringing *SR* to nearly twenty percentage points. The increases in tier capital are associated with an increase in the capital required to face shocks as a result of the early adoption of the Basel III framework by twelve of the banks under analysis, which is equivalent to 30.24% of the equity margin at the end of 2020.

II. 5.4 Probability of Regulatory Intervention

Figure II.5a shows the probability of regulatory intervention for different values of η over different periods during the COVID-19 crisis. Values of η of more than 9% were analyzed, considering the capital conservation and countercyclical buffers that must be added to abide by Basel III requirements. From January to April 2020, the curve shifts to the left, increasing the probability of regulatory intervention for different values of η. Beginning in July 2020, the curve shifts to the right. By January 2020, the probability of regulatory intervention was nearly zero for η all the values under analysis. For $\eta < 13\%$, the probability of regulatory intervention was nearly zero for all the periods under analysis. For η >13%, the probability of regulatory intervention was critical between March and June 2020, as shown in Figure II.5b, between 2.6% and 4.6% when estimated using a *GC CDF* (solid line) and between 0.7% and 5.9% when estimated using a normal *CDF* (dashed line). In most periods, the probability of regulatory intervention estimated using a normal *CDF* was below that when estimated using a *GC CDF*, except in April and June 2020, when the probability estimated using a normal *CDF* exceeded that estimated using a *GC CDF*.

Figure II.5 (a) Comparison of the probability of regulatory intervention estimated using the GC CDF for different regulatory solvency levels over different periods during the COVID-19 crisis. (b) The probability of regulatory intervention was estimated using a GC C

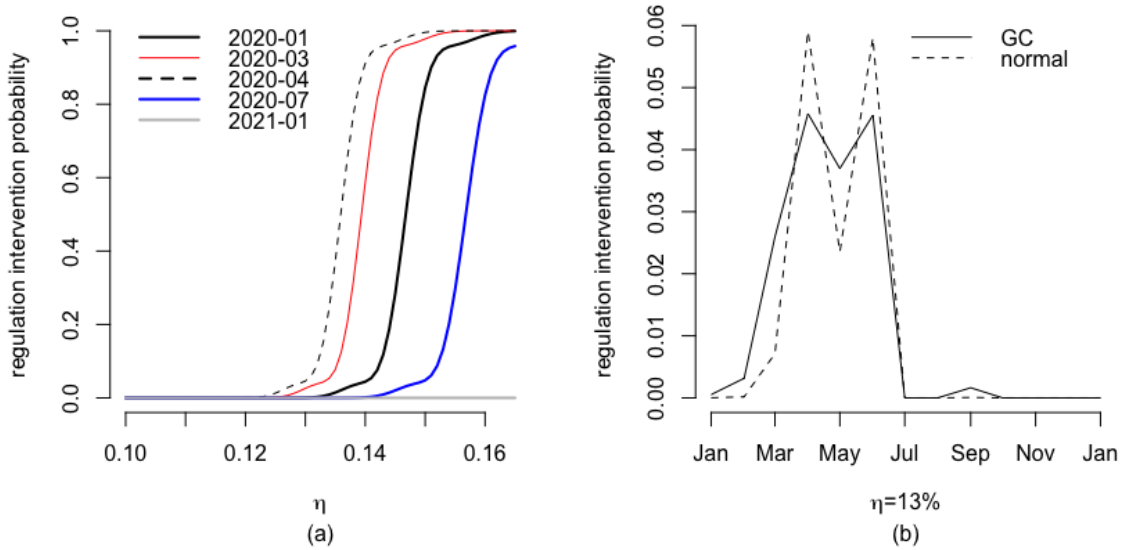

II. 5.5 Solvency Ratio Based on Quantile Risk Metrics over SDR

Based on the parameters estimated for the probability distributions of *SDR*, we calculated the *QRM-based SR*, which provides estimated scenarios involving banks' solvency loss, given a risk appetite α. Figure II.6 compares the monthly observed *SR* time series and the *QRM-based SR* estimated using a *GC CDF* (dashed black line) and a normal *CDF* (dashed blue line). Until the COVID-19 lockdown (February 2020), the observed *SR*s remained above the *QRM-based SR*. In March, April, May, and June 2020, when the COVID-19 monetary policy measures began to be implemented, the solvency observed fell below the *QRM-based SR*. The average difference between the *QRM-based SR* estimated using a *GC CDF* and that estimated using a normal *CDF* was 0.3 percentage points.

Figure II.6 Comparison between the monthly observed SR time series (solid line) and the QRM-based SR estimated using a GC CDF (dashed black line) and a normal CDF (dashed blue line) for a minimum regulatory solvency ratio (SR) of 13% (with a confidence level of 99% 99%) between January 2015 and December 2020

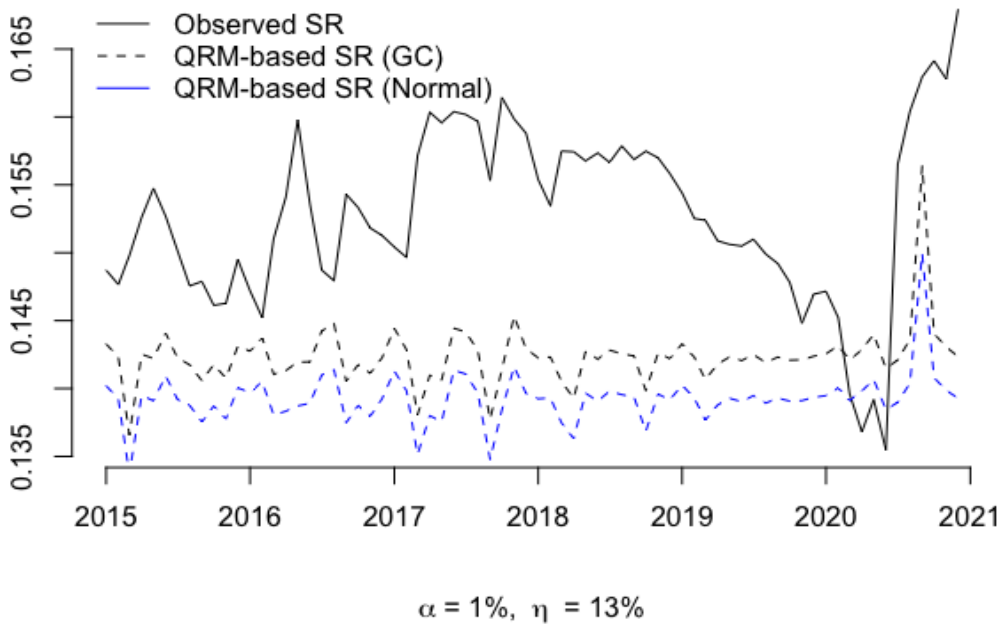

II. 6. Conclusions and Recommendations

This paper proposes risk measures for the risk-taking channel by modeling the probability functions of solvency risks. Modeling the *pdf*s of the solvency risk sources can be used to measure and constrain the impact of monetary policy on the banks' solvency used as a transmission channel. This is particularly useful for estimating the likelihood of an agent's *SR* falling below a given threshold at which the prudential regulator must intervene. Along these lines, to limit the solvency risk, we propose using a *SR* based on *QRMs*. Furthermore, the *GC pdf*s make it easier to manage solvency risk and improve the convergence of *RC* to *EC*. As a result, the risk profile can be incorporated by estimating the parameters that model the distortions caused by the higher-order moments of the observed frequency distributions concerning the normal distribution. This methodology is consistent with the requirements of the second pillar of the Basel framework and limits the risk appetite through the α parameter used in the value-at-risk model.

The magnitude of the impacts caused by the implementation of COVID-19 monetary policy measures in Colombia was calculated using the *pdf*s of variations in *SR*s in the risk portfolio and the capital supporting it. According to our findings, the frequency distributions of *SDR* and its components (*TDR* and *PGR*) had time-varying patterns in the mean and variance, which can be captured using ARMA and GARCH models, respectively. Regarding the higher moments of the probability distributions, the frequency distributions of the variables under analysis were leptokurtic, and *PGR* showed marked skewness to the right. The results of the performance tests indicate that the QRMs estimated using *GC pdf*s were more accurate than those estimated using normal *pdf*s. Also, the difference between the maximum likelihood fit of the *GC pdf* and that of the normal *pdf* is highly significant. Because of the lack of intramonthly data, the effects caused by the implementation of COVID-19 monetary policy measures in Colombia on the transmission channel were analyzed by considering aggregate monthly data on the policies implemented. This analysis leads us to conclude that the variations observed in *SR*s and their components are atypical, as they were found at the extreme end of the distribution tails. In the first four months after the COVID-19 monetary policy measures were implemented, solvency declined. However, the anticipated transition of twelve Colombian banks from Basel II to Basel III led to positive changes in solvency and

reduced risks to insignificant levels. These results confirm the hypothesis that transmission channel operators have a higher risk appetite in the context of the risk-taking channel and highlight the importance of considering this in implementing monetary policies.

Furthermore, we examined the probability of regulatory intervention under different intervention threshold scenarios. Because the Colombian banking system is transitioning from Basel II to Basel III, this implies an increase in the minimum *SR*s required by the prudential regulator. In this study, we considered a regulatory *SR* of 13%, which includes the capital conservation and countercyclical buffers established under Basel III. According to the results of this analysis, the probability of regulatory intervention significantly increased in the first four months after the COVID-19 monetary policy measures were implemented in Colombia, exceeding 4% (assuming an intervention threshold of 13%), which is beyond the risk appetite limit of 1% defined in the Basel framework for the estimation of *VaR* and *EC*. Concerning *SR*s based on *QRMs*, we analyzed historical data from 2015 to 2021. We found that, for a minimum regulatory *SR* of 13% and a risk appetite of 1%, solvency remained above the ratios based on *QRMs*, except between March and June 2020, which coincides with the period in which the COVID-19 monetary policy measures started to be implemented in Colombia. The *SR*s based on *QRMs* experienced an extreme shock, which corresponded to the percentile —a conservative scenario consistent with the Basel framework's provisions. Relative to the increase in the minimum regulatory *SR*s due to the Colombian banking system's transition from Basel II to Basel III, the risks assumed by the monetary policy transmission channel could be in a more critical position because the *SR*s based on *QRM*s increase exponentially as the minimum regulatory *SR*s and the risk appetite increase. The shock suffered by the risk portfolios at the beginning of the crisis because of the injection of liquidity into the different economies proves that this type of event must be considered when *EC* is allocated to support portfolio risk.

In the context of the Basel framework, the risk-taking channel needs to be included in the possible scenarios. The methodology proposed in this paper enables us to estimate the increases in *SR*s needed to absorb these types of shocks. Based on our findings, we recommend implementing prudential policies based on the estimation of *QRM*s, as merely considering the distance between the solvency observed and the regulatory threshold is

insufficient because each agent's risk profile is not considered, and these risk appetites cannot be regulated. Higher levels of disaggregation of the risk portfolio allow correlations between different risk modules and submodules to be analyzed, thus enabling portfolio rebalancing and optimization under certain capital constraints and assuming a minimum *SR*. The methodology proposed in this study can be applied to all levels of aggregation of the risk portfolio and the capital supporting it. It can also be used with more straightforward or complex models. If the components of creditworthiness are disaggregated, multivariate approaches could provide important information about the dynamics of the correlations between these components. Moreover, standard models could be made more flexible and adjusted to the dynamics of the risk portfolio and economic capital, tailoring them more to each financial institution. Also, future studies could consider the dynamics of the different distribution moments while maintaining simplicity.

References

Acharya, V. V., Cooley, T., Richardson, M., & Walter, I. (2010). Manufacturing tail risk: A perspective on the financial crisis of 2007–2009. *Foundations and Trends® in Finance*, *4*(4), 247–325. https://doi.org/10.1561/0500000025

Alexander, C. (2009). *Market Risk Analysis, Value at Risk Models* (1st ed.). John Wiley & Sons.

Bai, J., & Perron, P. (1998). Estimating and testing linear models with multiple structural changes. *Econometrica*, *66*(1), 47–78. http://www.jstor.org/stable/2998540

Balthazar, L. (2006). From Basel 1 to Basel 3. In: *From Basel 1 to Basel 3: The Integration of State-of-the-Art Risk Modeling in Banking Regulation* (pp. 209–213). Finance and Capital Markets Series. Palgrave Macmillan, London. https://doi.org/10.1057/9780230501171_15

Barrio Castro, T. del, Osborn, D. R., & Taylor, A. M. R. (2016). The performance of lag selection and detrending methods for HEGY seasonal unit root tests. Econometric Reviews, 35(1), 122–168. https://doi.org/10.1080/07474938.2013.807710

Basel Committee on Banking Supervision. (1988). *International convergence of capital measurement and capital standards*. Bank for International Settlements, Basel. https://www.bis.org/publ/bcbs04a.pdf

Basel Committee on Banking Supervision. (1998). *International convergence of capital measurement and capital standards*. Bank for International Settlements, Basel. https://www.bis.org/publ/bcbsc111.htm

Basel Committee on Banking Supervision. (2004). International convergence of capital measurement and capital standards: A revised framework. Bank for International Settlements, Basel. https://www.bis.org/publ/bcbs107.htm

Bateni, L., Vakilifard, H., & Asghari, F. (2014). The influential factors on capital adequacy ratio in iranian banks. *International Journal of Economics and Finance*, *6*(11), 108–116. https://doi.org/10.5539/ijef.v6n11p108

Belkin, B., Suchower, S., & Forest, L. R. (1998). The effect of systematic credit risk on loan portfolio value-at-risk and loan pricing. *CreditMetrics Monitor*, First Quarter, 17–28. https://www.z-riskengine.com/media/1037/the-effect-of-systematic-credit-risk-on-loan-portfolios-and-loan-pricing.pdf

Borio, C. E. (2008). The financial turmoil of 2007-?: A preliminary assessment and some policy considerations. BIS Working Papers, 251, Basel. https://www.bis.org/publ/work251.pdf

Borio, C., & Zhu, H. (2012). Capital regulation, risk-taking and monetary policy: A missing link in the transmission mechanism? *Journal of Financial Stability*, *8*(4), 236–251. https://doi.org/10.1016/j.jfs.2011.12.003

Brio, E. B. D., Ñíguez, T.-M., & Perote, J. (2009). Gram–Charlier densities: A multivariate approach. *Quantitative Finance*, *9*(7), 855–868. https://doi.org/10.1080/14697680902773611

Brio, E. B. D., & Perote, J. (2012). Gram–Charlier densities: Maximum likelihood versus the method of moments. *Insurance: Mathematics and Economics*, *51*(3), 531–537. https://doi.org/10.1016/j.insmatheco.2012.07.005

Bølviken, E., & Guillen, M. (2017). Risk aggregation in solvency ii through recursive log-normals. *Insurance: Mathematics and Economics*, *73*, 20–26. https://doi.org/10.1016/j.insmatheco.2016.12.006

Cantú, C., Cavallino, P., De Fiore, F., Yetman, J., et al. (2021). *A Global Database on Central Banks' Monetary Responses to COVID-19*. Bank for International Settlements, Monetary Economic Department.

Caruana, J. (2005). Implementation of Basel II. *Financial Markets, Institutions & Instruments*, *14*(5), 253–265. https://doi.org/10.1111/j.0963-8008.2005.00107.x

Chava, S., Stefanescu, C., & Turnbull, S. (2011). Modeling the loss distribution. *Management Science*, *57*(7), 1267–1287. https://doi.org/10.1287/mnsc.1110.1345

Chen, C., & Liu, L.-M. (1993). Joint estimation of model parameters and outlier effects in time series. Journal of the American Statistical Association, 88(421), 284–297. *https://doi.org/10.1080/01621459.1993.10594321*

Connolly, E. (2009). Banking crises and economic activity: Observations from past crises in developed countries. *Economic Papers: A Journal of Applied Economics and Policy*, *28*(3), 206–216. https://doi.org/10.1111/j.1759-3441.2009.00031.x

Corrado, C. J., & Su, T. (1996). Skewness and kurtosis in S&P 500 index returns implied by option prices. *Journal of Financial Research*, *19*(2), 175–192. https://doi.org/10.1111/j.1475-6803.1996.tb00592.x

Cortés, L. M., Mora-Valencia, A., & Perote, J. (2016). The productivity of top researchers: A semi-nonparametric approach. *Scientometrics*, *109*(2), 891–915. https://doi.org/10.1007/s11192-016-2072-5

Davis, A. W. (1976). Statistical distributions in univariate and multivariate Edgeworth populations. *Biometrika*, *63*(3), 661–670. https://doi.org/10.1093/biomet/63.3.661

De Fontnouvelle, P., Jesus-Rueff, D., Jordan, J. S., Rosengren, E. S., et al. (2003). Using loss data to quantify operational risk. Working paper, Federal Reserve Bank of Boston. Available at SSRN 395083. http://dx.doi.org/10.2139/ssrn.395083

de Moraes, C. O., Montes, G. C., & Antunes, J. A. P. (2016). How does capital regulation react to monetary policy? New evidence on the risk-taking channel. *Economic Modelling*, *56*, 177–186. https://doi.org/10.1016/j.econmod.2016.03.025

Dutta, K., & Perry, J. (2006). A tale of tails: An empirical analysis of loss distribution models for estimating operational risk capital. Federal Reserve Bank of Boston, Working Paper No 06-13. https://www.bostonfed.org/publications/research-department-working-paper/2006/a-tale-of-tails-an-empirical-analysis-of-loss-distribution-models-for-estimating-operational-risk-capital.aspx

Edgeworth, F. (1896). XI. The asymmetrical probability-curve. *The London, Edinburgh, and Dublin Philosophical Magazine and Journal of Science*, *41*(249), 90–99. https://doi.org/10.1080/14786449608620818

Elizalde, A., & Repullo, R. (2007). Economic and regulatory capital. What is the difference? *International Journal of Central Banking*, *3*(3), 87-117. https://www.ijcb.org/journal/ijcb07q3a3.pdf

Elliott, G., Rothenberg, T. J., & Stock, J. H. (1996). Efficient tests for an autoregressive unit root. Econometrica, 64(4), 813–836. http://www.jstor.org/stable/2171846

Fahlenbrach, R., Prilmeier, R., & Stulz, R. M. (2012). This time is the same: Using bank performance in 1998 to explain bank performance during the recent financial crisis. *Journal of Finance*, *67*(6), 2139–2185. https://doi.org/10.1111/j.1540-6261.2012.01783.x

Feria-Domínguez, J. M., Jimenez-Rodriguez, E., & Sholarin, O. (2015). Tackling the over-dispersion of operational risk: Implications on capital adequacy requirements. *North American Journal of Economics and Finance*, *31*, 206–221. https://doi.org/10.1016/j.najef.2014.11.004

Frachot, A., Georges, P., & Roncalli, T. (2001). Loss distribution approach for operational risk. Working Paper, Crédit Lyonnais, Groupe de Recherche Opérationnelle. Available at SSRN 1032523. https://papers.ssrn.com/sol3/papers.cfm?abstract_id=1032523

Franses, P. H., & Haldrup, N. (1994). The effects of additive outliers on tests for unit roots and cointegration. Journal of Business & Economic Statistics, 12(4), 471–478. *https://doi.org/10.1080/07350015.1994.10524569*

Haldrup, N., Montanés, A., & Sanso, A. (2005). Measurement errors and outliers in seasonal unit root testing. Journal of Econometrics, 127(1), 103–128. https://doi.org/https://doi.org/10.1016/j.jeconom.2004.06.005

Hernández, C., Torres, N., Walteros, Liliana, & Gamba, C. (2018). Documento técnico convergencia a los requerimientos de capital de Basilea III para los establecimientos de crédito. *Publicaciones Unidad de Proyección Normativa Estudios de Regulación Financiera*. https://www.urf.gov.co/webcenter/ShowProperty?nodeId=%2FConexionContent%2FWCC_CLUSTER-106150%2F%2FidcPrimaryFile&revision=latestreleased

Huang, X., Zhou, H., & Zhu, H. (2012). Assessing the systemic risk of a heterogeneous portfolio of banks during the recent financial crisis. *Journal of Financial Stability*, *8*(3), 193–205. https://doi.org/10.1016/j.jfs.2011.10.004

Hylleberg, S., Engle, R. F., Granger, C. W. J., & Yoo, B. S. (1990). Seasonal integration and cointegration. Journal of Econometrics, 44(1), 215–238. https://doi.org/https://doi.org/10.1016/0304-4076(90)90080-D

International Monetary Fund. (2020). *Global Financial Stability Report, April 20: Markets in the Time of COVID-19*. International Monetary Fund. https://www.imf.org/en/Publications/GFSR/Issues/2020/04/14/Global-Financial-Stability-Report-April-2020-49020

Jacod, J., & Protter, P. (2012). *Probability essentials*. Berlin. Springer Science & Business Media.

Jarrow, R., & Rudd, A. (1982). Approximate option valuation for arbitrary stochastic processes. *Journal of Financial Economics*, *10*(3), 347–369. https://doi.org/10.1016/0304-405X(82)90007-1

Jiménez, G., & Mencía, J. (2009). Modelling the distribution of credit losses with observable and latent factors. *Journal of Empirical Finance*, *16*(2), 235–253. https://doi.org/10.1016/j.jempfin.2008.10.003

Jondeau, E., & Rockinger, M. (2001). Gram–Charlier densities. *Journal of Economic Dynamics and Control*, *25*(10), 1457–1483. https://doi.org/10.1016/S0165-1889(99)00082-2

KPMG. (2020). Making sense of solvency, capital and COVID-19 for the insurance sector. https://home.kpmg/xx/en/home/insights/2020/04/COVID-19-solvency-capital-and-the-insurance-sector.html.

Kolassa, J. E. (2006). *Series approximation methods in statistics*. New York Springer Science & Business Media.

Kretzschmar, G., McNeil, A. J., & Kirchner, A. (2010). Integrated models of capital adequacy: Why banks are undercapitalised. *Journal of Banking & Finance*, *34*(12), 2838–2850. https://doi.org/10.1016/j.jbankfin.2010.02.028

Lee, L.-F. (1984). Tests for the bivariate normal distribution in econometric models with selectivity. *Econometrica*, *52*(4), 843–863. http://www.jstor.org/stable/1911187

Le Maistre, A., & Planchet, F. (2013). A proposal of interest rate dampener for solvency II framework introducing a three-factors mean reversion model. *ISFA-Laboratory SAF*. http://www.actuaries.org/lyon2013/papers/AFIR_Lemaistre_Planchet.pdf

Macey, J. (2017). Error and regulatory risk in financial institution regulation. *Supreme Court Economic Review*, *25*(1), 155–192. https://www.journals.uchicago.edu/doi/full/10.1086/694089

Madan, D. B. (2009). Capital requirements, acceptable risks and profits. *Quantitative Finance*, *9*(7), 767–773. https://doi.org/10.1080/14697680903314456

Mauleón, I., & Perote, J. (2000). Testing densities with financial data: An empirical comparison of the EdgeworthSargan density to the Students t. *European Journal of Finance*, *6*(2), 225–239. https://doi.org/10.1080/13518470050020851

Merton, R. (1973). Theory of rational option pricing. *Bell Journal of Economics and Management Science*, *4*(1), 229–288. https://doi.org/10.1142/9789812701022_0008

Merton, R. C. (1974). On the pricing of corporate debt: The risk structure of interest rates. *Journal of Finance*, *29*(2), 449–470. https://onlinelibrary.wiley.com/doi/10.1111/j.1540-6261.1974.tb03058.x

Ng, T. Y. J., & Roychowdhury, S. (2014). Loan loss reserves, regulatory capital, and bank failures: Evidence from the 2008-2009 economic crisis. *Review of Accounting Studies*. Research Collection School Of Accountancy.

https://ink.library.smu.edu.sg/soa_research/1192

Ñíguez, T.-M., & Perote, J. (2012). Forecasting heavy-tailed densities with positive edgeworth and gram-charlier expansions. *Oxford Bulletin of Economics and Statistics*, *74*(4), 600–627. https://doi.org/10.1111/j.1468-0084.2011.00663.x

Perron, P., & Rodríguez, G. (2003). Searching for additive outliers in nonstationary time series. *Journal of Time Series Analysis*, *24*(2), 193–220. https://doi.org/https://doi.org/10.1111/1467-9892.00303

Rötheli, T. F. (2010). Causes of the financial crisis: Risk misperception, policy mistakes, and banks' bounded rationality. *Journal of Socio-Economics*, *39*(2), 119–126. https://doi.org/10.1016/j.socec.2010.02.016

Sandström, A. (2007). Solvency II: Calibration for skewness. *Scandinavian Actuarial Journal*, *2007*(2), 126–134. https://doi.org/10.1080/03461230701250481

Sargan, J. D. (1975). Gram-Charlier approximations applied to t ratios of k-class estimators. *Econometrica*, *43*(2), 327–346. http://www.jstor.org/stable/1913589

Shevchenko, P. V. (2010). Implementing loss distribution approach for operational risk. *Applied Stochastic Models in Business and Industry*, *26*(3), 277–307. https://onlinelibrary.wiley.com/doi/10.1002/asmb.812

Tiesset, M., & Troussard, P. (2005). Regulatory capital and economic capital. *Financial Stability Review*, *7*, 59–74. https://ideas.repec.org/a/bfr/fisrev/200572.html

Vasicek, O. (2002). The distribution of loan portfolio value. *Risk*, *15*(12), 160–162.

Wason, A. W., Stuart Party, Kannan, R., Conger, B., & Mango, D. (2004). A global framework for insurer solvency assessment. *Report of the Insurer Solvency Assessment Working Party, International Actuarial Association*, *14*, 2013. https://www.actuaries.org/LIBRARY/Papers/Global_Framework_Insurer_Solvency_Assessment-public.pdf

Wirch, J.L., & Hardy, M. R. (1999). A synthesis of risk measures for capital adequacy. Insurance: Mathematics and Economics, 25(3), 337–347. https://doi.org/https://doi.org/10.1016/S0167-6687(99)00036-0

Wu, X., Xia, M., & Zhang, H. (2020). Forecasting VaR using realized EGARCH model with skewness and kurtosis. *Finance Research Letters*, *32*, 101090. https://doi.org/10.1016/j.frl.2019.01.002

Appendix II.1

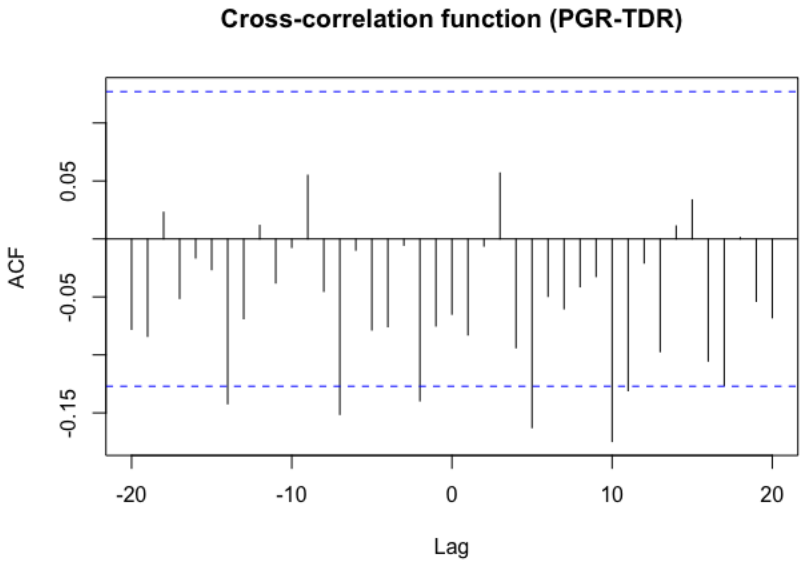

Appendix II.1 Figure 1. Cross-correlation between variations in the risk portfolio and in tier capital.

Notes: This cross-correlation diagram shows that the highest correlation between *PGR* and *TDR* occurs at lags 5 and 10, which means that tier capital adjustments are five months ahead of the variations in this component. However, a high correlation is observed in period -2, which means that some increases in the risk portfolio are compensated by capital increases two months later.

CHAPTER III. Countercyclical Bank Capital Buffer estimation and its relation to monetary policy

III.1. Introduction

The banking system has become essential to worldwide economies, being fundamental in financial intermediation and monetary policy transmission, thus its proper regulation have a deep impacting economic growth (see e.g., Stewart et al. (2021)). The role of banks as financial intermediaries involves the assumption of financial risks that can lead to bankruptcy, which represents a systemic risk for the economy. In this context, prudential regulation ensures the financial system's stability by strengthening solvency and liquidity. At the international level, the Basel Committee on Banking Supervision (BCBS) has defined capital adequacy as a pillar to support the financial risks faced by banks. The BCBS proposed the Capital Adequacy Ratio (CAR) as a solvency indicator calculated from a bank's Capital to its Risk Weighted Assets (RWA). For a bank to be considered solvent, its CAR must be above a certain minimum threshold established as a prudential policy. The bank capital framework based on the Basel I (BCBS, 1988) and Basel II (Basel, 2004) accords was insufficient to protect the international banking system from the events that triggered the 2008 financial crisis, revealing the need for changes in prudential regulation (Borio, 2008). In response to this requirement, the Basel III Accord (BCBS, 2011) introduced a capital conservation buffer equivalent to 2.5% of RWA and a Countercyclical Capital Buffer (CCB) between 0% and 2.5% of RWA. These buffers complement the minimum Capital required by Basel III. They were added to absorb losses that could cause the bank's solvency to fall below the minimum solvency level set by Total Capital.

The need to incorporate appropriate measures of solvency risk in prudential policy decision-making is still an open question. It involves the measurement of the probability of exceeding the minimum capital threshold set and the establishment of the CCB set under the Basel III accord, which mitigates insolvency and systemic risks. In this paper, we propose solvency risk measures based on the semi-nonparametric modeling of the probability density function (pdf) of the CAR proposed by the Basel Committee. A stochastic Ornstein-Uhlenbeck model

is used to measure the Probability of Breaching the Minimum Capital Threshold (PBT) and estimate the size of the CCB that must be kept above a minimum level for a one-year horizon, based on the modeling of the CAR's pdf. For this purpose, the cyclical behavior of the CAR is incorporated by using Fourier series accounting for in the first moment of the pdf. Furthermore, the salient empirical features of the CAR pdf are fitted by a flexible Gram-Charlier distribution, which allow the modeling of skewness and kurtosis. The estimation of the CCB is achieved from Quantile Risk Metrics (QRMs), which are an extension of the Value at Risk (VaR) concept used in the Basel regulatory framework. Additionally, this paper provides evidence of the existence of the bank-capital and risk-taking channels based on the relationship between the monetary policy interest rate and the PBT.

The rest of the paper is organized as follows: Section 2 presents a literature review on PBT measurement and determination of CCB size and timing. Section 3 presents the methodology applied, including the basics of the Ornstein-Uhlenbeck process and the Gram-Charlier expansions. Section 4 presents the empirical analyses for four representative countries and discusses the PBT in relation to the recent monetary policy. Section 5 summarizes the conclusions.

III.2. Literature review

The problem raised by the probability of exceeding the minimum capital threshold has been analyzed by authors such as Borio & Zhu (2012), who study the Capital Threshold Effect, defining it as the effect of the minimum level of Capital set by prudential policy on banks' lending decisions. The bank must support the funding costs of the Capital backing the loan portfolio to avoid the costs generated by failing to meet the minimum capital threshold regarding restrictive regulatory interventions, reputational costs, and adverse market reactions. The Capital Threshold Effect is considered a cost that varies with the size and volatility of the capital buffer above the regulatory minimum and operates over the long term, given the expectation that the bank will breach the minimum capital requirement. Under the Basel framework (BCBS, 1988), the restriction imposed by financial regulation on the transmission channel operates through the threat of non-compliance with the minimum

solvency levels, which depends on the distance between the level of bank solvency and the minimum regulatory threshold, measured through the CAR, and the volatility of the CAR.

The PBT has been modeled by authors such as Spiegeleer et al. (2017) through a geometric Brownian stochastic process without drift, i.e., the probability that the Basel III Common Equity Tier 1 (CET1) ratio reaches a certain threshold that determines the activation (trigger) of Contingent Convertible bonds or CoCos, for a specific time horizon. Russo et al. (2020) use the CET1 model proposed by Merton (1974) to estimate the probability that a financial institution fails to comply with the capital requirements under the Basel III regulatory framework, adapting a geometric Brownian motion to model bank assets that allows estimating their implied volatility. Jarrow (2013) defines the probability of insolvency at time t projected to time $t + \Delta$ as the probability that debt is greater than assets, i.e., the probability that equity is negative. Modeling bank solvency risk based on stochastic processes that do not allow incorporating terms that take into account the cyclical behavior of businesses may not be appropriate in prudential policy decision-making since the size of the capital buffer may depend on exogenous factors, such as the state of the economic cycle, idiosyncratic shocks to the bank's balance sheet and the bank's optimization strategies (Borio, 2008).

The Basel III accord (BCBS, 2011) argues that it is not possible to increase the risk sensitivity of banks at a given point in time without introducing some degree of cyclicality in minimum capital requirements over time and introducing a framework that promotes the reduction of procyclicality through the preservation and accumulation of capital buffers above the minimum threshold, which contribute to increasing resilience in recessionary phases and can be used in times of stress. Athanasoglou et al. (2014) analyze the effect that procyclicality has on the financial system, making an account within the literature of the causes of procyclicality and proposals to mitigate it. Under BCBS rules, credit, market, and operational risk estimates assume that loss distributions approximate the normal distribution. This assumption may be implausible given that, in the modeling of banking risks, evidence is found that the pdfs associated with banking risks show significant distortions with respect to the normal distribution that may lead to the under or overvaluation of risks, especially when quantile measures such as the VaR are used. Different authors have documented in the financial literature the presence of heavy tails in the loss distributions of financial solvency.

Authors such as Sandström (2007), Bølviken & Guillen (2017), and Le Maistre & Planchet (2013) conclude that in order not to underestimate the capital requirements, the bias in the aggregation of the different risk modules must be considered.

For calibration of the timing and size of the CCB, the Basel III framework establishes guidelines for prudential authorities applying the CCB regime (BCBS, 2010). These guidelines use the credit-to-GDP gap, defined as the difference between the credit-to-GDP ratio and its long-term trend. High levels of the credit-to-GDP ratio indicate that credit is growing out of proportion to the economy and leading to a financial crisis. Drehmann & Tsatsaronis (2014) point out the limitations of the credit-GDP gap in determining the size and timing of the CCB, focusing on the appropriateness of the indicator given the purpose of the CCB, its properties as an early warning indicator, and its practical measurement problems. The Hodrick-Prescott filter recommended by the BCBS to filter the trend in the credit-to-GDP ratio uses an arbitrary smoothing parameter that assumes a much longer credit cycle than has been empirically documented in many countries (Galán, 2019).

Finally, in this paper, we explore the relationship between PBT and monetary policy since the effect of monetary policy on the real and financial economy is one of the main instruments available to the economic authorities to achieve their growth and stability objectives. PBT can restrict the transmission of monetary policy, and monetary policy can affect PBT. Bruno & Shin (2015) underline the little attention that conventional monetary economics has paid to the role of the banking sector in the management of the financial conditions of the transmission channel, where changes in monetary policy interest rates affect the term spread of the yield curve, which affects the profitability of new loans and, thus, the decisions to grant new loans. The interaction of monetary and prudential policies raises the need to jointly analyze them. Central banks should adopt interest rate strategies that take into account capital adequacy requirements to avoid conflict between monetary policy, which seeks to ensure that there is sufficient lending to support stable economic growth, and prudential policy, which seeks to prevent excessive risk-taking and may limit banks' lending capacities (Cecchetti & Li, 2008). Angeloni & Faia (2013) suggest the possibility of interactions between the conduct of monetary policy and prudential regulatory policies through the combination of countercyclical capital ratios, such as those proposed by Basel III, and monetary policy

responding to shocks to asset prices or bank leverage, to help control systematic risk in the financial sector.

The interest rate channel is the conventional channel through which monetary policy is transmitted to households and firms' saving and investment decisions. Bernanke & Gertler (1995) also document the credit channel and the Balance Sheet Channel. The Credit Channel is defined as the interest rate's effect on credit volumes and is an amplifier of the interest rate channel. The Balance Sheet Channel is defined as the potential impact of changes in monetary policy on borrowers' balance sheets and income statements, including variables such as net worth, cash, and liquid assets. Recent advances in prudential policy have made regulatory bank capital more relevant in lending decisions (Markovic, 2006). Thus, the effectiveness of banks in transmitting monetary policy impulses will depend on how well-capitalized they are to cover the risks of their assets. Minimum capital requirements have an increasing influence on the behavior of banks and have implications for the transmission mechanism based on the differential cost of funding Capital, which is called the Bank-Capital Channel that operates on the transmission channel through the threat of non-compliance with minimum capital requirements, and through the Risk-Taking Channel defined as the effect that monetary policy has on the perception and valuation of risk by economic agents, and which affects banks' risky asset portfolios, altering lending decisions (Borio & Zhu, 2012).

The Bank Capital Channel, which operates through the constraints imposed by bank capital requirements on the effects of monetary policy on the economy, has been studied by authors such as Van den Heuvel (2007), Imbierowicz et al. (2021), Aiyar et al. (2016), Cappelletti et al. (2022), Gambacorta & Mistrulli (2004), Gambacorta & Shin (2018), Markovic (2006), among others. They generally find that low bank capital levels or increases in capital requirements weaken the transmission of monetary policy by affecting credit growth and causing banks to react in a lagged and amplified manner to changes in interest rates. On the other hand, they conclude that actions that increase bank capital, such as profit retention, contribute to monetary policy transmission. Adrian et al. (2019), Dell'Ariccia et al. (2017), Angeloni & Faia (2013) De Moraes et al. (2016) present empirical evidence of the Risk-Taking-Channel from the effect of monetary policy on risk appetite and risk pricing of bank assets.

III.3. Methodology

It is assumed that bank solvency, which determines capital adequacy, follows a mean-reverted Ornstein-Uhlenbeck process, as expressed in Eq.1.

$$CAR_t = \mu(t) + X_t, \tag{1}$$

where $\mu(t)$ is a deterministic function in the time domain, and X_t is the stochastic process described in Eq.2.

$$dX_t = -\kappa X_t dt + \sigma dW, \tag{2}$$

where $\kappa > 0$ is a parameter measuring the speed of reversion of CAR to $\mu(t)$, σ is a constant representing the volatility of demand, and $dW = \epsilon\sqrt{dt}$ is the spread of a standard Wiener process (ϵ being a standard normally distributed random variable). It is also assumed that for t=0, solvency has a known value of CAR_0. Following Lucia & Schwartz (2002), the stochastic differential equation can be expressed as in Eq. 3:

$$dCAR_t = \kappa(\mu(t) - CAR_t)dt + \sigma dW. \tag{3}$$

The conditional mean and variance of the process are given by expression 4:

$$E_0(CAR_t) = E(CAR_t/X_0) = \mu(t) + \big(CAR_0 - f(0)\big)e^{-\kappa(t-t_o)}$$

$$var_0(CAR_t) = var(CAR_t/X_0) = \frac{\sigma^2}{2\kappa}\big(1 - e^{-2\kappa(t-t_0)}\big)$$

$$X_0 = CAR_0 - \mu(0) \tag{4}$$

To measure the probability of insolvency, we start from the Capital Threshold Effect described by Borio & Zhu (2012), in which the threshold effect varies with the size and volatility of the buffer above the threshold and operates in the long run.

Figure III.1 Illustration of the mean reversion model

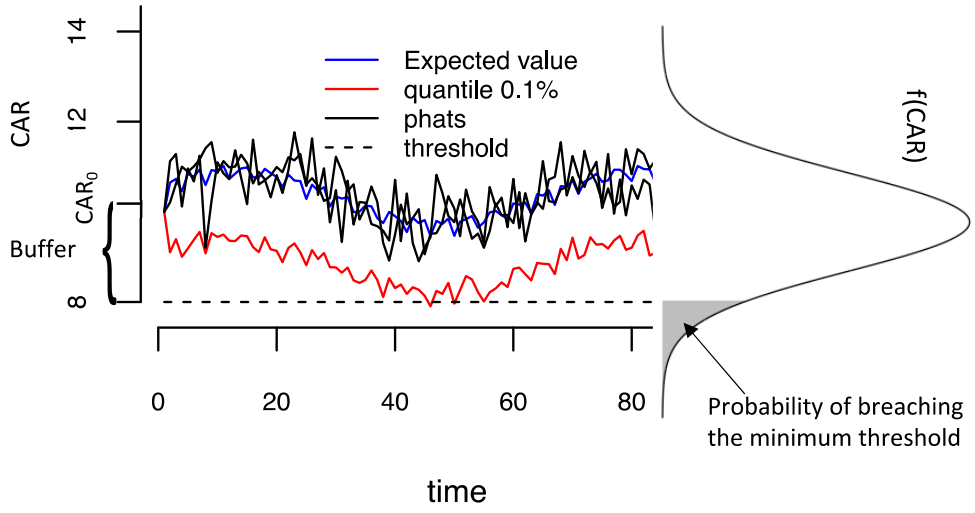

Figure III.1 illustrates the functioning of the mean reversion model. The blue line represents the expected solvency value, modeled through the linear combination of trigonometric functions that model the cyclicality of the CAR solvency indicator. The red line represents the 0.1% percentile, so the probability that CAR is below this percentile is 0.1%. The dotted line is the minimum regulatory threshold, and there is a probability α that the CAR indicator is below the minimum threshold. The black lines are paths simulated under the normality assumption, with a scale parameter equal to 0.5 and a parameter κ of 0.5. It is observed how the probability of breaching the minimum threshold increases in the downward phase of the cycle.

Measurement of the Probability of Breaching the Minimum Capital Threshold (PBT)

Suppose η is the regulatory minimum threshold at a time t_0. In that case, one can express the PBT_0 at a given time t in the future (e.g., one year ahead), as expressed in Eq. 5:

$$PBT_0(CAR_t < \eta) = F_{CAR}(d),$$
$$d = \frac{\eta - \mu(t) - (CAR_0 - \mu(0))e^{-\kappa(t-t_0)}}{\sigma\sqrt{\frac{1-e^{-2\kappa(t-t_0)}}{2\kappa}}}, \quad (5)$$

where F_{CAR} is CAR's standard cumulative density function (CDF) at time t in the future.

The parameter d depends on the distance between the minimum threshold η and the function μ at time t, on the distance between the observed solvency and the value of the function μ, at time t_0, affected by an exponential decay factor that depends on the decay rate κ, on the

time horizon $t - t_0$, and the scaling parameter σ. Finally, PBT_0 depends on the functional form of F_{CAR}, especially on the shape of the tail over which the risk of non-compliance with the regulatory minimum threshold occurs.

Policies for determining the Countercyclical Capital Buffer (CCB), based on Quantile Risk Metrics (QRMs)

Alexander (2009) defines QRMs, for some α between 0 and 1, as the quantile x_α of the distribution of a continuous random variable X such that $p(X \leq x_\alpha) = \alpha$.

$$QRM_\alpha^X = F_X^{-1}(\alpha) = inf\{x \in R: \alpha \leq F_X(x)\}, \qquad (6)$$

F_X^{-1} is the quantile function associated with X.

Determining prudential policies of CCB size from QRMs allows limiting the risk assumption from the parameter α and incorporating stylized features from the pdf with which the insolvency risk is measured.

By equating the value of the minimum solvency threshold to the QRM_α^{CAR} of CAR ($QRM_\alpha^{CAR} = \eta$), it is possible to determine the size of the CCB_0, that a financial institution must have above the minimum regulatory threshold at a time t_0, such that the probability of being below the threshold η at a horizon $t - t_0$ (e.g., one year ahead) is equal to the parameter α, which the prudential regulator must set as a policy $p_o(CAR_t \leq \eta) = \alpha$), to limit the risk of insolvency.

$$CCB_0 = max\left\{\mu(0) + \eta\left(e^{\kappa(t-t_0)} - 1\right) - \left(\mu(t) + F_{std}^{-1}(\alpha)\sigma\sqrt{\frac{e^{2\kappa(t-t_0)}-1}{2\kappa}}\right)e^{\kappa(t-t_0)}, 0\right\}. \quad (7)$$

In Eq. 7, the CCB_0 must be positive and depends on the level of the regulatory threshold, the time domain function μ, the standard quantile function evaluated at α ($F_{std}^{-1}(\alpha)$), the speed of reversion to the mean κ and the projection horizon $t - t_0$.

Incorporating the Fourier series in the function μ allows us to parameterize the characteristics of CAR dynamics, such as seasonal patterns generated by banks' frequency of financial reporting and cyclical phenomena typical of banking systems. In addition, the particularities of the probability distribution of solvency (e.g., volatility, skewness, and kurtosis) can be modeled through the quantile function and the scale parameter σ.

Determination of the pdf of CAR

For the measurement of the probability of default of the minimum capital threshold and the determination of the capital buffer based on QRMs, it is required to model the pdf of the CAR indicator. This paper makes use of the Fourier transform as a tool for modeling the cyclicality of the stochastic process with which the solvency indicator is characterized through spectral analysis and deviations of the tails of the empirical risk distributions, concerning the normal distribution, accounted by the Taylor series expansion of the conjugate Fourier transform of the normal pdf, which is known as Gram-Charlier expansion.

Deterministic component

As BCBS (2011) established, a certain degree of cyclicality must be included in the minimum capital requirements to increase risk sensitivity. Spectral analysis allows the determination of Fourier series that model bank solvency's cyclical and seasonal behavior based on the linear combination of trigonometric functions. Thus, the deterministic component $\mu(t)$ can be expressed according to Eq. 8.

$$\mu(t) = \theta + \sum_{i=0}^{n} C_i * cos\left(\tau_i + \frac{\omega_i 2\pi * t}{T}\right), \quad (8)$$

Where θ is a constant, C_i, τ_i, ω_i are the amplitude, phase, and frequency of each cycle i, and T is the number of observed periods per year.

The autocovariance function $\gamma(\tau)$ can be expressed in terms of the combination of variances such that $\gamma(\tau) = \sum_{i=1}^{n} \sigma_i^2 \, cos(\omega_i \cdot \tau)$, where σ_i^2 is the variance of the harmonic with frequency ω_i. Thus, the variance of a stochastic process can be expressed as $\gamma(0) = \sum_{i=1}^{n} \sigma_i^2$.

Gram-Charlier expansions

The CAR pdf's distortions concerning the normal distribution (e.g., skewness, excess kurtosis, or wavy tails) may lead to underestimating the risk of non-compliance with the minimum capital threshold and the amount of regulatory Capital required to cover the risk with a given probability level. The Gram-Charlier expansions make the distributional assumption flexible by explicitly incorporating skewness, kurtosis, and high-order moments.

Based on a reference parametric pdf f_Y associated with a random variable Y, an approximation of a pdf g_Y is obtained from the conjugate Fourier transform of the reference parametric pdf. The Fourier transform ζ of a pdf is a parameterized function on an auxiliary real variable β (frequency) defined by applying the expectation operator E to the complex function $e^{i\beta Y}$ (i is the imaginary unit). The so-obtained characteristic function characterizes the pdf in a univocal way from the application of the Fourier inversion theorem. Moreover, this function always exists since it is defined on a complex plane. The derivative of the characteristic function at the point $\beta = 0$ generates the ordinary moments of the distribution, corresponding to the order of derivation.

$$\zeta_f(\beta) = E\left[e^{i\beta Y}\right] = \int_{-\infty}^{\infty} e^{i\beta y} f(x). \tag{9}$$

Following Kolassa (2006) and Davis (1976), the characteristic function can be expressed in terms of the power series expansion:

$$\zeta_f(\beta) = exp\left[\sum_{j=1}^{\infty}(\kappa_j)\frac{(i\beta)^j}{j!}\right]. \tag{10}$$

The coefficients κ_j of the power series terms correspond to the j th order cumulants of f_y, and $log\big(\zeta_Y(\beta)\big)$ defines the cumulant generating function. We define the differential operator D_Y and its adjoint $D_Y^{\dagger}$ as:

$$D_Y = \frac{d}{dy}, \quad D_Y^{\dagger} = -\frac{d}{dy}. \tag{11}$$

Following Cohen 1988), given two density functions, $f(y)$ and $g(y)$, and their respective characteristic functions $\zeta_f(\beta)$ and $\zeta_g(\beta)$, these can be related through a kernel $\Psi(\beta)$ which is a function of the two pdfs, such that:

$$\Psi(\beta) = \frac{\zeta_g(\beta)}{\zeta_f(\beta)}. \tag{12}$$

Given the property of the derivative of the Fourier transforms, $D_Y^{\dagger} exp(-i\beta y) = -i\beta * exp(-i\beta y)$, we replace $-i\beta$ with the differential operator $D_Y^{\dagger}$ such that:

$$g(y) = \Psi\big(D_Y^{\dagger}\big) f(y),$$

$$g(y) = \frac{\zeta_g(\beta)}{\zeta_f(\beta)} f(y),$$

$$g(y) = exp\left[\sum_{j=1}^{\infty}\left(\kappa_j^g - \kappa_j^f\right)\frac{(i\beta)^j}{j!}\right] f(y),$$

$$g(y) = exp\left[\sum_{j=1}^{\infty}\left(\kappa_j^g - \kappa_j^f\right)\frac{(D^{\dagger})^j}{j!}\right] f(y), \quad (13)$$

κ_j^g and κ_j^f are the cumulants of $g(y)$ and $f(y)$, respectively.

Taking the standard normal distribution $\phi(y)$ as a reference pdf, $g(y)$ can be expressed in terms of the conjugate inverse Fourier transform, such that:

$$g(y) = \frac{1}{2\pi}\int_{-\infty}^{\infty} e\, xp[-i\beta y] * exp\left[\sum_{j=1}^{\infty}\frac{\left(\kappa_j^g\right)(i\beta)^j}{j!}\right] d\beta. \quad (14)$$

Expanding the first two terms of the series and substituting $i\beta$ for the operator $D_Y^{\dagger}$ we have that:

$$g(y) = \exp\left[\sum_{j=3}^{\infty}\kappa_j\frac{\left(D_Y^{\dagger}\right)^j}{j!}\right] * \frac{1}{2\pi}\int_{-\infty}^{\infty} e\, xp[-i\beta y] * exp\left[k_1 i\beta - \frac{k_2}{2}\beta^2\right] d\beta \quad (15)$$

The term $\frac{1}{2\pi}\int_{-\infty}^{\infty} e\, xp[-i\beta y] * exp\left[k_1 i\beta - \frac{k_2}{2}\beta^2\right]$ corresponds with the inverse transform of the characteristic function that recovers the normal pdf, therefore if $k_1 = \mu, k_2 = \sigma^2$, $g(y)$ is expressed as in Eq. 16:

$$g(y) = \exp\left[\sum_{j=3}^{\infty}\kappa_j\frac{\left(D_Y^{\dagger}\right)^j}{j!}\right]\phi(y), \quad (16)$$

where $\phi(y)$ is the normal standard pdf with mean μ and variance σ^2.

Thus $\exp\left[\sum_{j=3}^{\infty}\kappa_j\frac{\left(D_Y^{\dagger}\right)^j}{j!}\right]$ is the kernel $\Psi\left(D_Y^{\dagger}\right)$ which relates $g(y)$ to $\phi(y)$ and is orthogonal to $\phi(y|\mu,\sigma^2)$. Following Davis (1976), the kernel can be expressed as a Maclaurin series:

$$g(y) = \left[\sum_{j=3}^{\infty} c_j\frac{\left(D_Y^{\dagger}\right)^j}{j!}\right]\phi(y|\mu,\sigma^2). \quad (17)$$

For empirical applications of the model, the orthogonality property of Ψ concerning ϕ allows truncating the kernel to finite order J, thus:

$$g(y) = \left[\sum_{j=3}^{J} c_j \frac{\left(D_Y^{\dagger}\right)^j}{j!}\right]\phi(y). \tag{18}$$

Assuming that ϕ is the standard normal distribution with $\mu = 0$ and $\sigma^2 = 1$, we expand the series up to $J = 4$, such that:

$$g(y) = \left[1 + \frac{c_3(x^3 - 3x)}{6} + \frac{c_4(x^4 - 6x^2 + 3)}{24}\right]\phi(y)$$

$$= \left[1 + \frac{c_3 h_3}{6} + \frac{c_4 h_4}{24}\right]\phi(y). \tag{19}$$

In general:

$$h_j = \frac{D_Y^{\dagger(j)}\phi(y)}{\phi(y)}, \tag{20}$$

h_j corresponds with a polynomial function known as Hermite Polynomial (HP) of order j, which forms an orthonormal basis with respect to the reference function $\phi(x)$, such that:

$$\int_{-\infty}^{\infty} h_j\,(z)h_i(z)\phi(y) = 0, \quad \forall j \neq i. \tag{21}$$

This property allows truncating the series of HPs at finite order $j = J$, preserving up to one integration of $g(y)$ under certain regularity conditions (Cramér, 1925).

In general, $g(y)$ can be expressed as

$$g(y; d) = \left[1 + \sum_{j=3}^{J} d_j\, h_j(x)\right]\phi(x), \tag{22}$$

where d is a vector of parameters $\left(d_1, d_2, \ldots, d_J,\right)$ containing the corresponding information of the distortions of the cumulants of $g(y)$ with respect to those of the normal distribution.

Integrating on both sides of Eq. 22 yields an approximation to the CDF of Y, as expressed in 23:

$$G(y; d) = \int_{-\infty}^{y} g_n\,(t)dt, = \Phi(y) - \sum_{j=1}^{J} h_{j-1}\,(y)d_j\phi(y). \tag{23}$$

In Eq. 23, Φ is the standard normal CDF.

Parameter estimation

Deterministic component

The deterministic component $\mu(t)$, expressed in Eq. 8, depends on the amplitude, phase, and frequency parameters of the wave spectrum used to describe the periodic behavior of CAR. To identify the contribution of each wave function with frequency ω_i to the variance of the stochastic process describing CAR, we use the periodogram, which is a function corresponding to the discrete Fourier transform of the autocovariance function $\gamma(\tau)$. The frequencies ω_i that contribute most to the variance of the stochastic process will be those where the value of the periodogram function is the largest. Since the discrete Fourier transform starts from an arbitrary set of frequencies, the exact value of the frequencies ω_i is unknown; therefore, the frequency parameter must also be estimated. For the estimation of these parameters, a nonlinear least squares regression is carried out, for which the frequencies of the periodogram are used as the initial values for ω_i. Following Lucia & Schwartz (2002), the discrete version of Eq. 3 can be written according to Eq. 24:

$$CAR_t = \phi CAR_{t-1} + \mu(t) - \phi\big(\mu(t-1)\big) + a_t, \tag{24}$$

$\kappa = \phi - 1$ and a_t is a random error.

Gram-Charlier parameters

In most applications of Gram-Charlier expansions, the parameters are estimated using the Maximum Likelihood (ML) method. Assuming that the first two moments of the distribution are well specified, global optima guarantee that $g(y; d)$ is positive (Del Brio &Perote, 2012). For a sample of size T, the log-likelihood function $log(L)$ is given by:

$$log(L) = -\frac{T}{2} log(2\pi) - \frac{1}{2}\sum_{t=1}^{T} l\,og(y_t^2) + \sum_{t=1}^{T} l\,og\big(\big[1 + \sum_{j=3}^{n} d_j\, h_j(y_t)\big]\big). \tag{25}$$

III.4. Empirical Analysis

This section presents the results of the empirical analysis of the application of the model on a sample of the historical time series of the CAR of four countries, the Netherlands, the

United States of America (USA), Germany, and Colombia. In the first part, a description of the sample data is given. The second part presents the pdfs' estimated parameters and then the estimated PBT and CCB series. Finally, the VAR model results that relate the PBT to the monetary policy interest rate are presented.

The historical CAR time series sample was taken from the CEIC database, which provides the CAR reported by different countries. For modeling, we take complete available data from the most ancient date till the most recent date at the moment of the sampling, at the higher disposable frequency.

The countries to be analyzed were selected based on the size of the available samples so that their behavior at critical moments, such as the 2008 crisis and the impact of COVID-19, could be observed, and their global systemic importance. Banking in the USA is of great importance globally due to the size of its financial market, the dominance of the US dollar, its role in financial innovation, and its regulatory influence. As a result, banks in USA are essential players in international financial markets, and their performance impacts the global economy. European Union (E.U.) banking is also one of the critical global players due to the size of its financial market, its economic influence, and its role in financial regulation globally, with regulations such as Basel III and MiFID II (Markets in Financial Instruments Directive II) having a significant impact on banking and financial markets worldwide. On the other hand, banking in emerging countries is becoming increasingly important globally due to economic growth, geographic diversification, innovation, and new players in international financial markets. As these banks expand and acquire a more significant presence in global financial markets, they are expected to have an increasing impact on the global economy and the banking industry worldwide.

III.4.1 Description of the sample

Table III.1 presents descriptive statistics for the four countries in the sample. The frequency of the series for the Netherlands, USA, and Germany are quarterly, while for Colombia, the

data are monthly. Germany has an average CAR of 17.62%, the highest in the sample, followed by the Netherlands, with an average of 15.28%. The USA has the lowest average but has the lowest volatility (1.03 quarterly). The highest volatility is that of the Netherlands, being 4.38% quarterly, followed by Colombia, which has a monthly volatility of 1.81%, which under the normality assumption is equivalent to 3.62% quarterly. The Netherlands and Colombia have a positive skewness, while the USA and Germany have a negative skewness. The Netherlands and USA series are platykurtic, while the German and Colombian series are leptokurtic.

Table III.1 Descriptive statistics for CAR

Country	Frequency	Start	End	Average	Std	Skew	K	Min	Max
Netherlands	Quarterly	1998-03	2021-06	15.28	4.38	0.79	-1.09	10.90	23.20
USA	Quarterly	2001-12	2021-06	13.82	1.03	-0.21	-1.40	12.15	15.57
Germany	Quarterly	2008-12	2020-12	17.62	1.53	-1.03	0.01	13.54	19.38
Colombia	monthly	2002-01	2021-11	14.48	1.81	1.03	2.18	10.91	20.39

Note: This table shows the descriptive statistics for the four countries in the sample: the Netherlands, the United States (USA), Germany, and Colombia. Start and End correspond to the dates the series begins and ends, respectively. Std=standard deviation, Skew=skewness, K=excess kurtosis coefficient, Min= minimum CAR, Max=maximum CAR.

III.4.2 Outlier detection

Figure III.2 presents the CAR's time series graph, adjusted for outliers and outliers for the analyzed sample. The series for the Netherlands shows an exponential growth trend after the 2008 financial crisis. The average solvency of the Netherlands until 2008 was 11.77%. However, after the crisis, the average increased to 18.25%, implying a more than 50% rise in the indicator level. The USA series also shows a significant increase in solvency levels after the 2008 financial crisis, with the average rising from 12.71% to 14.68%. The time series of bank solvency in Germany converges logarithmically to a value close to 19%. For Colombia, the series converges to a value close to 15% until December 2020. In January 2021, a significant increase in solvency levels was observed, reaching a level close to 20%. According to Franses & Haldrup (1994), the existence of outliers can generate type I error by rejecting the null hypothesis that states the presence of unit roots. To control for the

existence of outliers in the unit root hypothesis testing, we apply the approach described by Chen & Liu (1993) in which the detection of additive innovational outliers ("IO"), additive outliers ("AO"), level shifts ("LS"), temporary changes ("TC") and seasonal level shifts ("SLS") is implemented. The Netherlands series presents AO in February and April 2008, February 2010, and LS in March 2009, March 2009, March 2014, January and April 0216, and February 2017. The USA series presents AO in January 2016 and January 2022. Germany presented a level change in January 2016, and Colombia presented LS in May 2006, August 2013, July 2020, and January 2021.

Figure III.2 Evolution of CAR, CAR adjusted by outliers, and outliers for the Netherlands, USA, Germany, and Colombia

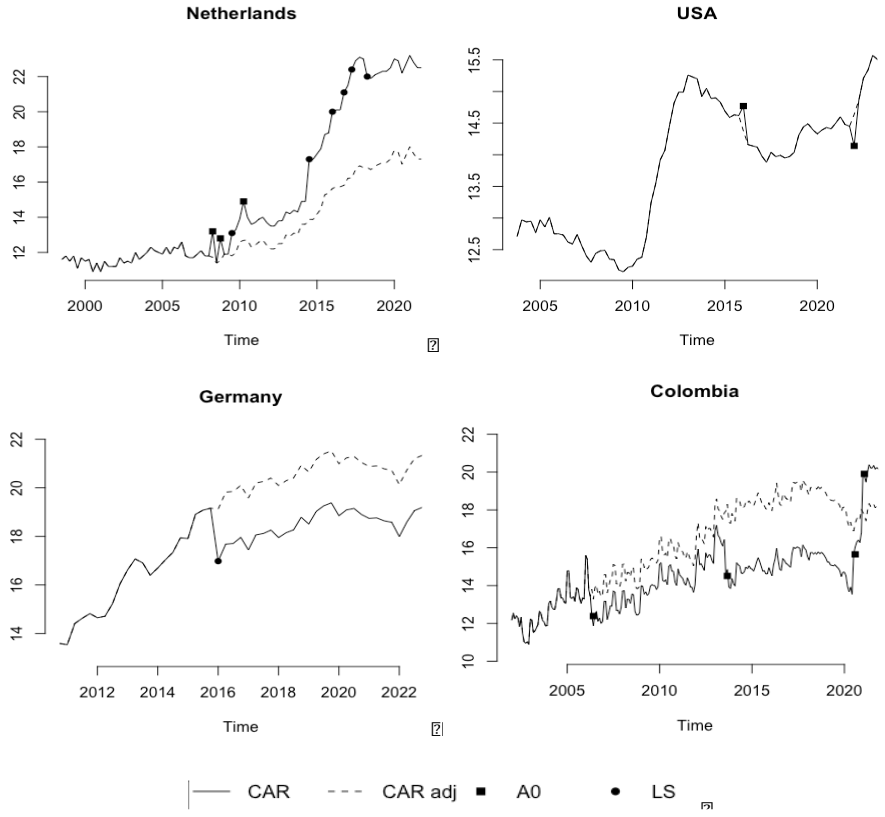

Table III.2 Unit root test

	p-value (Netherlands)	p-value (USA)	p-value (Germany)	p-value (Colombia)
Augmented Dickey-Fuller				
$\mathbf{y_{t-1}}$	1.90e-06	0.087020	0.01089	0.0785
ADF-GLS				
$\mathbf{y_{t-1}}$	0.01715	0.001840	0.0568	0.00082
HEGY				
Ha	0.0652	0.0655	0.0433	0.044
Hb	---	---	---	0.0013
Hc	---	---	---	3e-04
Hd	---	---	---	0.0492
He	0.0069	0.0115	0.0182	0.0027
Hf	---	---	---	0.0632
Hg	0.000	0.000	0.000	0.000

Note: This table presents the p-values of the Augmented Dickey-Fuller, DF-GLS, and HEGY unit root tests of CAR adjusted for the Netherlands, USA, Germany, and Colombia. The Augmented Dickey-Fuller test includes drift for the Netherlands, Germany, and Colombia and trend for Germany, and the number of lags is selected using the BIC criterion. The ADF-GLS test includes drift for the Netherlands and Trend for the United States (USA), Germany, and Colombia. The HEGY test consists of drift and seasonal dummies for the Netherlands and Germany and drift and trend for the USA and Colombia. The number of lags is selected using the AIC criterion. The presence of unit roots is tested with the corresponding null hypotheses: Ha: non-seasonal unit root, Hb: bi-monthly unit root, Hc: unit root for four-month periods, Hd: quarterly unit root, He: semi-annual unit root, Hf: root at the frequency $5\pi/6$, Hg: annual unit root.

Table III.2 presents the p-values of the unit root tests for the time series analyzed. For the classical Dickey-Fuller test, the null hypothesis that states the presence of unit roots is rejected at 1% significance for the Netherlands, 5% for Germany, and 10% for the USA and Colombia. The DF-GLS test proposed by Elliott et al. (1996), which improves the power of the test by considering the serial correlation, rejects the null hypothesis at 1% for USA and Colombia, 5% for the Netherlands, and 10% for Germany. The HEGY test proposed by Hylleberg et al. (1990), which tests for the presence of seasonal unit roots, rejects the null hypothesis that states the existence of non-seasonal and seasonal unit roots at a maximum significance level of 10%.

III.4.3 Estimated parameters

Table III.3 presents the estimated parameters of the deterministic component and the Gram-Charlier pdfs of the series under analysis. For the Netherlands, cycles with periods of approximately one year, 7.5 years, and 0.5 years (annual frequency of 0.952, 0.133, and 2.11), respectively, are identified (annual frequency of 0.952, 0.133, and 2.11, respectively),

being the cycle with a period of 7.5, the one with the largest amplitude, with a difference between peak and trough of 1.46%. Given the exponential growth of the Dutch time series, a trend parameter is included, which indicates that solvency grows approximately 0.2% quarterly, implying annual growth of 0.82%.

For the USA, cycles with periods of 10.5 years, six years, 0.5 years, and 1.9 years are identified, with the cycle with a period of 0.5 being the one with the largest amplitude, with a difference between peak and trough of 1.52%. Given the jump observed in the USA. series after the 2008 financial crisis, a dummy variable is included, which indicates that the solvency level increased by 1.57% on average. For Germany, cycles of one year, 4.6 years, and 0.5 years are identified, being the 4.6-year cycle the one with the highest variability, with a difference between peak and trough of approximately 1%. For Colombia, cycles with periods of 0.5 years, four years, and one year are identified. The 4-year cycle has the highest variability, with a difference between peak and trough of approximately 1.7%. In terms of the Gram-Charlier parameters, it is found that the skewness and excess kurtosis parameters are significant for the Netherlands and Colombia.

In contrast, for Germany, only the excess kurtosis parameter is significant. For the USA, neither parameter is significant, which implies that the normality assumption can be assumed without significant loss of precision. The standard deviation of USA solvency is less than half that of the other countries (under the assumption of normality, Colombia's standard deviation is 0.93% quarterly).

Table III.3 Fitted parameters of the Ornstein-Uhlenbeck process under Gram-Charlier pdf

	Netherlands		*USA*		*Germany*		*Colombia*	
parameter	Estimate	p-value	Estimate	p-value	Estimate	p-value	Estimate	p-value
$\boldsymbol{\theta}$	4.54	0.201	14.609	0.000	18.799	0.000	15.379	0.000
$\boldsymbol{C_1}$	0.142	0.018	-0.761	0.000	-0.208	0.002	0.164	0.001
$\boldsymbol{\tau_1}$	17.67	0.000	10.209	0.000	18.699	0.000	4.116	0.000
$\boldsymbol{\omega_1}$	0.952	0.000	0.096	0.000	0.997	0.000	2.052	0.000
$\boldsymbol{C_2}$	-0.73	0.062	0.286	0.001	0.48	0.069	0.859	0.027
$\boldsymbol{\tau_2}$	25.02	0.000	3.282	0.000	19.657	0.000	1.34	0.154
$\boldsymbol{\omega_2}$	0.133	0.000	0.169	0.000	0.218	0.000	0.241	0.000
$\boldsymbol{C_3}$	0.112	0.007	-0.032	0.024	0.153	0.003	0.199	0.042
$\boldsymbol{\tau_3}$	18.022	0.000	3.756	0.000	20.543	0.000	5.267	0.000
$\boldsymbol{\omega_3}$	2.11	0.000	1.907	0.000	2.04	0.000	0.993	0.000
$\boldsymbol{C_4}$			0.061	0.091				

τ_4			-0.108	0.927				
ω_4			0.527	0.000				
Dum Crisis			-1.569	0.000				
Trend	0.205	0.000						
	0.940	0.000	0.739	0.000	0.898	0.000	0.965	0.000
Std dvt	0.541		0.157		0.403		0.536	
d_3	0.12297	0.007					0.0795	0.024
d_4	0.07361	0.003			0.10603	0.002	0.10347	0.000

Note: This table presents the estimated parameters and p-values of the deterministic component and the Gram-Charlier pdfs of the series under analysis. The countries in the sample are the Netherlands, the United States (USA), Germany, and Colombia. θ is a constant, C_i, τ_i, ω_i are the amplitude, phase, and frequency of each cycle i.

Figure III.3 Comparison between the frequency histograms of the normalized residuals of the mean model, the normal (solid line), and G.C. (dashed line) probability density functions

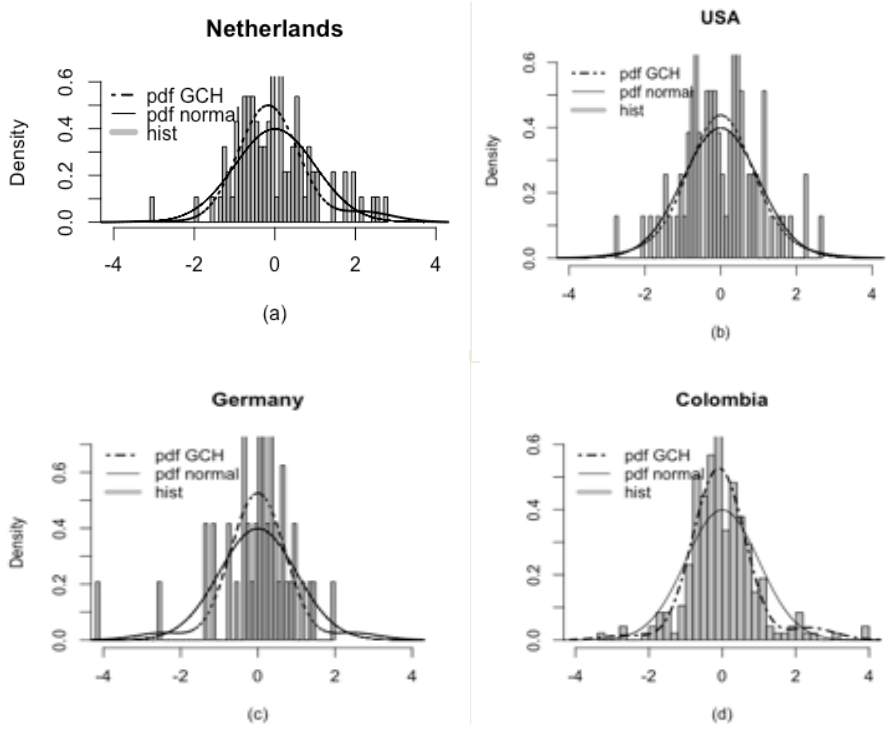

This Figure compares the fits of the normal and the Gram-Charlier pdfs to the frequency histogram of the analyzed series. In general, it is observed that the right tail of the Gram-Charlier pdf is fatter than the normal pdf, except for the USA series, for which no significant differences are observed.

Figure III.4 presents the PBT within one year, estimated from Eq. 5. The minimum solvency levels were arbitrarily set such that the probability was binding. The minimum solvency requirements have varied over time, according to the regulatory changes introduced in the different versions of the Basel Accord. This risk indicator has a cyclical behavior governed

by the estimated mean function. It depends on the estimated standard deviation, skewness, and kurtosis, as well as the speed of mean reversion.

Figure III.4 Estimated series of the probability of breaching the minimum solvency requirements one year ahead

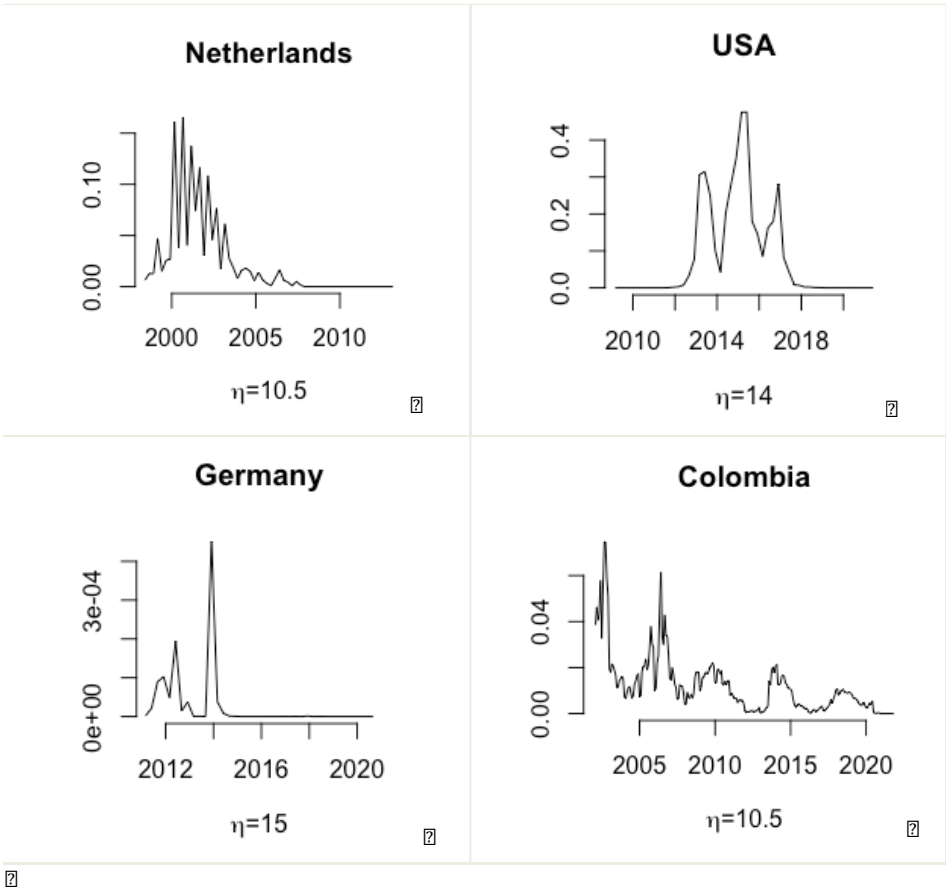

III.4.4 Estimated CCB

Figure III.5 presents the CCB estimated from Eq. 7, assuming that the probability of breaking the minimum solvency requirement threshold within one year is less than or equal to 1%. For the Netherlands and the USA, the required CCB levels decreased markedly after the shock caused by the 2008 crisis. For Germany and Colombia, the required levels of the CCB fluctuate more homogeneously within the analyzed period.

Figure III.5 The Countercyclical Capital Buffer estimated series with parameter α=1% for a time horizon of one year

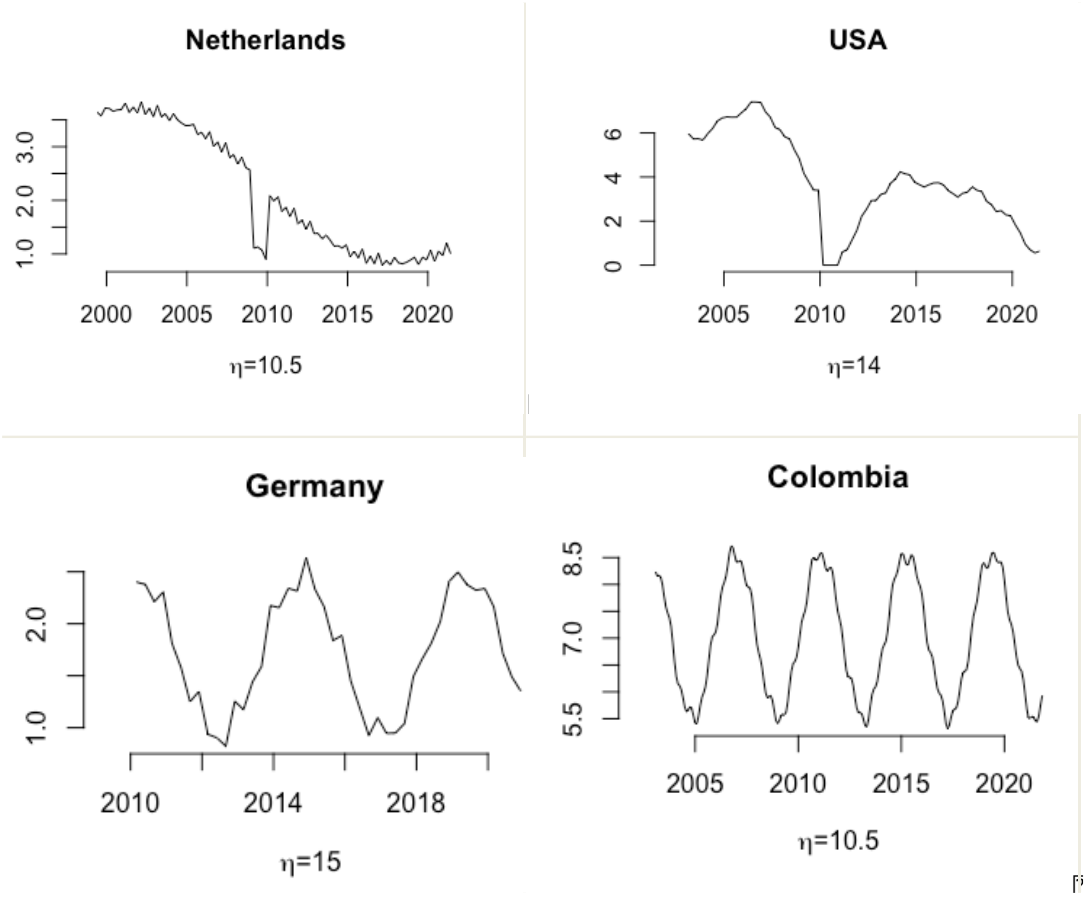

Figure III.6 shows the responses of the probability of breaching the minimum solvency threshold (PBT_0) to monetary policy interest rate shocks (6a, 6c, 6e, and 6g) and the responses of the volume of loans granted by banks to changes in the probability of breaching the minimum solvency threshold (6b, 6d, 6f, and 6h). These results are then obtained from the estimation of Vector Autoregressive (VAR) models where the PBT_0 is chosen as the most endogenous variable. The variables used in the model for each country are the unemployment level indexes, the GDP indexes, the monetary policy interest rate, the level of loans granted by banks, and the inflation indexes with a quarterly frequency. Figures III.6a, 6c, 6e, and 6g show that interest rate raises lead to an increase in PBT_0, although, for Germany and Colombia, the change in PBT_0 is initially negative. For the Netherlands and the USA, the effect of monetary policy interest rate shocks persists up to about two years; for Germany, the effect persists up to about five years; for Colombia, the effect persists for four years. The response of lending volumes to increases in PBT_0 is positive for the USA and negative for

the Netherlands and Germany. Colombia presents a negative response in the first year and a positive one after that, persisting for approximately five years.

Figure III.6 Responses of the probability of breaching the minimum solvency threshold to monetary policy interest rate shocks (6a, 6c, 6e, and 6g). Response of the volume of credit provided by banks to changes in the probability of breaching the minimum solvency threshold (6b, 6d, 6f, and 6h)

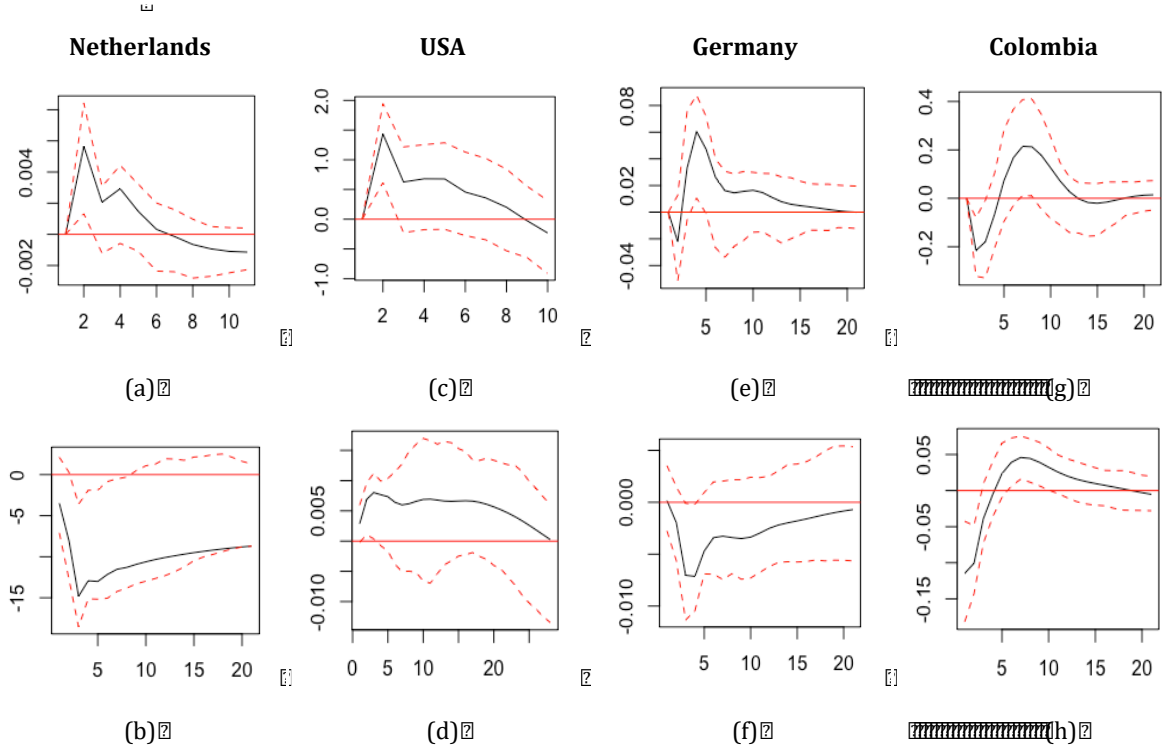

III.5. Conclusions

This article proposes a model to estimate the PBT and the CCB established in the Basel III agreement, considering the cyclical behavior of business that affects bank solvency levels and the characteristics of the bank solvency ratio pdf. As a by-product, and on the basis of a Vector Autoregressive model, the effect of the monetary policy interest rate on the probability of breaching the minimum capital threshold and the effect of this probability on credit granting decisions is discussed.

The results indicate that prudential policies based on the accurate estimation of regulatory Capital are relevant in lending decisions, affecting banks' effectiveness in transmitting

monetary policy. The effect of the interest rate on PBT is a combined effect of the Bank-Capital Channel and the Risk-Taking Channel, referred to as the bank-solvency channel. These channels are key to understand how monetary policy decisions affect financial stability. Monetary policy interest rate shocks affect lending decisions through the effect of the monetary policy interest rate on PBT. This evidence suggests that prudential and monetary policy decisions should be made jointly.

The significance of the skewness and kurtosis parameters proves that the solvency pdfs exhibit heavy tails. Failure to consider these stylized facts leads to under- or overestimating risk, which can affect lending decisions. Given the convergence of CAR to levels that limit insolvency risk and do not make banks' profitability more expensive, the mean reversion assumption underlying the Ornstein-Uhlenbeck processes seems appropriate for CAR modeling.

Determining the CCB through QRMs allows for limiting the risk through insolvency by considering the risk appetite, the distance between the observed solvency and the minimum capital threshold, the volatility of solvency, and the behavior of the tails of its probability distribution. Spectral analysis is a practical methodology for determining insolvency risk and the size of CCB.

The analyzed samples of the bank solvency indicator present short and long-term periodic behaviors. The estimated waves with periods of one year or less can be explained by seasonal effects related to the frequency of accounting reports and distribution of dividends; cycles with periods longer than one year can be associated with phenomena related to business cycles and credit activity. In the analyzed sample, the cycles with the most extended duration also have the most significant variability.

The effects of the monetary policy rate increase the PBT, and the effect persists in the long term. Increases in the PBT negatively affected the credit supply for the Netherlands, Germany, and Colombia, which can be associated with an increase in the cost of Capital. For the USA, increases in interest rates increased lending levels, which may be associated with the higher profitability of loans associated with higher interest rates.

PBT measurement and CCB determination are essential tools for financial institutions and regulators because they help to anticipate potential losses and take preventive measures to avoid insolvency, increase resilience, facilitate effective regulation, and maintain transparency and confidence in the financial system. On the other hand, the analysis of the relationship between the PBT and the monetary policy interest rate is of particular importance for economic regulation, given the effect it has on inflation, investment decisions, consumption, and employment. A change in the interest rate can increase the risk of PBT and decrease banks' capacity as a transmission channel for monetary policy.

A potential limitation of our methodology is the fact that the analyses of the CAR series are performed at a univariate basis. For future research, the multivariate analysis of CAR with macroeconomic variables, such as GDP and the monetary policy interest rate, could allow cross-correlation parameters to identify lags between CAR and economic cycles so that prudential decisions can be made depending on the phases of the economic cycle.

References

Adrian, T., Estrella, A., & Shin, H. S. (2019). Risk-taking channel of monetary policy. *Financial Management*, *48*(3), 725–738. https://doi.org/https://doi.org/10.1111/fima.12256

Aiyar, S., Calomiris, C. W., & Wieladek, T. (2016). How does credit supply respond to monetary policy and bank minimum capital requirements? *European Economic Review*, pp. *82*, 142–165. https://doi.org/https://doi.org/10.1016/j.euroecorev.2015.07.021

Alexander, C. (2008). *Value-at-risk models*. John Wiley & Sons. https://www.wiley.com/en-us/Market+Risk+Analysis%2C+Volume+IV%2C+Value+at+Risk+Models-p-9780470997888

Angeloni, I., & Faia, E. (2013). Capital regulation and monetary policy with fragile banks. *Journal of Monetary Economics*, *60*(3), 311–324. https://doi.org/https://doi.org/10.1016/j.jmoneco.2013.01.003

Athanasoglou, P. P., Daniilidis, I., & Delis, M. D. (2014). Bank procyclicality and output: Issues and policies. *Journal of Economics and Business*, *72*, 58–83. https://doi.org/https://doi.org/10.1016/j.jeconbus.2013.10.003

Basel Committee on Banking Supervision (2004). International convergence of capital measurement and capital standards: A revised framework. *Bank for International Settlements*.

Basel Committee on Banking Supervision (2010): Guidance for national authorities operating the countercyclical capital buffer, December

Basel Committee on Banking Supervision (1988). *International convergence of capital measurement and capital standards*. https://www.bis.org/publ/bcbs04a.pdf

Basel Committee on Banking Supervision (2011). Basel III: A global regulatory framework for more resilient banks and banking systems. *Bank for International Settlements, Basel, Switzerland*. https://www.bis.org/publ/bcbs189.htm

Bernanke, B. S., & Gertler, M. (1995). Inside the black box: The credit channel of monetary policy transmission. *Journal of Economic Perspectives*, *9*(4), 27–48.

Bølviken, E., & Guillen, M. (2017). Risk aggregation in solvency II through recursive log-normals. *Insurance: Mathematics and Economics*, *73*, 20–26. https://doi.org/https://doi.org/10.1016/j.insmatheco.2016.12.006

Borio, C. E. (2008). *The financial turmoil of 2007-?: A preliminary assessment and some policy considerations*. https://www.bis.org/publ/work251.pdf

Borio, C., & Zhu, H. (2012). Capital regulation, risk-taking and monetary policy: A missing link in the transmission mechanism? *Journal of Financial Stability*, *8*(4), 236–251. https://doi.org/https://doi.org/10.1016/j.jfs.2011.12.003

Bruno, V., & Shin, H. S. (2015). Capital flows and the risk-taking channel of monetary policy. *Journal of Monetary Economics*, pp. *71*, 119–132. https://doi.org/https://doi.org/10.1016/j.jmoneco.2014.11.011

Cappelletti, G., Reghezza, A., Rodríguez d'Acri, C., & Spaggiari, M. (2022). Compositional effects of bank capital buffers and interactions with monetary policy. *Journal of Banking & Finance*, *140*, 106530. https://doi.org/https://doi.org/10.1016/j.jbankfin.2022.106530

Cecchetti, S. G., & Li, L. (2008). Do capital adequacy requirements matter for monetary policy? *Economic Inquiry*, *46*(4), 643–659.

Chen, C., & Liu, L.-M. (1993). Joint estimation of model parameters and outlier effects in time series. Journal of the American Statistical Association, 88(421), 284–297. https://doi.org/10.1080/01621459.1993.10594321

Cohen, L. (1998). Generalization of the gram-charlier/edgeworth series and application to time-frequency analysis. *Multidimensional Systems and Signal Processing*, *9*(4), 363–372. https://doi.org/https://doi.org/10.1023/A:1008454223082

Cramér, H. (1925). *On some classes of series used in mathematical statistics* (pp. 329–425). Sixth Scandinavian Congress of Mathematicians.

Davis, A. W. (1976). Statistical distributions in univariate and multivariate Edgeworth populations. *Biometrika*, *63*(3), 661–670. https://doi.org/10.1093/biomet/63.3.661

de Moraes, C. O., Montes, G. C., & Antunes, J. A. P. (2016). How does capital regulation react to monetary policy? New evidence on the risk-taking channel. *Economic Modelling*, pp. *56*, 177–186. https://doi.org/https://doi.org/10.1016/j.econmod.2016.03.025

DELL'ARICCIA, G., LAEVEN, L., & SUAREZ, G. A. (2017). Bank leverage and monetary policy's risk-taking channel: Evidence from the united states. *The Journal of Finance*, *72*(2), 613–654. https://doi.org/https://doi.org/10.1111/jofi.12467

Drehmann, M., & Tsatsaronis, K. (2014). The credit-to-GDP gap and countercyclical capital buffers: Questions and answers. *BIS Quarterly Review March*.

Elliott, G., Rothenberg, T. J., & Stock, J. H. (1996). Efficient tests for an autoregressive unit root. Econometrica, 64(4), 813–836. http://www.jstor.org/stable/2171846

Franses, P. H., & Haldrup, N. (1994). The effects of additive outliers on tests for unit roots and cointegration. Journal of Business & Economic Statistics, 12(4), 471–478. *https://doi.org/10.1080/07350015.1994.10524569*

Galán, J. (2019). Measuring credit-to-GDP gaps. The Hodrick-Prescott filter revisited. *The Hodrick-Prescott Filter Revisited (May 8, 2019). Banco de Espana Occasional Paper*, *1906*.

Gambacorta, L., & Mistrulli, P. E. (2004). Does bank capital affect lending behavior? *Journal of Financial Intermediation*, *13*(4), 436–457. https://doi.org/https://doi.org/10.1016/j.jfi.2004.06.001

Gambacorta, L., & Shin, H. S. (2018). Why bank Capital matters for monetary policy. *Journal of Financial Intermediation*, pp. *35*, 17–29. https://doi.org/https://doi.org/10.1016/j.jfi.2016.09.005

Imbierowicz, B., Löffler, A., & Vogel, U. (2021). The transmission of bank capital requirements and monetary policy to bank lending in Germany. *Review of International Economics*, *29*(1), 144–164. https://doi.org/https://doi.org/10.1111/roie.12500

Jarrow, R. (2013). A leverage ratio rule for capital adequacy. *Journal of Banking & Finance*, *37*(3), 973–976.

Del Brio, E. B., & Perote, J. (2012). Gram–Charlier densities: Maximum likelihood versus the method of moments. *Insurance: Mathematics and Economics*, *51*(3), 531–537. https://doi.org/https://doi.org/10.1016/j.insmatheco.2012.07.005

Kolassa, J. E. (2006). *Series approximation methods in statistics* (Vol. 88). Springer Science & Business Media. https://link.springer.com/book/10.1007/0-387-32227-2

Le Maistre, A., & Planchet, F. (2013). A proposal of interest rate dampener for Solvency II framework introducing a three factors mean reversion model. *ISFA-Laboratory SAF*. https://www.semanticscholar.org/paper/A-proposal-of-interest-rate-dampener-for-Solvency-a-Maistre/00bc83d8d5ebc17e062d86456a67a5ae44d46cfe

Lucia, J. J., & Schwartz, E. S. (2002). Electricity prices and power derivatives: Evidence from the nordic power exchange. *Review of Derivatives Research*, *5*(1), 5–50. https://doi.org/https://doi.org/10.1023/A:1013846631785

Markovic, B. (2006). *Bank capital channels in the monetary transmission mechanism* [Bank of England working papers]. Bank of England. https://EconPapers.repec.org/RePEc:boe:boeewp:313

Merton, R. C. (1974). On the pricing of corporate debt: The risk structure of interest rates. *The Journal of Finance*, *29*(2), 449–470. https://onlinelibrary.wiley.com/doi/10.1111/j.1540-6261.1974.tb03058.x

Russo, V., Lagasio, V., Brogi, M., & Fabozzi, F. J. (2020). Application of the Merton model to estimate the probability of breaching the capital requirements under Basel III rules. *Annals of Finance*, *16*(1), 141–157.

Sandström, A. (2007). Solvency II: Calibration for skewness. *Scandinavian Actuarial Journal*, *2007*(2), 126–134. https://doi.org/10.1080/03461230701250481

Spiegeleer, J. D., Höcht, S., Marquet, I., & Schoutens, W. (2017). CoCo bonds and implied CET1 volatility. *Quantitative Finance*, *17*(6), 813–824. https://doi.org/10.1080/14697688.2016.1249019

Stewart, R., Chowdhury, M., & Arjoon, V. (2021). Interdependencies between regulatory capital, credit extension and economic growth. *Journal of Economics and Business*, *117*, 106010. https://doi.org/10.1016/j.jeconbus.2021.106010

Van den Heuvel, S. (2007). The bank capital channel of monetary policy. *Society for Economic Dynamics 2006 Meeting Papers*, *512*.

CHAPTER IV. Macroprudential Stress Testing Using a Semi-nonparametric Approach

IV.1 Introduction

Monetary policy is today one of the main elements in maintaining economic stability. The central bank strategy of target inflation that seeks to stabilize prices in the economy by controlling the money supply and the reference interest rate has been implemented in different economies globally (Vega & Winkelried, 2005). Within economic stability, the prudential policy plays a fundamental role, given that the financial system is essential for economic transactions and represents the main transmission channel for monetary policy(Claessens, 2015) . A stable financial system efficiently allocates economic resources and manages financial risks, which implies the absorption of losses caused by materializing risks.

The financial crisis in 2007-08, unleashed by the materialization of systemic risks in the banking sector in the United States and some countries globally, have raised the relevance of macroprudential policy to prevent excessive risk-taking in the financial sector and mitigate its potential effects on the real economy (Bengtsson, 2020).. The relationship between the stability of the financial system as a whole and the economy's performance has become a priority for policymakers and academics as the conception of financial stability policy has changed (Ebrahimi Kahou & Lehar, 2017) . After the 2008 financial crisis, the Basel Committee of Banking Supervision (BCBS) recognized in the Basel III accord the importance of macroprudential policies and, particularly, (i) the provision of countercyclical capital buffers and additional buffers for the most systemically entities at the global and local level; and (ii) the implementation of stress testing as a fundamental risk management tool for banking supervisors and macroprudential authorities(Committee, 2018).

Le Quang & Scialom (2022) argue that before the crisis, it was assumed that the combination of microprudential policies based on the individual stability of financial institutions and monetary policies that kept inflation under control was sufficient to ensure financial stability..

Borio (2003) makes a comparison between micro and macroprudential perspectives, noting that while the microprudential perspective aims to limit the risks of individual institutions in order to protect depositors and investors, the macroprudential policy aims to limit risks in the financial system to avoid the costs generated by banking instability on economic growth. In addition, it is crucial to consider correlation and common exposures across the system from the macroprudential perspective.

At the beginning of the 2020s, financial stability had to face the effect of the coronavirus pandemic (COVID-19), where policymakers adopted expansionary monetary policy regimes to ensure a sufficient supply of credit, which caused a generalized increase in leverage levels and a substantial decline in creditworthiness (Rendón et al., 2021). Subsequently, inflation globally began to accelerate, driven mainly by low-interest rates, the climate crisis, the war in Ukraine, and increased geopolitical risks caused by political tensions between China and the United States (IMF,2023).

In response, central banks rapidly increased monetary policy interest rates. For example, the US Federal Reserve's interest rate rose from 0.25% to 5% between the first quarter of 2022 and the first quarter of 2023. This situation has led to banking instability, which has resulted in a decrease in liquidity and bank solvency, and the collapse of Silicon Valley Bank (SVB) in early 2023. SVB had concentrated most of its assets in fixed-income instruments, such as US Treasury bonds. These bonds fell sharply in value as interest rates rose. When they were required to meet the demand for liquidity generated by deposit withdrawals that exceeded cash reserves, they realized losses that undermined the confidence of their customers, leading to a run on the banks. The collapse of SVB increased systemic risk, with consequences for other banks, such as Signature Bank, which also had to be closed. In April 2023, First Republic Bank (FRB) collapsed for similar reasons to SVB, having to be intervened by the Federal Deposit Insurance Corporation (FDIC), which as a rescue strategy, allowed the acquisition of FRB by JP Morgan Chase.

The International Monetary Fund in the Global Financial Stability Report published in April 2023 (IMF, 2023) lays out the challenge for policymakers to safeguard financial stability in an environment of high inflation, high geopolitical risks, and fragile financial market confidence. Le Quang & Scialom (2022) argue that, although the 2007-08 crisis has prompted

a renewal of financial regulation toward adopting macroprudential policies, this regulation is still incomplete, failing to consider extreme external risks such as a pandemic, geopolitical or climate risks. Borio & White (2004) posits the need to modify the current monetary and prudential policy frameworks to mutually reinforce price and financial stability to prevent financial imbalances that might jeopardize the objectives of both policies.

In this context, monetary and prudential policy decisions are linked. Monetary policy must consider the capital constraints due to the composition of the risk and liquidity portfolios of the banks used as transmission channels. On the other hand, prudential policy should be set, considering the needs of monetary policy transmission. Formulating macroprudential policies requires methodologies allowing adequate systemic risk measurement in both its cross-sectional and time series dimensions (Borio, 2003). In its cross-sectional dimension, it is required to establish the connection between financial entities and their contribution to the systemic risk – see Adrian & Brunnermeier (2011) for a VaR measure based on the marginal contributions of financial entities to systemic risk. The time series dimension is also relevant for measuring the procyclicality between macrofinancial stability indicators and macroeconomic variables.

This paper proposes a methodology for conducting macroprudential stress tests, focusing on the joint modeling of the probability distributions of a leverage indicator (used as an indicator of the stability of a financial system) and the monetary policy interest rate (as a variable that can affect the stability of a financial system). For modeling the dynamics between variables and their probability distributions, we use the Dynamic Conditional Correlation - Semi-nonparametric (DCC-SNP) model that allows modeling stylized facts such as the skewness and kurtosis of the marginal probability density function (pdf) and the dynamic conditional correlation between variables. In addition, bivariate spectral analysis is applied to analyze the cyclical dynamics between interest rate and bank leverage. As an application case, we use the monthly series of the ratio of equity to total assets of US commercial banks as an indicator of leverage and the 3-month Treasury Bill as an indicator of the interest rate to estimate the model parameters. Finally, we performed macroprudential stress tests of the impact of the interest rate on the leverage indicator for a 5-year horizon, using Monte Carlo simulations. We find that, for the projection period, high and low-interest rate scenarios increase leverage, while a medium-rate scenario has a decreasing effect on bank leverage.

The Dynamic Conditional Correlation (DCC) model (Engle, 2002) is one of the most successful approaches to parameterizing the variance-covariance matrix. This model presents the dependence structure in a parsimonious way. However, its extension beyond the normality assumption is not trivial. Therefore, different solutions have been provided to model the non-Gaussian multivariate distribution (Engle & Gonzalez-Rivera, 1991; Engle & Sheppard, 2001; Bauwens, Laurent, & Rombouts, 2006). Another approach is the semi-nonparametric approach (SNP) corresponding to an extension of the multivariate Gaussian through the Gram-Charlier series that are valid asymptotic approximations to any empirical distribution under regularity conditions (Sargan, 1975; Phillips, 1977). In the field of finance, different authors have used a multivariate SNP extension to capture the distribution of financial returns, with a applications to different fields, including risk quantification or cryptocurrency portfolios (Mauleón, 2003; Mauleón, 2006; Del Brio et al., 2011; Mora-Valencia, 2017; Jiménez et al., 2020).

Stress testing encompasses different methodologies that can be performed at different degrees of portfolio aggregation, ranging from the individual analysis of an asset to an institutional and systemic level of aggregation that assesses the effects of possible extreme macroeconomic stress events. The Basel Committee on Banking Supervision (BCBS) published 2018 a document that updates the guidelines for conducting stress tests as a tool for risk management and informing business decision-making. This document states that the models and methodologies to assess the impact of different macroeconomic scenarios must have the appropriate level of sophistication to achieve the objectives of the exercise and for the importance of the portfolios that these models are monitored (BCBS, 2018).

Stress tests are performed on various indicators that evaluate a financial institution's capacity to withstand adverse market shocks. The leading indicators used include (i) the Capital Adequacy Ratio, which is a solvency indicator calculated as the ratio between Tier Capital and risk-weighted assets; (ii) liquidity indicators that measure the capacity of a financial institution to meet its short-term obligations without incurring losses from the liquidation of assets; and (iii) the Leverage Ratio, which measures the ratio between Tier Capital and total non-risk-weighted assets. These indicators are subject to adverse shocks related to interest rate changes, increases in credit default levels, and increased market risks.

The results show that stress tests should consider the asymmetries and heavy tails of the pdfs associated with financial stability indicators and the dynamics of the correlation between financial stability indicators and macroeconomic variables.

The remainder of this article is organized as follows: Section 2 presents the methodology employed, including the mathematical model and the methodology for parameter estimation. Section 3 presents an application case for the United States, discussing the results on the model estimation and the stress testing analysis of different interest rate scenarios. Finally, concluding remarks and recommendations are presented in the last section.

IV.2. Methodology

IV2.1 Stochastic process

Let the interest rate and the leverage ratio (LR) follow a multivariate Ornstein-Uhlenbeck stochastic process as expressed in equation 1,

$$Y_t = \mu(t) + X_t, \tag{1}$$

where Y_t is a multi-dimensional vector representing the interest rate, and LR. $\mu(t)$ is a multi-dimensional vector containing deterministic functions in the time domain for each variable and X_t is a multi-dimensional stochastic process governed by a Stochastic Differential Equation (SDE) described below.

$$dX_t = -\kappa X_t dt + \sigma dW_t, \tag{2}$$

where κ y σ are real square matrices of order d, and W_t is a standard Wiener process. Therefore, it follows that

$$dX_t = \kappa(\mu(t) - X_t)dt + \sigma dW_t, \tag{3}$$

and, according to Vatiwutipong & Phewchean (2019), the conditional mean and variance of the process are given in equation 4:

$$M_0(t) = E(Y_t/X_0) = (I - e^{-\kappa t})\mu(t) + (X_0)e^{-\kappa(t)}$$

$$X_0 = Y_0 - \mu(0)$$

$$\Sigma_0(t) = var(Y_t/X_0) = \int_0^t e^{\kappa(t-s)}\,\sigma\sigma^T e^{\kappa^T(s-t)} ds. \tag{4}$$

The joint pdf of Y_t is

$$f(Y_t) = \frac{exp\left(-\frac{1}{2}\left(Y_t - M_0(t)\right)^T)\Sigma_0^{-1}(t)\left(Y_t - M_0(t)\right)\right)}{\sqrt{|2\pi\Sigma_0(t)|}}, \tag{5}$$

and each component $\mu_i(t)$ of the vector $\mu(t)$ can be expressed as in equation 6:

$$\mu_i(t) = \alpha_i + \sum_{j=0}^{n} C_{ji} * cos\left(\tau_{ji} + \frac{\omega_{ji} 2\pi * t}{T}\right), \tag{6}$$

where α_i is a constant; $C_{ji}, \tau_{ji},$ and ω_{ji} are the amplitude, phase, and frequency of each wave component; and T is the number of observed periods per year.

IV.2.2 Joint DCC-SNP density function.

The multivariate Ornstein-Uhlenbeck stochastic process assumes that the pdf presented in equation 5 is a multivariate normal distribution with constant variance-covariance matrix. In order to capture stylized facts of the marginal distributions of the interest rate and LR, such as skewness and kurtosis, and the correlation dynamics, we use the DCC-SNP model proposed by Del Brio et al. (2011) and Jiménez et al. (2020), which generalizes the Dynamic Conditional Correlation model proposed by Engle (2002), from the Taylor series expansion of the characteristic function of the gaussian pdf, which allows the estimation of parameters for the upper moments of the marginal pdfs.

Following the vector notation proposed by Dharmani (2018), we define $Y_t = (y_1, y_2, \ldots, y_d)$ as a d-dimensional random vector, and $f(Y_t)$ being the joint pdf associated with Y_t. The characteristic function $\mathcal{F}(\beta)$ associated with Y_t is defined as the expected value of $e^{iY_t'\beta}$, with i being the imaginary unit and $\beta = (\beta_1, \beta_2, \ldots, \beta_d) \in \mathbb{R}^{d.}$

$$\mathcal{F}(\beta) = E\left[e^{i\beta Y_t'}\right] = \int_{-\infty}^{\infty} \ldots \int_{-\infty}^{\infty} e^{i\beta Y_t'} f(Y_t) dY_t. \tag{7}$$

Expanding $\mathcal{F}(\beta)$ as a Maclaurin series, we have that

$$\mathcal{F}(\beta) = \sum_{j=0}^{\infty} c_j' \frac{(i\beta)^{\otimes j}}{j!} = exp\left[\sum_{j=1}^{\infty} \kappa_j' \frac{(i\beta)^{\otimes j}}{j!}\right], \tag{8}$$

where c_j and κ_j correspond to the vector of moments and the vector of cumulants of order j, respectively, $\otimes$ is the Kronecker product operator and $(.)^{\otimes j} = (.) \otimes (.) \otimes \ldots \otimes (.)$ (j times).

Let the differential operator ∇_Y and its adjoint $\nabla_Y^{\dagger}$ be

$$\nabla_Y = \left(\frac{\partial}{\partial y_1}, \frac{\partial}{\partial y_2}\right)' \text{ and } \quad \nabla_Y^{\dagger} = \left(-\frac{\partial}{\partial y_1}, -\frac{\partial}{\partial y_2}\right)'. \tag{9}$$

Assuming that function $f(Y_t)$ is differentiable m times, the Kronecker product between ∇_Y and $f(Y_{t.})$ is

$$\nabla_Y^{\otimes} f(Y_t) = Vec\left(\frac{\partial f}{\partial Y_t}\right) \quad ", \tag{10}$$

where $\nabla_Y^{\otimes}$ is the Kronecker derivative operator, and Vec is an operator that converts the $m \times d$ matrix into a column vector $md \times 1$.

Following Cohen (1998), given two joint density functions $f(Y_t)$ and $g(Y_t)$, and their respective characteristic functions $\zeta_f(\beta)$ and $\zeta_g(\beta)$ and these can be related through a $\Psi(\beta)$ kernel that is a function of the two pdfs, such that

$$\Psi(\beta) = \frac{\zeta_g(i\beta)}{\zeta_f(i\beta)}. \tag{11}$$

Given the properties of the derivative of the Fourier transform, where $\nabla_Y^{\dagger} exp\left(-i\beta Y_t^{'}\right) = -i\beta * exp\left(-i\beta Y_t \quad\right)'$, the differential operator $\nabla_Y^{\dagger}$ that can replace $-i\beta$:

$$g(Y_t) = \Psi\left(\nabla_Y^{\dagger}\right) f(Y_t). \tag{12}$$

The kernel Ψ and f are orthogonal.

$$g(Y_t) = \frac{\zeta_g(\beta)}{\zeta_f(\beta)} f(Y_t), \tag{13}$$

$$g(Y_t) = exp\left[\sum_{j=1}^{\infty}\left(\kappa_j^g - \kappa_j^f\right)' \frac{(i\beta)^{\otimes j}}{j!}\right] f(Y_t), \tag{14}$$

$$g(Y_t) = \sum_{j=0}^{\infty}\left(c_j^g - c_j^f\right)' \frac{\nabla_Y^{\dagger\otimes j}}{j!} f(Y_t) = exp\left[\sum_{j=1}^{\infty}\left(\kappa_j^g - \kappa_j^f\right)' \frac{\nabla_Y^{\dagger\otimes j}}{j!}\right] f(Y_t). \tag{15}$$

If $\Phi(Y_t)$ is the multivariate normal distribution and assuming $\kappa_1^g = \kappa_1^{\Phi}, \kappa_2^g = \kappa_2^{\Phi}$ and knowing that $\kappa_{j>2}^{\Phi} = 0$

$$g(Y_t) = \left[\sum_{j=3}^{\infty}(c^g)' \frac{\nabla_Y^{\dagger\otimes j}}{j!}\right] \Phi(Y_t). \tag{16}$$

For empirical applications of the model, the orthogonality property of Ψ concerning Φ allows the kernel to be truncated to finite order J, thus

$$g(Y_t) = \left[\sum_{j=3}^{J}(c^g)' \frac{\nabla_Y^{\dagger\otimes j}}{j!}\right] \Phi(Y_t) \tag{17}$$

In general,

$$H_j = \frac{\nabla_Y^{\dagger\otimes j}\Phi(Y_t)}{\Phi(Y_t)}. \tag{18}$$

H_j corresponds to a vector of polynomial functions known as Hermite Polynomials (HPs), such that:

$$g(Y_t) = \left[\sum_{j=3}^{J}\frac{\left(c_j^g\right)'}{j!}\right] H_j\Phi(Y_t). \tag{19}$$

The pdf $g(Y_t)$ is known as the multivariate Gram Charlier Type A distribution.

For empirical applications, Del Brio et al,(2011) and Jiménez et al. (2020) formulate in terms of the product of the marginal Gram-Charlier distributions of each component of Y_t,

$$g(Y_t) = \frac{1}{d}\prod_{m=1}^{d}\phi\,(y_{mt})\sum_{m=1}^{d}\mathcal{H}_m\,(y_{mt}) = \frac{1}{d}\Phi(Y_t)\sum_{m=1}^{d}\mathcal{H}_m\,(y_{mt}), \qquad (20)$$

where $\phi(y_{mt})$ corresponds to the standard normal pdf, and $\mathcal{H}_m(y_{mt})$ is a *j*-order Gram-Charlier expansion (without loss of generality, the same *J* is considered for all dimensions) expressed in terms of the HPs:

$$\mathcal{H}_m(y_{mt}) = \left[1 + \sum_{j=2}^{J}\delta_{jm}\,h_m(y_{mt})\right], \qquad (21)$$

$$h_j(y_{mt}) = \frac{D_Y^{\dagger(j)}\phi(y_{mt})}{\phi(y_{mt})}, \qquad (22)$$

where $D_Y^{\dagger} = -\frac{d}{dy}$.

To avoid possible negativity problems in the truncated Gram-Charlier pdf, one could use the modification proposed by Ñíguez & Perote (2012)and presented in Equation 23. This transformation can be necessary when applying backtesting techniques:

$$\mathcal{H}_m(y_{mt}) = \frac{1}{1 + \sum_{j=2}^{J} j\,!\,\delta_{jm}^2}\left[1 + \sum_{j=2}^{J}\delta_{jm}^2\,h_j(y_{mt})^2\right]. \qquad (23)$$

HPs satisfy the well-known orthogonality properties,

$$\int_{-\infty}^{\infty} h_j\,(y_{mt})\phi(y_{mt}) = 0, \quad \forall j > 0. \qquad (24)$$

$$\int_{-\infty}^{\infty} h_j\,(y_{mt})h_n(y_{mt})\phi(y_{mt})dy_{mt} = \begin{cases} 0, & \forall j \neq n, \\ j!, & \forall j = n, \end{cases} \qquad (25)$$

$$\int_{-\infty}^{\infty} h_j\,(y_{mt})^2 h_n(y_{mt})^2\phi(y_{mt})dy_{mt} = j!\,n!, \quad j \neq n. \qquad (26)$$

Given the orthogonality condition HPs multivariate SNP distributions satisfy specific properties presented in Del Brio et al., (2011), among which it is stated that the marginal pdfs are also Gram-Charlier. The marginal pdf is expressed as in equation 27, considering equation 23.

$$g_m(y_{mt}) = \phi(y_{mt})\left[\frac{d-1}{d} + \frac{1}{d}\left(\frac{1}{1+\sum_{j=2}^{J} j!\delta_{jm}^2}\left[1 + \sum_{j=2}^{J} \delta_{jm}^2\, h_m(y_{mt})^2\right]\right)\right] \quad (27)$$

Another property of multivariate Gram-Charlier pdf is that the linear transformations and combinations are also Gram-Charlier distributed. This property is exploited to incorporate the correlation between variables. Given the linear transformation $\mathcal{U}_t = \mathrm{R}_t^{1/2}\mathrm{Y}_t$ with zero mean and variance-covariance matrix Σ_t that can be decomposed in terms of a diagonal matrix of the conditional standard deviations $D_t = diag[\sigma_{1t}, \sigma_{2t}, \ldots, \sigma_{dt}]$ and the correlation matrix R_t, as presented in equation 28.

$$\Sigma_t = D_t R_t D_t = D_t R_t^{1/2} R_t^{1/2} D_t \quad , \quad (28)$$

where $R = R^{1/2}R^{1/2}$ is a symmetric spectral decomposition. Given the standard vector $\epsilon_t = D_t^{-1}\mathcal{U}_t$, its multivariate SNP density can be expressed as

$$F(\epsilon_t) = (2\pi)^{-\frac{j}{2}}|R_t|^{-\frac{1}{2}} exp\left[-\frac{1}{2}\epsilon' R^{-1}\epsilon\right] \times \frac{1}{d}\left[\sum_{m=1}^{d} \mathcal{H}_m\,(y_m)\left(R^{-\frac{1}{2}}\epsilon\right)\right]. \quad (29)$$

IV.2.3 The Dynamic Conditional Correlation Model.

Engle (2002) introduces a new class of multivariate Gaussian GARCH model, and its estimators called dynamic conditional correlation or DCC from the variance-covariance matrix decomposition in equation 28. Equations 30, 31, 32, 33 and 34 present the statistical specification of the DCC model. ι is a vector of ones A, B, and $\iota' - A - B$ are positive definite matrices and $\circ$ is the Hadamard product obtained by multiplying element by element two matrices of the same size.

For a d-dimensional vector Y_t the full DCC model can be parameterized as follows:

$$Y_t \mid \Omega_{t-1} \sim N(0, D_t R_t D_t), \quad (30)$$

$$D_t^2 = diag\{\omega_i\} + diag\{\omega_i\} \circ Y_{t-1}Y_{t-1}' + diag\{\lambda_i\} \circ D_{t-1}^2, \quad (31)$$

$$\epsilon = D^{-1}\mathcal{U}. \quad (32)$$

$$Q_t = S \circ (\iota\iota' - A - B) + A \circ \epsilon_{t-1}\epsilon_{t-1}^{'} + B \circ Q_{t-1}, \quad (33)$$

$$R_t = diag\{Q_t\}^{-1} Q_t diag\{Q_t\}^{-1}. \quad (34)$$

Let the parameters in D be denoted by θ, and the other parameters in *R* be denoted by ρ. The log-likelihood can be written as the sum of volatility and correlation components.

$$L(\theta, \rho) = L_v(\theta) + L_c(\theta, \rho). \quad (35)$$

Del Brio et al. (2011) propose the DCC-SNP model where the shape parameters (γ) are estimated jointly with those of the correlation component, allowing estimation in two stages: In the first stage, the dynamic variances of the d variables are fitted, and in the second stage the correlation parameters and the shape parameters are estimated by maximizing the log-likelihood $L_{CSNP}(\theta, \varphi)$, $\varphi = (\rho, \gamma)$.

IV.2.4 Parameter estimation.

Deterministic Component

To model the deterministic component $\mu(t)$, we used harmonic analysis, which allows for representing a time series as a trigonometric Fourier series, as expressed in equation 6. To estimate the frequency parameters, we used the cross-spectrum, which corresponds to the Fourier transform of the cross-correlation function and determines the relationship of two-time series in the frequency domain from the contribution of each spectral component to the total correlation. The contribution is estimated as the modulus of the complex number resulting from the transformation. The cross-spectrum can be plotted on a contour plot.

For the estimation of the amplitude, phase, and reversion-to-mean parameters (parameter k of equations 2 and 3) of each spectral component, the nonlinear least squares (NLS) method suggested by Lucia & Schwartz (2002) is used.

Estimation of dynamic variance, correlation, and shape parameters.

The conditional variance, dynamic conditional correlation and the shape parameters are estimated by maximum likelihood method, given the log-likelihood functions in Equations 36 and 37 and the two-step procedure described in the above section.

$$L_V(\theta) = -\frac{1}{2}\sum_{m=1}^{d}\left[T ln(2\pi) + \sum_{t=1}^{T} l\, n(\sigma_{mt}^2) + \frac{(y_{mt} - \mu_{mt})^2}{\sigma_{mt}^2}\right], \qquad (36)$$

$$L_{CSNP}(\theta, \varphi) = \sum_{t=1}^{T}\{ ln\left[\sum_{m=1}^{d} \mathcal{H}_m\,(y_m)\left(R_t^{-1/2}\epsilon_t\right)\right] - \frac{1}{2}\left(ln|R_t| + \epsilon_t^{'} R_t^{-1}\epsilon_t\right)\}. \qquad (37)$$

IV.3 Empirical application

Description of the data.

The proposed methodology is applied to monthly series of the Leverage Ratio of all US commercial banks from January 2000 until February 2023, calculated as the ratio between total equity (difference between total assets and total liabilities) and total assets of all commercial banks, not seasonally adjusted and extracted from the Federal Reserve Bank of St Louis and the US.

According to BCBS (2014), the leverage ratio is calculated based on Tier capital. We use total equity since the Tier time series is published at quarterly basis, which provides little data for estimation. Comparing the quarterly Tier 1 Leverage Capital series published by the Federal Reserve Bank with the total capital series, they correlate over 99%, and Tier 1 is, on average, 92% of total capital. The benchmark monetary policy interest rate in the United States is the Federal Funds Effective Rate (FFER), which is calculated as a weighted average of the rates at which depository institutions exchange federal funds with each other overnight. It is market-determined but is influenced by the Federal Reserve through open market operations to achieve the Fed's target rates. This series remains constant during some sample periods. Therefore, we used the 3-month Treasury bill secondary market rate to proxy the monetary policy rate. This variable exhibits variations for all periods and correlates more than 99% with FFER.

IV. 4 Results

Figure IV.1 shows the interest rate and LR evolution from January 2000 to February 2023. It can be seen that in 2000 the interest rate (Figure IV.1.a) had values close to 6% per annum and that by 2001 it fell rapidly to a level close to 1.6%, which implies a decrease of more than 70% in its value, while the LR had an increase of approximately 9% for this same period. From 2002 until 2004, the rate continued to fall to levels close to zero, from where it began to rise again in an accelerated manner, until the beginning of 2007, reaching levels close to 5%, to then fall again to levels close to zero that were maintained until 2017 where the interest rate began to rise to levels above 2% until the end of 2019.

The LR maintained an increasing trend until the end of 2008, when a sudden drop was observed. However, it quickly returned to growth until the beginning of 2012, when it reached a maximum of 11.58% and then remained at levels close to 11% until the beginning of 2020, when an accelerated drop was observed, reaching levels close to 9% by the end of 2022, which implied a decrease in the LR value of approximately 20%. Although the average correlation between the interest rate and LR is about -50%, the evolution of the interest rate and LR presents different relationships between their trends, showing that the relationship is positive in some time intervals; but negative in others. The interest rate can affect the LR both for the equity and for the assets. On the one hand, equity is sensitive to the cost of capital, which depends directly on the interest rates of the economy. On the other hand, bank assets are affected by the interest rate through the sensitivity of credit demand to the interest rate or through changes in the value of assets in the investment portfolio, such as bonds, stocks, and other types of financial instruments that depend on the interest rate.

Figure IV.1 Monthly evolution of interest rate and Leverage Ratio

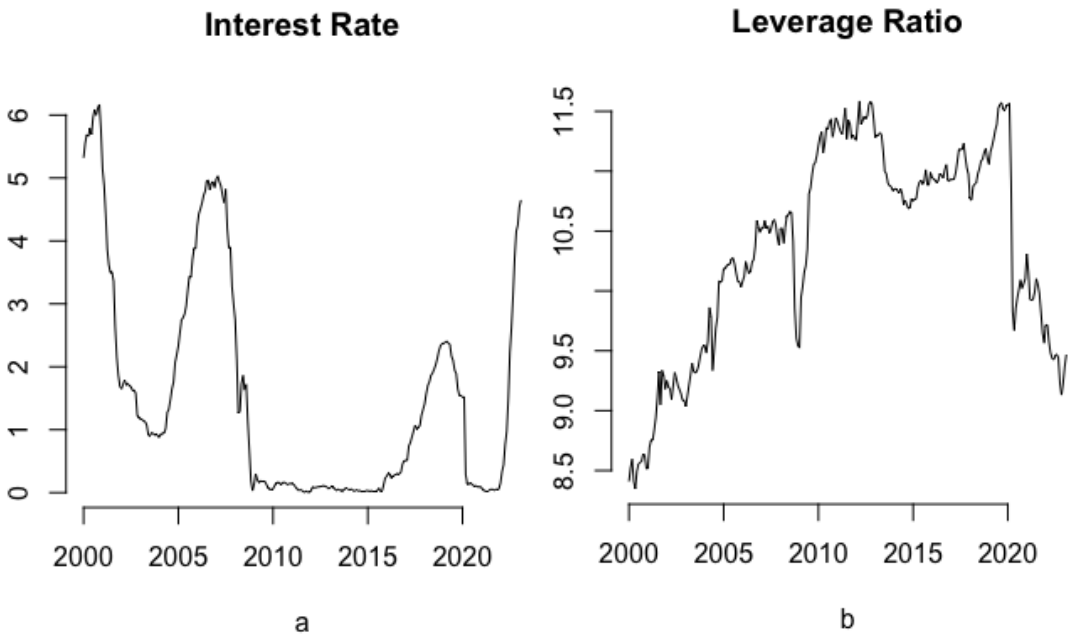

Table IV.1 presents the descriptive statistics for the interest rate and LR. The minimum interest rate is close to zero. This value corresponds to the period starting after the 2008 crisis, where a near-zero interest rate regime was maintained until the beginning of 2017. The maximum value is close to 6% and is found at the beginning of the series. The monthly average interest rate has been 1.5%, and its monthly volatility is 1.75%. The skewness parameter indicates right tail skewness and excess kurtosis is close to zero. LR has ranged from 8.35% to 11.6% and averaged 10.4% with monthly volatility of 0.86%. The skewness and excess kurtosis are close to zero.

Table IV.1 Descriptive statistics for Interest Rate and LR

	Max	Min	Mean	Std	Skew	K
Interest Rate	6.170	0.010	1.545	1.751	1.079	-0.018
LR	11.586	8.349	10.365	0.859	-0.511	-0.821

Note: This table shows the descriptive statistics for the Interest Rate and Leverage Ratio. Max and Max correspond to the maximum and minimum value, respectively. Std=standard deviation, Skew=skewness, K=excess kurtosis coefficient.

Figure IV.2 depicts the cross-periodogram between interest rate and LR. The horizontal axis corresponds to the annual frequencies of LR, and the vertical axis corresponds to the annual frequencies of the interest rate. The contour map corresponds to the modulus of the complex value corresponding to the cross-periodogram between the interest rate and LR, where the warmer colored areas represent the absolute and local maxima of the cross-periodogram function. In comparison, the darker areas correspond to the minimum values. Figure IV.2.a shows a maximum at a frequency of 0.04 cycles per year (24-year period) and a maximum at a frequency of 0.17 cycles per year, corresponding to a cycle of 6 years. Figures IV.2.a, 2.b, 2.c, and 2.d show other local maxima at frequencies near 0.8, 1.3, and 2, among other local maxima. The maxima of the function indicate the frequencies at which the interest rate and LR are most closely related.

Figure IV.2 Cross Periodogram Interest Rate and Leverage Ratio

a

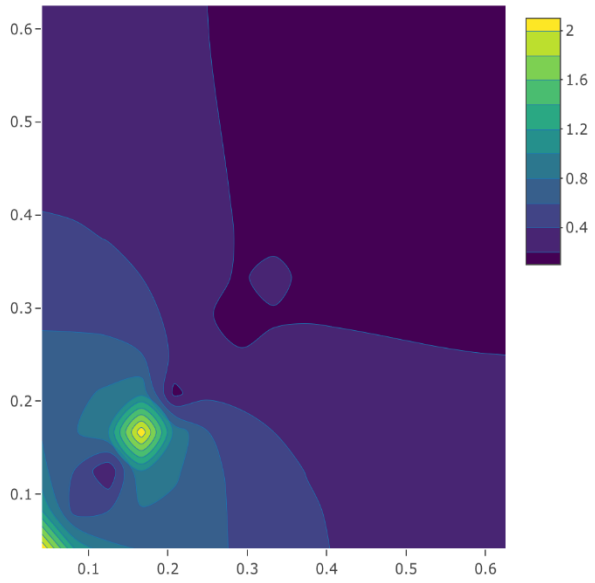

b

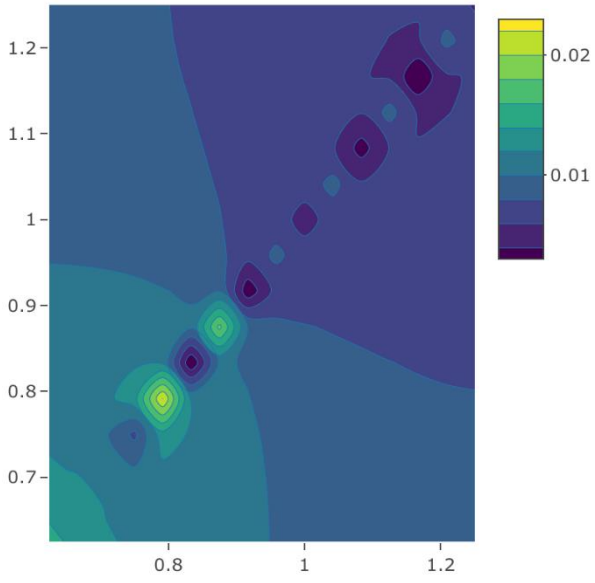

c

d

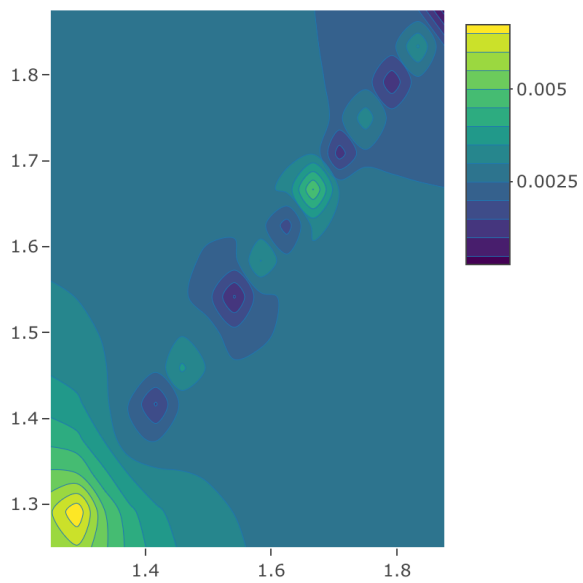

c.

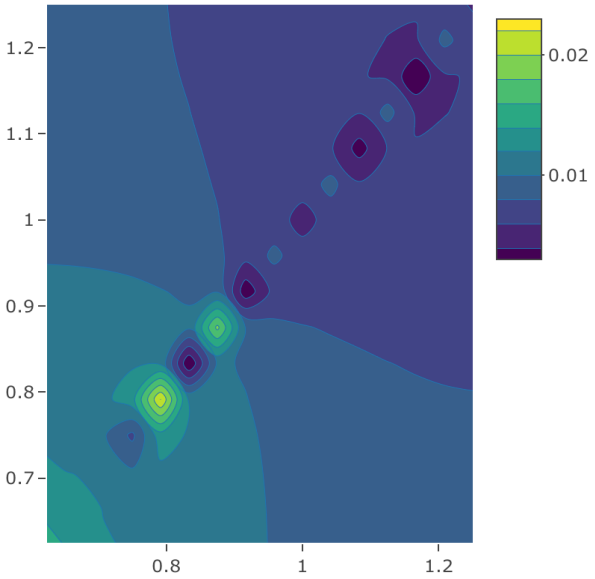

d.

Table IV.2 shows the amplitude and phase parameters for 14 different frequencies determined from the interest rate and LR cross-periodogram. The frequencies with the highest amplitudes for the interest rate and LR are those of the annual frequencies 0.167, 0.042, and 0.125, corresponding to periods of 6, 24, and 8 years, respectively. The high-frequency spectra tend to have lower amplitudes.

Table IV.2 Estimated parameters for the moments of the pdfs and the correlation of interest rate and LR

	Interest Rate				Leverage Ratio			
	Estimate	Std. Error	t value	p-value	Estimate	Std. Error	t value	p-value
α_i	1.699	0.041	40.973	0.000	10.403	0.098	105.933	0.000
ω_1				0.167				0.167
C_1	-1.665	0.059	-28.187	0.000	-0.219	0.093	-2.354	0.019
τ_1	2.648	0.034	78.414	0.000	2.780	0.408	6.815	0.000
ω_2				0.042				0.042
C_2	-1.706	0.059	-28.696	0.000	-0.931	0.139	-6.684	0.000
τ_2	2.535	0.034	75.381	0.000	12.071	0.137	88.138	0.000
ω_3				0.125				0.125
C_3	1.193	0.06	19.858	1.193	0.234	0.105	2.238	0.026
τ_3	6.439	0.045	142.694	6.439	-9.081	0.455	-19.980	0.000
ω_4				0.250				0.33
C_4	-0.484	0.050	-9.606	0.000	0.116	0.057	2.048	0.042
τ_4	4.272	0.105	40.504	0.000	3.408	0.477	7.144	0.000
ω_5				0.2				0.42
C_5	-0.495	0.058	-8.569	0.000	0.128	0.045	2.827	0.005

τ_5	3.305	0.113	29.279	0.000	-1.220	0.357	-3.422	0.001
ω_6				0.5				0.5
C_6	-0.168	0.039	-4.353	0.000	0.096	0.039	2.465	0.014
τ_6	-0.175	0.231	-0.759	0.449	-18.141	0.403	-45.033	0.000
ω_7				0.29				0.7
C_7	0.228	0.050	4.556	0.000	0.085	0.029	2.945	0.004
τ_7	0.438	0.207	2.118	0.035	-87.264	0.341	-256.014	0.000
ω_8				0.46				0.95
C_8	-0.125	0.041	-3.061	0.002	-0.048	0.021	-2.273	0.024
τ_8	-0.062	0.320	-0.192	0.848	3.792	0.440	8.616	0.000
ω_9				0.54				1.5
C_9	0.138	0.037	3.733	0.000	0.026	0.014	1.907	0.058
τ_9	-2.975	0.267	-11.126	0.000	-0.330	0.522	-0.632	0.528
ω_{10}				0.63				0.63
C_{10}	-0.059	0.033	-1.787	0.075	0.090	0.032	2.844	0.005
τ_{10}	0.033	0.557	0.059	0.953	-1.466	0.354	-4.147	0.000
ω_{11}				1.12				1.2
C_{11}	-0.041	0.021	-1.960	0.051	0.051	0.017	2.999	0.003
τ_{11}	-0.251	0.509	-0.492	0.623	-0.134	0.332	-0.404	0.687
ω_{12}				2				2
C_{12}	0.032	0.013	2.495	0.013	0.031	0.010	3.002	0.003
τ_{12}	-0.464	0.399	-1.162	0.246	-1.292	0.333	-3.875	0.000
ω_{13}				0.58				3.16
C_{13}	-0.120	0.036	-3.383	0.001	-0.019	0.007	-2.693	0.008
τ_{13}	-11.850	0.294	-40.322	0.000	-0.092	0.372	-0.248	0.804
ω_{14}				4				4.04
C_{14}	-0.018	0.007	-2.442	0.015	0.011	0.006	1.852	0.065
τ_{14}	-10.886	0.409	-26.629	0.000	17.461	0.539	32.393	0.000
1-κ	0.794	0.038	20.807	0.000	0.925	0.022	41.835	0.000
θ_0	0.001	0.000	2.772	0.006	0.002	0.001	1.606	0.108
θ_1 (ARCH)	0.457	0.107	4.253	0.000	0.349	0.101	3.445	0.001
θ_2 (GARCH)	0.523	0.084	6.209	0.000	0.506	0.168	3.015	0.003
δ 3	-0.037	0.060	-0.617	0.537	-0.019	0.063	-0.298	0.766
δ 4	0.096	0.032	3.018	0.003	0.090	0.031	2.937	0.003
ρ_1	0.636	0.235	2.709	0.007				
ρ_2	0.087	0.047	1.865	0.062				

Note: This table shows the amplitude and phase parameters for 14 different frequencies determined from the Interest Rate and Leverage Rate cross-periodogram.

Figure IV.3 shows the monthly series of the spectral components with periods of 6, 24, and 8 years (figures IV.3.a, 3.b, and 3.c, respectively), which are the components that explain the most significant variability (given that the estimated amplitudes), and the series of the sum of the entire estimated spectrum (Figure IV.3.d) of the interest rate (continuous line) and the LR (dotted line).

This graph allows us to analyze the relationship between interest rates and LR trends at different times. The trends of the variables overlap in the component with six years (Figure

IV.3.a) since there is no lag between the waves. When LR is in the low phase of the cycle, the decreases (increases) in the interest rate are procyclical (countercyclical). The last peak of this component was in June 2018, and the last trough was in June 2021. Its next peak and trough will be in June 2024 and 2027, respectively.

The components with 24 years (Figure IV.3.b) present a half-cycle lag, which implies that the trends of the variables are inverse and that the peaks (valleys) of the interest rate component coincide with the valleys (peaks) of the LR.

For the analysis horizon, the interest rate peaks in May 2002 and February 2026, and a trough in March 2014, while LR peaks in October 2013 and troughs in December 2001 and September 2025. In this phase, given that as the interest rate rises, LR falls, interest rate increases will have procyclical effects on LR. The components with eight years (Figure IV.3.c) also present a 4-year lag, which implies the coincidence of the interest rate peaks with the LR valleys.

Figure IV.3.d presents the linear combination of the estimated frequency spectrum. It is observed that for the projection of the next five years (from February 2023 to February 2028), the combination of wave spectra produces low levels of LR, which is mainly determined by the 24-year component that has the highest amplitude (see Table IV.2) and reinforced by other cycles of lower amplitude that have valleys during this time interval. For this same time interval, the combination of the spectral components of the interest rate results in an increasing trend of the interest rate until September 2024, when it reaches a peak mainly determined by the peak of the 24-year component. From October 2025 onwards, a negative trend begins, mainly determined by the six and 8-year components, which coincide in a maximum (peak) in the first half of 2024 and a minimum in the second half of 2027.

Figure IV.3 Standardized estimated spectral components for the interest rate and LR

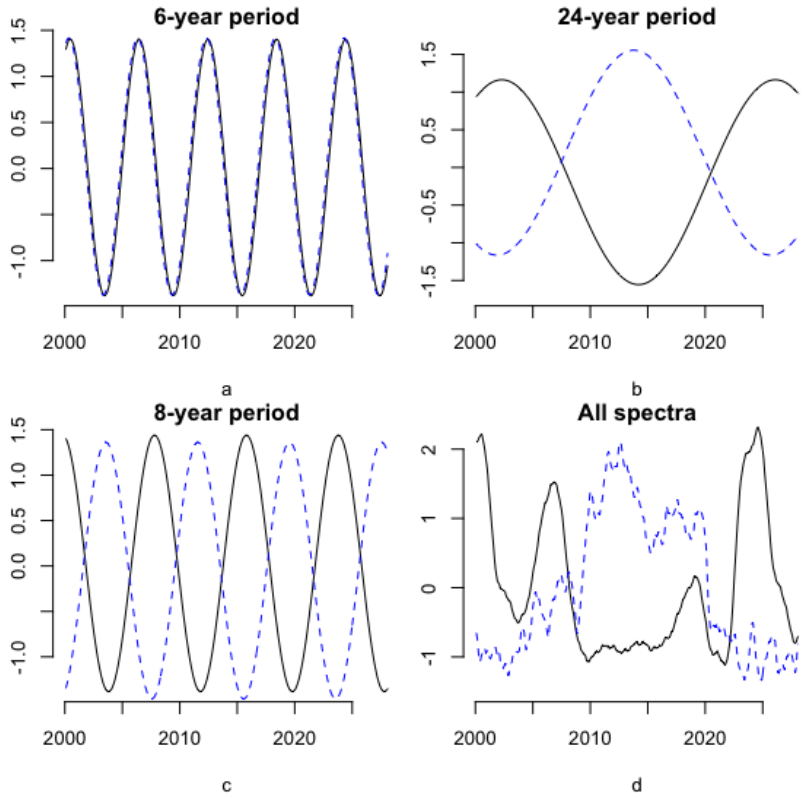

Figure IV.4 shows the time series of the correlation estimated under the DCC-SNP model. It can be seen that the correlation sign shifts at different points in time. The maximum negative correlation value is observed in July 2004, when it reaches a value close to -50%, followed by the value in January 2023, which is close to -36%. The maximum positive correlation values are presented in the first half of 2020, just when the monetary policy interest rate measures to mitigate the effects of the COVID-19 pandemic began to be applied. The correlation rose from 14% in December 2019 to over 48% in January 2020, reaching a value above 99% in May 2020.

Figure IV.4 Dynamic Conditional Correlation Between the interest Rate and LR

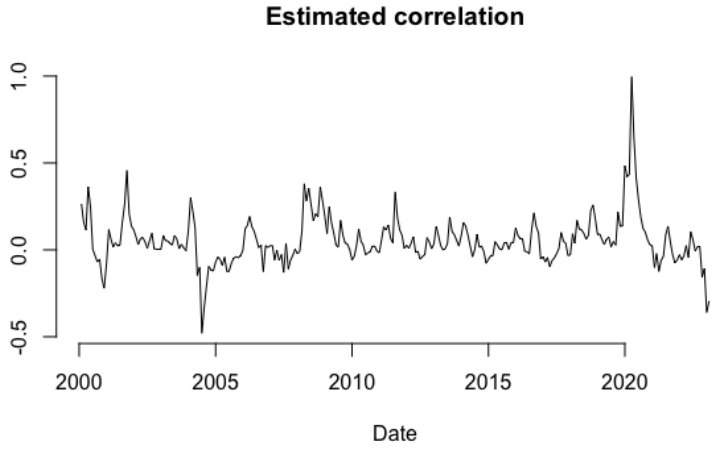

IV.4.1 Performance tests

To compare the performance of the model concerning the estimation of the 1st percentile under the assumption of normality and constant variance-covariance matrix with the estimation of the 1st percentile under DCC-SNP, we use the test proposed by Kupiec (1995) and the test proposed by Lopez (1997) for the monthly series for the interval between February 2000 and February 2023. Table IV.3 shows the results of the tests. The null hypothesis, which states that the proportion of QRM exceptions is equal to 1%, is rejected for the model under the assumption of normality and constant correlation. In contrast, the DCC-SNP model is not rejected. In the Lopez test, the score under the assumption of normality and constant correlation is more than the double of the score obtained under DCC-SNP.

Table IV.3 Forecasting performance tests under DCC-SNP and normal distributions

p-value Kupiec's test DCC-SNP	p-value Kupiec's test Normal	Score Lopez' test DCC-SNP	Score Lopez' test Normal
0.536	0.036	4.03	9.118

Note: This table presents the performance of the model concerning the estimation of the 1st percentile under the assumption of normality and constant variance-covariance matrix with the estimation of the 1st percentile under DCC-SNP.

IV.4.2 Scenario simulation

To graphically evaluate the behavior of the in-sample model, a 5-year Monte Carlo simulation is performed using the estimated parameters of the DCC-SNP model presented in Table IV.2. Figure IV.5 shows the simulation results from March 2018 to February 2023 with a monthly frequency. The solid blue line represents the simulated mean. The dashed blue line represents a bounded interval between the 1st and 99th percentiles of the marginal SNP pdfs of the interest rate and LR, and the solid black line is the observed variable. In the simulation, the interest rate was conditioned to positive values. The variables generally remain within the simulated interval, and only at the points where accelerated changes occur do the variables approach the interval limits. For the interval between the beginning of 2020 and the beginning of 2022, the 1st percentile is close to zero, given the non-negativity constraint in the simulation.

Figure IV.5 Simulation monthly interest rate and LR

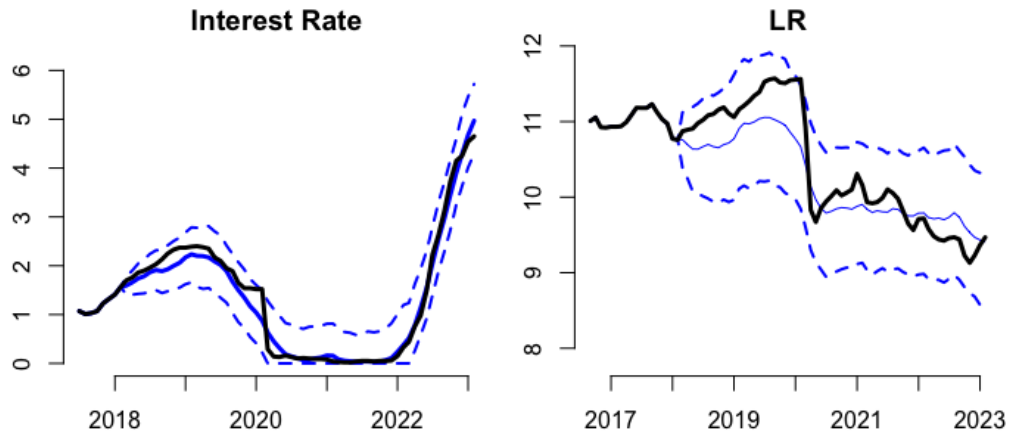

Figure IV.6 depicts the results on the simulation of three scenarios for the interest rate and the monthly LR between February 2018 and February 2023. The proposed scenarios are obtained from the 10th, 50th, and 90th percentiles from the interest rate simulation under the SNP marginal pdf. The blue line corresponds to the scenario obtained from the 90th percentile. Under this scenario, the interest rate continues to rise from its initial value of 4.65% in February 2023 to reach a level close to 7.8% in August 2024 and then declines to

levels between 3.5% and 4% by the end of 2027. The black line corresponds to the scenario obtained from the 50th percentile. In this scenario, the interest rate continues to rise until August 2024, reaching levels close to 6.5% before falling below 4% in early 2028. The red line corresponds to a scenario obtained from the 1st percentile of the simulated interest rate. In this scenario, the interest rate does not continue to rise and remains close to 5% until the end of 2024, when it begins to fall to levels close to zero.

The LR results show that the most favorable scenario is obtained with the 50th percentile, and the most unfavorable scenario is obtained with the 90th percentile. The worst-case scenario for LR is that the rate continues to rise and remains relatively high.

Figure IV.6 Monthly out-off sample simulation of interest rate and LR

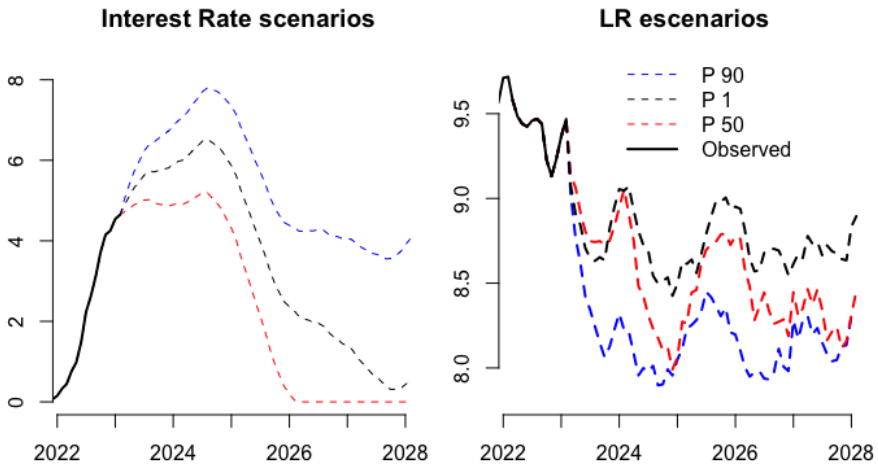

IV. 5 Conclusions and recommendations

This paper proposes a mathematical model and a methodology for macroprudential stress testing based on the joint modeling of the probability distributions of macrofinancial stability indicators and the macroeconomic variables that affect them. Specifically, we have analyzed the Bank Leverage Ratio and the monetary policy interest rate in the United States.

One main conclusion from the results is that the relationship between the Leverage Ratio and the interest rate presents dynamic statistical conditions. Their marginal probability distributions present heavy tails reflected in the skewness and kurtosis parameters. These features should be incorporated in macroprudential stress test models to provide reliable and accurate risk measures. The evidence show that the assumption of a constant conditional correlation matrix and normal distributed marginals lead to the underestimation of the risk of the measurement model. However, by incorporating dynamic conditional correlation, conditional variance deviation, skewness, and kurtosis features simulations seem to successfully pass the performance tests.

The harmonic analysis provides a tool to establish long-term relationships between the cyclical behavior of financial stability indicators and the macroeconomic variables that affect them, based on the contributions to the total variation of each wave component reflected in the amplitude parameters and the parameters that measure the lags between waves. This approach generalizes harmonic analysis by including wave spectra in which the cross-periodogram modulus is maximized. This model could be used to establish simple timing rules for the accumulation and decumulation of countercyclical capital buffers. The DCC-SNP model provides an early warning model for assessing the effects of macroeconomic shocks. The cross-periodogram allows us to identify the peaks (valleys) of the LR, where financial institutions will be more (less) leveraged. If required to adopt interest rate regimes such as those provided by the 1st and 90th percentile of the rate pdf, banks may need to raise more capital or decrease their assets to avoid excessive leverage.

The effects of the interest rate on the LR change over time since the conditional correlation between the variables changes in sign and intensity over time, which implies that in specific periods increases (decreases) in the interest rate may cause an increase (decrease) in leverage levels and other periods may imply a decrease (increase) in leverage.

The proposed model provides interest rate scenarios based on scenarios that depend on the pdfs of the interest rate and allows testing extreme scenarios, such as those obtained from the distribution's tails, as well as base scenarios that can be obtained from the center of the distribution. According to the results obtained for the projection horizon, the monetary policy interest rate regime obtained from the time series of the simulated median of the interest rate

pdf is recommended. The scenario obtained with the median is the one that most favor financial stability.

References

Adrian, T., & Brunnermeier, M. K. (2011). *CoVaR* (Working Paper No. 17454; Working Paper Series). National Bureau of Economic Research. https://doi.org/10.3386/w17454

Basel Committee on Banking Supervision. (2009). *Principles for sound stress testing practices and supervision*. Bank for International Settlements Basel.

Basel Committee on Banking Supervision. (2014). Basel III leverage ratio framework and disclosure requirements. Basel Committee on Banking Supervision.

Banking Supervision, B. C. on. (2018). *Stress testing principles*. Bank for International Settlements Basel.

Bengtsson, E. (2020). Macroprudential policy in the EU: A political economy perspective. *Global Finance Journal*, *46*, 100490. https://doi.org/https://doi.org/10.1016/j.gfj.2019.100490

Borio, C. (2003). Towards a macroprudential framework for financial supervision and regulation? *CESifo Economic Studies*, *49*(2), 181–215. https://doi.org/http://dx.doi.org/10.2139/ssrn.841306

Borio, C. (2011). Central banking post-crisis: What compass for uncharted waters. *Central Banking at a Crossroads*, p. *191*.

Borio, C. E., & Lowe, P. W. (2002). *Asset prices, financial and monetary stability: Exploring the nexus*.

Borio, C. E., & White, W. R. (2004). *Whither monetary and financial stability? The implications of evolving policy regimes*.

Borio, C., Drehmann, M., & Tsatsaronis, K. (2014). Stress-testing macro stress testing: Does it live up to expectations? *Journal of Financial Stability*, *12*, 3–15. https://doi.org/https://doi.org/10.1016/j.jfs.2013.06.001

Claessens, S. (2015). An overview of macroprudential policy tools. *Annual Review of Financial Economics*, *7*(1), 397–422. https://doi.org/10.1146/annurev-financial-111914-041807

Cohen, L. (1998). Generalization of the Gram-Charlier/Edgeworth series and application to time-frequency analysis. *Multi-dimensional Systems and Signal Processing*, *9*(4), 363–372. https://doi.org/https://doi.org/10.1023/A:1008454223082

Committee, B. (2018). Basel Committee on Banking Supervision Charter. *International Law Documents*, *October*, 322–328. https://doi.org/10.1017/9781316577226.047

Del Brio, E. B., Ñíguez, T.-M., & Perote, J. (2011). Multivariate semi-nonparametric distributions with dynamic conditional correlations. *International Journal of Forecasting*, *27*(2), 347–364. https://doi.org/https://doi.org/10.1016/j.ijforecast.2010.02.005

Dharmani, B. C. (2018). Multivariate generalized Gram–Charlier series in vector notations. *Journal of Mathematical Chemistry*, *56*, 1631–1655.

Ebrahimi Kahou, M., & Lehar, A. (2017). Macroprudential policy: A review. *Journal of Financial Stability*, *29*, 92–105. https://doi.org/https://doi.org/10.1016/j.jfs.2016.12.005

Engle, R. (2002). Dynamic conditional correlation. *Journal of Business & Economic Statistics*, *20*(3), 339–350. https://doi.org/10.1198/073500102288618487

International Monetary Fund. (2023). Global financial stability report: Safeguarding financial stability amid high inflation and geopolitical risks. *Washington DC*.

Jiménez, I., Mora-Valencia, A., Ñíguez, T.-M., & Perote, J. (2020). Portfolio risk assessment under dynamic (equi)correlation and semi-nonparametric estimation: An application to cryptocurrencies. *Mathematics*, *8*(12). https://doi.org/10.3390/math8122110

Kupiec, P. H. (1995). Techniques for verifying the accuracy of risk measurement models. *Journal of Derivatives*, *3*, 73–84.

Le Quang, G., & Scialom, L. (2022). Better safe than sorry: Macroprudential policy, covid 19 and climate change. *International Economics*, *172*, 403–413. https://doi.org/https://doi.org/10.1016/j.inteco.2021.07.002

Lopez, J. A. (1997). Regulatory evaluation of value-at-risk models. *FRB of New York Staff Report*, *33*.

Lucia, J. J., & Schwartz, E. S. (2002). Electricity prices and power derivatives: Evidence from the Nordic power exchange. *Review of Derivatives Research*, *5*(1), 5–50. https://doi.org/https://doi.org/10.1023/A:1013846631785

Mauleón, I. (2003). Financial densities in emerging markets: an application of the multivariate ES density. Emerging Markets Review, 4(2), 197–223.

Mauleón, I. (2006). Modelling multivariate moments in European stock markets. European Journal of Finance, 12(03), 241–263.

Mora-Valencia, A., Ñíguez, T. M., & Perote, J. (2017). Multivariate approximations to portfolio return distribution. Computational and Mathematical Organization Theory, 23, 347-361.

Rendón, J. F., Cortes, L., & Perote, J. (2021). Determining the banking solvency risk in times of COVID-19 through Gram-Charlier expansions. Available at SSRN 3928191.

Ñíguez, T.-M., & Perote, J. (2012). Forecasting heavy-tailed densities with positive Edgeworth and Gram-Charlier expansions*. *Oxford Bulletin of Economics and Statistics*, *74*(4), 600–627. https://doi.org/https://doi.org/10.1111/j.1468-0084.2011.00663.x

Vatiwutipong, P., & Phewchean, N. (2019). Alternative way to derive the distribution of the multivariate Ornstein–Uhlenbeck process. *Advances in Difference Equations*, *2019*(1), 1–7.

Vega, M., & Winkelried, D. (2005). Inflation targeting and inflation behavior: A successful story? International Journal of Central Banking, 1(3), 153–175.

Conclusions

This thesis proposes a methodology for measuring financial risks in banking systems based on modeling the pdfs associated with solvency and leverage risks, both in univariate and multivariate framework. The Gram-Charlier expansions are used to model stylized facts of the pdfs, such as asymmetry and heavy tails, which generalize the normal pdf. Performance tests comparing models under normality assumptions and models under SNP assumptions indicate that they justify the use of Gram-Charlier expansions to obtain more accurate risk measures than those obtained under the normality assumption.

The models are used to propose tools that facilitate macroprudential policy decisions to maintain a financial system's stability and can be used in financial systems operating under the parameters established by Basel Committee of Banking Supervision (BCBS) in BCBS (2011) since they are based on a common theoretical framework, where economic capital is established as the basis for maintaining financial stability. This methodology reinforces the second pillar established by BCBS, which implies the development of risk management policies based on measures that reflect banks' profiles and risk propensity. The models can be used under both standardized and internal risk measurement methods.

The analysis of the characteristics of the empirical probability distributions of the macroprudential stability indicators shows that they present skewness and kurtosis distortions concerning the normal distribution. This result is evidenced in the literature review, where it is shown that these distortions are present in the measurement of banking risks associated with a wide range of financial variables, also exhibited by the descriptive statistics of the variables, but especially in the significance of estimated parameters of skewness and kurtosis.

The analysis of the behavior of the first moment of the pdfs showed seasonal and cyclical behavior both in the first difference of the variables and in levels. The variables in the first difference were modeled from ARMA models. The variables in levels were modeled from stochastic processes of reversion to the mean where the expected value of the process incorporates a deterministic component that was defined using the harmonic analysis that

facilitates the decomposition of a time series in a set of trigonometric Fourier series, both in the univariate and multivariate cases.

The analysis of the behavior of the second moment shows mixed behavior, given that significant GARCH parameter were found in the variance modeling. In contrast, for the models of the variables in levels, only significant GARCH parameters were found for the multivariate case. Heteroscedasticity was not detected in the variance of the univariate variables in levels. It was modeled from the historical estimator of the unconditional variance of the errors of the mean model.

The results of the multivariate analysis between financial stability indicators and macroeconomic variables revealed the dynamic behavior of the correlation, where it varies in a wide range that fluctuates between positive and negative values. The change of sign in the correlation is an important finding since it reveals that the effects of macroeconomic variables on financial stability are time-varying, which implies that the application of the same macroeconomic policy (e.g., monetary policies) can have procyclical effects at some moments and countercyclical effects at others, therefore, decision-makers should use models that measure the correlation dynamics between financial stability indicators and macroeconomic variables.

The results of the application of the proposed models for risk measurement in macro-financial stability indicators show that the use of monthly and quarterly data samples is appropriate; however, for many developed and emerging countries, the length of the data series published by the prudential authorities is not sufficient for the proposed models to be applied. In this sense, financial authorities should improve the availability of data in order to reinforce Pillar III established by the BCBS, which recommends that financial institutions provide clear information on their risk profile in order to be more transparent on their capital structure and adequacy, and risk exposure.

Although this work only presents results at the macroprudential level, the models can be used in the microprudential context by regulators to monitor individual institutions and financial institutions, integrating them into their risk management system. This methodology can be used for different levels of data aggregation. It can be applied to levels of disaggregation that

involve the measurement of risk for a specific asset or a portfolio of assets, up to levels of aggregation that include the entire financial system.

The main objective of Chapter II was to propose measures of the probability that a bank or banking system could fall below the minimum solvency level required by prudential policy and to define policies regarding the capital levels that a bank or banking system must maintain to restrict the probability of falling below the minimum solvency level required, based on QRMs. The methodology was based on Gram-Charlier expansions to model the higher moments and on ARIMA-GARCH models to model the mean and variance of the pdfs related to changes in Tier capital, Risk-Weighted Assets, and Solvency Ratio. As a case study, the methodology was applied using data from the Colombian banking system. An analysis was made of the effects that the monetary policy regime had on the probability of being below the minimum solvency level required during the period of the beginning of the COVID-19 pandemic, finding that the monetary policy measures applied generated a significant increase in the probability of being below the minimum solvency level required. Monetary policy measures can destabilize the financial system, highlighting the need to consider monetary and prudential policy decisions together.

Chapter III proposes a new model for Measuring the Probability of Breaching the Minimum Capital Threshold (PBT) and estimating the countercyclical capital buffer (CCB) established in the Basel III Accord based on the assumption that the Capital-To-Risk Weighted Assets Ratio follows a stochastic Ornstein Uhlenbeck Gram-Charlier process. Analytical PBT and CCB solutions are obtained that depend on, the last observed solvency level, the minimum solvency level required by the regulator, a parameter that restricts risk appetite, and the parameters that model the moments of the pdf of the Capital Adequacy Ratio. The mean is modeled from harmonic analysis, introducing the Fourier series in the deterministic component of the model. These harmonic components allow businesses' cyclical behavior to be considered in estimating PBT and CCB. For the estimation of the second moment of the pdf, the unconditional variance estimator was used since no evidence of significant autocorrelations of the squared residuals resulting from the estimation of the mean models was found in the data analyzed. Once more, Gram-Charlier expansions were used to model the higher moments.

An application is made on a set of solvency ratio (SR) time series for the Netherlands, United States, Germany, and Colombia. PBT and CCB are estimated for the observed periods of each series.

To analyze the interaction between the monetary policy interest rate and the PBT related to prudential policy, a Vector Autoregressive model (VAR) including macroeconomic variables and a credit volume indicator is estimated. The results indicate that PBT is relevant in lending decisions, affecting the effectiveness of banks in the transmission of monetary policy. On the other hand, interest rate shocks affect lending decisions through the effect of the interest rate on PBT. This evidence suggests that prudential and monetary policy decisions should be made jointly.

This methodology could model the credit-to-GDP gap proposed in the Basel III agreement. The Fourier series can be used to avoid the problem of arbitrariness in the choice of the smoothing parameter of the Hodrick-Prescott filters used in this methodology. The results of this study indicate that assuming normality in the behavior of the pdf associated with the SR leads to an underestimation of PBT and CCB. Consistent with this result, it is suggested to include parameters that consider the bias and heavy tails in estimating regulatory capital. Finally, this study provides evidence of the existence of bank-capital and risk-taking channels from the relationship between the monetary policy interest rate and the PBT.

Chapter IV proposes a methodology for macroprudential stress tests based on the application of the DCC-SNP model, which involves modeling the joint pdf between a bank leverage indicator (used as an indicator of macrofinancial stability) and the monetary policy interest rate (which is assumed to be related to macrofinancial stability). In this chapter, we make a multivariate generalization of the model proposed in Chapter III. Thus, we start from a multivariate Ornstein Uhlenbeck stochastic process as the underlying stochastic process that contains variables representing a set of macrofinancial stability indicators and a set of macrofinancial variables that are assumed to be correlated with macrofinancial stability indicators. Cross-harmonic analysis was used to incorporate the Fourier series in the deterministic components of the models. The cross-harmonic analysis provides a tool to establish long-term relationships between macrofinancial stability indicators and macroeconomic variables. Finally, the model is applied to an indicator of the leverage of U.S.

commercial banks and the policy interest rate set by the U.S. Federal Reserve. The model provides scenarios of interest rate regimes based on the estimation of quantiles of the marginal pdf of the interest rate and the effect these scenarios have on the bank leverage indicator. The backtesting tests applied to measure the performance of the estimated models showed the need to use dynamic estimators for variances and correlations and to model the tails of the distributions. The model assuming normality of the pdf and non-conditional variance and correlation estimators did not perform well, while the DCC-SNP model showed better performance.

The methodologies proposed in this document focus on meeting the needs of the second pillar established by BCBS to acquire more accurate models for measuring financial risks, where in addition to considering credit, market, operational and liquidity risks, systemic risks should also be considered. In these terms, financial institutions and prudential authorities should implement models that consider the bias and kurtosis of financial stability indicators to avoid undervaluation of risks and the capital needed to cover them. These parameters can be estimated from sophisticated models such as the ones presented in this research and implemented in a standardized way (periodically updated) by incorporating factors that correct the financial stability indicators. These factors can be incorporated into the risk measurement models used by financial institutions and regulators, but it implies that the respective econometric measurements are made for each case. Given many methodologies academics and practitioners use for financial risk measurement, incorporating high moments pdfs constitutes a whole line of research within the financial risk area.

Conclusiones

Esta tesis propone una metodología para medir los riesgos financieros en los sistemas bancarios basada en la modelización de las funciones de densidad de probabilidad (pdf por sus siglas en inglés) asociadas a los riesgos de solvencia y apalancamiento, de manera univariante y multivariante. Se utilizan las expansiones de Gram-Charlier que generalizan la pdf normal, para modelizar hechos estilizados de las pdf, como la asimetría y las colas pesadas. Las pruebas de rendimiento que comparan modelos bajo supuestos de normalidad y SNP indican que se justifica el uso de las expansiones de Gram-Charlier para obtener medidas de riesgo que no subestimen el riesgo.

Los modelos se utilizan para proponer herramientas que faciliten las decisiones de política macroprudencial para mantener la estabilidad de un sistema financiero y pueden ser utilizados en sistemas financieros que operan bajo los parámetros establecidos por el Comité de Supervisión Bancaria de Basilea (BCBS) en BCBS (2011), ya que se basan en un marco teórico común, donde el capital económico se establece como la base para mantener la estabilidad financiera. Esta metodología refuerza el segundo pilar establecido por el BCBS, que implica el desarrollo de políticas de gestión del riesgo basadas en medidas que reflejen los perfiles de los bancos y su propensión al riesgo. Los modelos pueden utilizarse tanto bajos métodos estandarizados e internos de medición del riesgo.

El análisis de las características de las distribuciones empíricas de probabilidad de los indicadores de estabilidad macroprudencial evidencia la presencia de asimetría y curtosis con respecto a la distribución normal. Este resultado se verifica en la revisión de la literatura, donde se muestra que estas distorsiones están presentes en la medición de los riesgos bancarios asociados a una amplia gama de variables financieras, y en los estadísticos descriptivos de las variables analizadas, pero especialmente en la significación de los parámetros estimados de asimetría y curtosis.

El análisis del primer momento de las pdf mostró un comportamiento estacional y cíclico tanto en la primera diferencia de las variables como en niveles. Las variables en primera diferencia se modelaron a partir de modelos ARMA. Las variables en niveles se modelaron a partir de procesos estocásticos de reversión a la media, donde el valor esperado del proceso

incorpora una componente determinista que se definió utilizando el análisis armónico que facilita la descomposición de una serie de tiempo en un conjunto de series trigonométricas de Fourier, tanto en el caso univariado como multivariado.

El análisis del segundo momento muestra un comportamiento mixto, dado que se encontraron parámetros GARCH significativos en la modelización de la varianza. En cambio, para los modelos de las variables en niveles, solo se encontraron parámetros GARCH significativos para el caso multivariado. No se detectó heteroscedasticidad en la varianza de las variables univariantes en niveles. Se modeló a partir del estimador histórico de la varianza no condicional de los errores del modelo de medias.

Los resultados del análisis multivariado entre los indicadores de estabilidad financiera y las variables macroeconómicas revelaron el comportamiento dinámico de la correlación, que varía en un amplio rango que oscila entre valores positivos y negativos. El cambio de signo en la correlación es un hallazgo importante, ya que revela que los efectos de las variables macroeconómicas sobre la estabilidad financiera son variables en el tiempo, lo que implica que la aplicación de una misma política macroeconómica (por ejemplo, políticas monetarias) puede tener efectos procíclicos en algunos momentos y efectos contracíclicos en otros, por lo tanto, los tomadores de decisiones deben utilizar modelos que midan la dinámica de correlación entre los indicadores de estabilidad financiera y las variables macroeconómicas.

Los resultados de la aplicación de los modelos propuestos para la medición del riesgo en los indicadores de estabilidad macrofinanciera muestran que el uso de muestras de datos mensuales y trimestrales es adecuado; sin embargo, para muchos países desarrollados y emergentes, la longitud de las series de datos publicadas por las autoridades prudenciales no es suficiente para aplicar los modelos propuestos. En este sentido, las autoridades financieras deberían mejorar la disponibilidad de datos para reforzar el Pilar III establecido por el BCBS, que recomienda que las instituciones financieras proporcionen información clara sobre su perfil de riesgo para ser más transparentes sobre su estructura y adecuación de capital, y su exposición al riesgo.

Aunque en este trabajo solo se presentan resultados a nivel macroprudencial, los modelos pueden ser utilizados en el contexto microprudencial por los reguladores para supervisar instituciones individuales y entidades financieras, integrándolos en su sistema de gestión de

riesgos. Esta metodología puede utilizarse para distintos niveles de agregación de datos. Puede aplicarse a niveles de desagregación que impliquen la medición del riesgo para un activo específico o una cartera de activos, hasta niveles de agregación que incluyan todo el sistema financiero.

El principal objetivo del Capítulo II es proponer medidas de la probabilidad de que un banco o sistema bancario pudiera caer por debajo del nivel mínimo de solvencia exigido por la política prudencial y definir políticas relativas a los niveles de capital que un banco o sistema bancario debe mantener para restringir la probabilidad de caer por debajo del nivel mínimo de solvencia exigido, basándose en los QRM. La metodología se basó en expansiones de Gram-Charlier para modelar los momentos superiores y en modelos ARIMA-GARCH para modelar la media y la varianza de las pdf relacionadas con los cambios en el capital de nivel, los activos ponderados por riesgo y el coeficiente de solvencia. Como caso de estudio, se aplicó la metodología utilizando datos del sistema bancario colombiano. Se analizaron los efectos que tuvo el régimen de política monetaria sobre la probabilidad de estar por debajo del nivel mínimo de solvencia requerido durante el periodo de inicio de la pandemia COVID-19, encontrando que las medidas de política monetaria aplicadas generaron un aumento significativo en la probabilidad de estar por debajo del nivel mínimo de solvencia requerido. Las medidas de política monetaria pueden desestabilizar el sistema financiero, lo que pone de relieve la necesidad de considerar conjuntamente las decisiones de política monetaria y prudencial.

En el Capítulo III se propone un nuevo modelo para la Medición de la Probabilidad de Incumplimiento del Umbral Mínimo de Capital (PBT) y la estimación del colchón de capital anticíclico (CCB) establecidos en el Acuerdo de Basilea III basado en el supuesto de que el Ratio Capital-Activos Ponderados por Riesgo sigue un proceso estocástico Ornstein Uhlenbeck Gram-Charlier. Se obtienen soluciones analíticas de PBT y CCB que dependen, del último nivel de solvencia observado, del nivel de solvencia mínimo exigido por el regulador, de un parámetro que restringe el apetito por el riesgo, y de los parámetros que modelizan los momentos de la pdf del Ratio de Adecuación de Capital. La media se modela a partir del análisis armónico, introduciendo la serie de Fourier en el componente determinista del modelo. Estos componentes armónicos permiten considerar el

comportamiento cíclico de los negocios en la estimación de PBT y CCB. Para la estimación del segundo momento de la pdf se utilizó el estimador de varianza no condicional al no encontrarse en los datos analizados evidencia de autocorrelaciones significativas de los residuos al cuadrado resultantes de la estimación de los modelos de medias. Una vez más, se utilizaron expansiones de Gram-Charlier para modelizar los momentos superiores.

Se realiza una aplicación sobre un conjunto de series temporales del coeficiente de solvencia (SR) para los Países Bajos, Estados Unidos, Alemania y Colombia. Se estiman PBT y CCB para los periodos observados de cada serie.

Para analizar la interacción entre el tipo de interés de política monetaria y el PBT relacionado con la política prudencial, se estima un modelo vectorial autorregresivo (VAR) que incluye variables macroeconómicas y un indicador del volumen de crédito. Los resultados indican que el PBT es relevante en las decisiones de préstamo, afectando a la eficacia de los bancos en la transmisión de la política monetaria. Por otra parte, las perturbaciones de los tipos de interés afectan a las decisiones de préstamo a través del efecto del tipo de interés sobre el PBT. Esta evidencia sugiere que las decisiones de política prudencial y monetaria deberían tomarse conjuntamente.

Esta metodología podría modelizar la brecha entre crédito y PIB propuesta en el acuerdo de Basilea III. Las series de Fourier pueden utilizarse para evitar el problema de la arbitrariedad en la elección del parámetro de suavización de los filtros de Hodrick-Prescott utilizados en esta metodología.

Los resultados de este estudio indican que asumir normalidad en el comportamiento de la pdf asociada a la SR conduce a una subestimación de PBT y CCB. Consistente con este resultado, se sugiere incluir parámetros que consideren el sesgo y las colas pesadas en la estimación del capital regulatorio. Por último, este estudio aporta pruebas de la existencia de canales de capital bancario y asunción de riesgos a partir de la relación entre el tipo de interés de política monetaria y el PBT.

En el Capítulo IV se propone una metodología para las pruebas de tensión macroprudencial basada en la aplicación del modelo DCC-SNP, que consiste en modelizar el pdf conjunta de un indicador de apalancamiento bancario (utilizado como indicador de estabilidad

macrofinanciera) y el tipo de interés de política monetaria (que se supone relacionado con la estabilidad macrofinanciera). En este capítulo, hacemos una generalización multivariante del modelo propuesto en el Capítulo III. Así, partimos de un proceso estocástico multivariante de Ornstein Uhlenbeck como proceso estocástico subyacente que contiene variables que representan un conjunto de indicadores de estabilidad macrofinanciera y un conjunto de variables macrofinancieras que se supone están correlacionadas con los indicadores de estabilidad macrofinanciera. Se utilizó el análisis armónico cruzado para incorporar las series de Fourier en los componentes deterministas de los modelos. El análisis armónico cruzado proporciona una herramienta para establecer relaciones a largo plazo entre los indicadores de estabilidad macrofinanciera y las variables macroeconómicas. Por último, el modelo se aplica a un indicador del apalancamiento de los bancos comerciales estadounidenses y al tipo de interés oficial fijado por la Reserva Federal de Estados Unidos. El modelo proporciona escenarios de regímenes de tipos de interés basados en la estimación de cuantiles de la fdp marginal del tipo de interés y el efecto que estos escenarios tienen sobre el indicador de apalancamiento bancario.

Las pruebas de backtesting aplicadas para medir el rendimiento de los modelos estimados mostraron la necesidad de utilizar estimadores dinámicos para las varianzas y las correlaciones y de modelar las colas de las distribuciones. El modelo que asume la normalidad de la pdf y los estimadores no condicionales de varianzas y correlaciones no evidenciaron desempeños apropiados, mientras que el modelo DCC-SNP sí.

Las metodologías propuestas en este documento se centran en satisfacer las necesidades del segundo pilar establecido por el CBSB de adquirir modelos más precisos para la medición de los riesgos financieros, donde además de considerar los riesgos de crédito, mercado, operacional y liquidez, también se deben considerar los riesgos sistémicos. En estos términos, las entidades financieras y las autoridades prudenciales deben implementar modelos que consideren el sesgo y la curtosis de los indicadores de estabilidad financiera para evitar la subvaloración de los riesgos y del capital necesario para cubrirlos. Estos parámetros pueden estimarse a partir de modelos sofisticados como los presentados en esta investigación e implementarse de forma estandarizada (actualizados periódicamente) incorporando factores que corrijan los índices de estabilidad financiera por asimetría y colas pesadas. Estos factores

pueden ser incorporados a los modelos de medición de riesgo utilizados por las instituciones financieras y los reguladores, pero implica que se realicen las respectivas mediciones econométricas para cada caso. Dadas las múltiples metodologías que académicos y profesionales utilizan para la medición del riesgo financiero, la incorporación de momentos superiores de las pdf constituye toda una línea de investigación dentro del área de riesgos financieros.